RESEARCH STUDY ENTITLED

ADVANCED X-RAY ASTROPHYSICAL OBSERVATORY (AXAF)

(NASA-CR-161092) RESEARCH STUDY ENTITLED ADVANCED X-RAY ASTROPHYSICAL OBSERVATORY (AXAF) Final Report, 8 Aug. 1977 - 30 Nov. 1978 (Smithsonian Astrophysical Observatory) 138 p HC A07/MF A01 CSCL 03A G3/89

N79-17767

Unclas 13895

FINAL REPORT

NASA CONTRACT NAS8-32667

August 8, 1977 - November 30, 1978

January 1979

Prepared For

National Aeronautics And Space Administration
George C. Marshall Space Flight Center
Marshall Space Flight Center, Alabama 35812

RECEIVED
NASA STI FACILITY
FEB 1979

Submitted By

Smithsonian Institution
Astrophysical Observatory
Cambridge, Mass. 02138

The Smithsonian Astrophysical Observatory
And The Harvard College Observatory
Are Members Of The
Center For Astrophysics

RESEARCH STUDY ENTITLED

ADVANCED X-RAY ASTROPHYSICAL OBSERVATORY (AXAF)

FINAL REPORT

NASA CONTRACT NAS8-32667

August 8, 1977 - November 30, 1978

January 1979

Submitted By

Smithsonian Astrophysical Observatory
High Energy Astrophysics Division

Prepared By: Robert W. Rasche

Approvals:

Riccardo Giacconi
Associate Director

John W. Gerdes
AXAF Program Manager

TABLE OF CONTENTS

Section	Description	Page
1.0	INTRODUCTION	1-1
2.0	BACKGROUND	2-1
2.1	General	2-1
2.2	Comments On Horizontal Testing	2-2
2.3	Verification Of MSFC Preferred Concepts	2-3
2.4	Subcontracts	2-4
2.5	Future Work	2-5
2.6	Other Activities	2-6
3.0	OPTICAL DESIGN STUDIES	3-1
3.1	General	3-1
3.2	Baseline Optical Design	3-1
3.3	Effective Area Related To Energy	3-4
3.4	Mirror Parametric Studies	3-5
3.5	Baseline Off-Axis Properties	3-20
3.6	Scattering Effects	3-23
4.0	MIRROR SUPPORT CONCEPTS	4-1
4.1	General	4-1
4.2	Cantilever Support Cylinder Concept	4-5
4.3	Center Support Cylinder	4-9
4.4	Thermal Gradient Effects Trade	4-18
4.5	Work In Progress	4-18
5.0	MIRROR WEIGHT ESTIMATES	5-1
5.1	General	5-1
5.2	Weight Of Glass	5-1
5.3	Structure Weight	5-1
6.0	1 G EFFECTS ON MIRROR ELEMENTS	6-1
6.1	Comment	6-1
6.2	Deflection Vs. Support Plane	6-1
6.3	Sleeve Support Concept	6-4
7.0	MIRROR ASSEMBLY RESONANT FREQUENCIES	7-1
7.1	General	7-1
7.2	Mirror Element Resonant Frequencies	7-1
7.3	Lateral Assembly Frequencies	7-1
7.4	Axial Assembly Frequencies	7-1
8.0	OPTICAL BENCH CONSIDERATIONS	8-1
8.1	General	8-1
8.2	Model For Optical Bench Studies	8-1
8.3	Sources Of Error From Bench Deformations	8-1

TABLE OF CONTENTS, contd.

Section	Description	Page
8.4	Focal Length Changes (De-Focus)	8-3
8.5	Decentering Changes (ΔR)	8-7
8.6	Horizontal Testing Considerations	8-9
8.7	Typical Deformations	8-11
8.8	Ground Testing Dynamic Considerations	8-11
9.0	TEMPERATURE CONTROL OF MIRROR ASSEMBLY	9-1
9.1	General	9-1
9.2	Thermal Control Concept Model	9-1
9.3	Need For Optical Bench Control	9-3
9.4	Control Surface Effects	9-5
9.5	Baffle Studies	9-5
10.0	ASPECT DETERMINATION SYSTEM	10-1
10.1	General	10-1
10.2	Aspect Determination System (Baseline)	10-2
10.3	Control Of Focal Plane Motion	10-5
10.4	Preliminary Error Budget	10-6
10.5	Fine Aspect Sensor Studies	10-7
10.6	Summary Comment	10-13
	References	vii

LIST OF FIGURES

Figure #	Description	Page
3-1	X-ray Mirror Assembly Baseline Design Concept	3-2
3-2	Efficiency^2 x Grazing^2 For Energy Range Of 2-9 keV With Nickel Surface	3-6
3-3	Efficiency^2 x Grazing^2 For Energy Range Of 2-9 keV With Gold Surface	3-7
3-4	Effect Of Surface Materials	3-10
3-5	Area Vs. Energy Focal Length Dependance	3-12
3-6	Area Vs. Energy Radius Dependance	3-14
3-7	Ang. Res. Vs. Polar Angle Radius Dependance	3-16
3-8	Area Vs. Energy Segment Length Dependance	3-17
3-9	Ang. Res. Vs. Polar Angle Segment Length Dependance	3-18
3-10	Area Vs. Energy Segment Length Dependance	3-19
3-11	Baseline Off-Axis Response (Effective Area Vs. Energy)	3-21
3-12	Baseline Off-Axis Response (RMS Radius Vs. Inc. Polar Angle)	3-22
3-13	Scattering Effects	3-24
3-14	Scattering Effects	3-25
3-15	Scattering Effects	3-26
4-1	Length In Feet Of HEAO-B And AXAF	4-2
4-2	Weight - HEAO-B And AXAF	4-3
4-3a	Cantilevered Support Cylinder	4-4
4-3b	Center Supported Cylinder	4-4
4-4	Effect Of Cantilever Sag	4-6
4-5	Deflection Modes	4-11
4-6	Mounting Cylinder Rotation	4-13
4-7	Mounting Cylinder Decentering	4-15
4-8	Support Cylinder Decentering	4-16
4-9	Mounting Ring Deflection	4-17
5-1	Weight Of Glass Mirrors	5-2

LIST OF FIGURES, contd.

Figure #	Description	Page
6-1	Support Plane Locations	6-2
6-2	Maximum & Average Slope Error Vs. Support Distance	6-3
6-3	Resolution Vs. Support Plane Location (Outer Element)	6-5
6-4	Support Sleeve Concept	6-6
6-5	Effect Of G/E Cyl.-Invar Ring Support On Mirror Deflection	6-8
8-1	Simplified Optical Bench Model	8-2
8-2	Bench Curvature Effect On Focal Length	8-5
8-3	Rotation Effects On Image Plane	8-6
8-4	Support Concept	8-10
8-5	Effect Of Rotation About Node	8-12
8-6	1 g Static Deflection	8-13
8-7	1 g Static Rotation	8-14
8-8	Hot-Dog Effects	8-15
9-1	Simplified Thermal Control Concept	9-2
9-2	Model For Baffle Studies	9-6
9-3	Element Temperature Vs. Element Length	9-7
9-4	Element Temperature Vs. Length	9-8
9-5	Element Temperature Vs. Length	9-9
9-6	Element Temperature Vs. Length	9-10
9-7	Element Temperature Vs. Element Length	9-11
9-8	Element Temperature Vs. Element Length	9-12
9-9	Element Temperature Vs. Element Length	9-13
9-10	Element Temperature Vs. Element Length	9-14
9-11	Element Temperature Vs. Element Length	9-15
9-12	Element Temperature Vs. Element Length	9-16
9-13	Element Temperature Vs. Element Length	9-17
9-14	Element Temperature Vs. Element Length	9-18
9-15	Element Temperature Vs. Element Length	9-19
9-16	Element Temperature Vs. Element Length	9-20

LIST OF FIGURES, contd.

Figure #	Description	Page
9-17	Element Temperature Vs. Element Length	9-21
9-18	Element Temperature Vs. Element Length	9-22
9-19	Element Temperature Vs. Element Length	9-23
9-20	Element Temperature Vs. Element Length	9-24
9-21	Element Temperature Vs. Element Length	9-25
9-22	Element Temperature Vs. Element Length	9-26
9-23	Element Temperature Vs. Element Length	9-27
9-24	Element Temperature Vs. Element Length	9-28
9-25	Element Temperature Vs. Element Length	9-29
9-26	Aperture Power Loss Vs. Percent Of Baffle Heated	9-30
10-1	Aspect Determination Elements	10-1

LIST OF TABLES

Table #	Description	Page
3-1	Baseline Optical Design High Resolution Mirror Assembly	3-3
3-2	Angles, Arc-Minutes	3-8
4-1	Ground Rules	4-10
10-1	Aspect Determination System Elements	10-3
10-2	CCD Activities	10-8

REFERENCES

1. American Science And Engineering, Inc. Report, ASE-4302, "Advanced X-ray Astrophysics Facility (AXAF) Mirror 1 G Deflection Parametric Study", June 22, 1978.

2. Ball Aerospace Systems Division, "A Comparative Evaluation Of Solid State vs Image Dissector Tube Detectors For The AXAF Star Sensor", November 10, 1978.

3. MSFC, "Advanced X-ray Astrophysics Facility, Conceptual Design", May 1978.

1.0 INTRODUCTION

This report is the Final Report required by Contract NAS8-32667. It documents and summarizes the principal and significant results of the work to date (November 30, 1978) and includes recommendations and conclusions as appropriate based upon the experience and results obtained.

It must be recognized that the activities implied by this report are part of SAO's continuing and, with the successful launch of HEAO-B, accelerating technical support to the AXAF program as part of the MSFC/SAO team concept. Because the work is on-going the results reported here are not always conclusive nor in some cases complete and should be regarded more as indicative of what has been done than as a final position or conclusion on a particular subject.

The technical program at SAO is carried out in response to a total X-ray Telescope Assembly (XTA) system engineering overview wherein the many contributing factors determining the ultimate performance of the AXAF and test thereof are treated in an integrated and coordinated fashion. Thus, many of what are presented in this report as apparently separate topics are, in fact, closely interrelated and represent sensitivity, feasibility, or other system studies. For example, the analysis of thermal and 1 g deflections of the optical bench are not so much related to the design of an optical bench *per se*, but rather to establish that the deflection constraints can be satisfied with a realizable system and, in particular, by the concept put forth by the MSFC Program Development activity.

Section 2.0 contains some general background and overview material. The thrust of on-going and near term future activities is summarized and interim conclusions are stated.

Sections 3.0 through 10.0 deal with specific subject areas.

This report does not deal with the "optical technology" activity because selection and contract award activities are currently in progress.

2.0 BACKGROUND

2.1 General

The work at SAO reflected in this report began in summer 1977 in parallel with the X-ray test of the HEAO-B X-ray mirror at the test facility at MSFC. This test experience established for the first time that the optical measurements made during mirror manufacture and final assembly and alignment, if properly made and interpreted, can provide a high degree of confidence in general alignment integrity. A key point established was that while in-process X-ray testing is certainly desirable it is not absolutely necessary to manufacture and assemble a properly figured and aligned mirror.

The second point which was established was the need for full aperture test of the mirror assembly in X-rays to establish resolution and total energy response and to provide boresight information for use in the on-orbit alignment of X-ray axis to aspect sensor axis. The total test experience at MSFC established the futility of subaperture testing and subsequent superposition to derive total mirror response.

The third and probably most important point which emerged from the HEAO-B mirror test activity and subsequent analysis of results was that the mirror performed very well and that the limitations on performance due to surface roughness, thermal effects during assembly, etc. were well understood in a reasonably quantitative way. The limit on resolution can be expected to be established by surface finish rather than alignment and figure given the state of the art at present. Upon review and reflection of the HEAO-B mirror fabrication and test experience, the SAO group concluded that the AXAF mirror assembly resolution goal should be 0.5 arc-seconds and that on the basis of all

available information such a goal while certainly difficult was entirely feasible. This conclusion remains intact.

In order to exploit the resolution of the mirror it is necessary to establish post facto aspect to a relative accuracy comparable to the resolution of the mirror. Individual photon events taken over many orbits can then be superimposed in celestial coordinates with a "spread" no greater than that produced by the mirror's finite resolution. Absolute accuracy is determined by on-orbit bore sighting of X-ray sources with known optical counterparts and the maintenance of the stability of the aspect determination system alignment. The performance objectives for post facto aspect determination are 0.5 arc-seconds relative accuracy and 1.0 arc-sec absolute accuracy. These are state of the art for systems employing fixed head sensors. Nevertheless, after more than one year of study, these performance goals are still considered feasible.

These twin goals of 0.5 arc-sec resolution and post facto aspect determination are the system engineering drivers constraining and defining work at SAO. The consequence of these goals is that the entire XTA must be considered as an integral system and SAO is carrying out its mission in such a way.

2.2 Comments On Horizontal Testing

Full aperture testing in X-rays is essential to establish AXAF performance characteristics. It has been assumed that such testing will be done at MSFC after some modification to the existing facility is accomplished and that the distance from the X-ray source to the mirror will be between 1500 and 2000 feet. This approach which appears to be the only feasible one requires that the XTA be tested with its optical axis horizontal with the

consequence that reasonably severe 1 g distortions can be introduced. These deformations can be controlled but not eliminated.

It turns out to be as important to understand the effects of these 1 g distortions as it is to control them within practical limits. When these 1 g deformations are taken together and in some cases individually their effect on measured resolution at finite source distances is greater than that from the postulated (and desired) scattering due to mirror surface roughness (assuming this is the principal component of resolution degradation). In order to accurately predict the on-orbit resolution of the XTA it is necessary to make a number of first order corrections for 1 g effects (at specified source distances) and in order to make these corrections it is necessary to establish design concepts that permit the accurate calculation of 1 g deformations and the resultant degradation of XTA performance. Consequently, much of the work performed and much of the material in this report deals with horizontal testing issues. Work to date indicates it is feasible to correct measured resolution to the residual 0.5 arc-sec due to inherent mirror scattering.

2.3 Verification Of MSFC Preferred Concepts

At the time SAO began work, the Program Development activity at MSFC had already identified several concepts and had developed one in some detail. Work at SAO was therefore directed towards identifying system issues and constraints and assessing the MSFC work in that context to ensure compatibility with the performance objectives*. As would be expected, different assumptions, preferences, and perspectives have produced different

*For example, most of the SAO work assumed a cylindrical optical bench tube of graphite epoxy supported at the minimum deflection point.

conclusions in some instances. However, a result of the SAO work to date is verification that the MSFC preferred concept offers a high probability of meeting the AXAF performance objectives. This is considered a significant result since the total MSFC-SAO effort relative to the concept which is appreciable, complementary for the most part, and in general agreement now can serve as an excellent point of reference in the evaluation and trade off of new and different concepts which are beginning to be proposed by interested private organizations.

2.4 Subcontracts

A substantial portion of the work reported here has been performed under subcontracts from SAO to three organizations.

2.4.1 Ernst Armand and Botti Associates (EAB)

EAB has provided engineering design and analysis support to SAO in the areas of thermal, structural, and structural dynamics engineering. With the acquisition of a structural systems engineer at SAO in early fall, the EAB work has been primarily in the area of thermal engineering. EAB was selected on the basis of competitive hourly rates and unique thermal engineering expertise.

2.4.2 American Science and Engineering, Inc.

AS&E has provided support in several areas. Some early work relative to movable mirror systems was performed and incorporated in Ref. 3. AS&E was utilized to perform some of the deflection analysis summarized in Section 6.0. Two candidate

support concepts were developed by AS&E to the point where preliminary structural analysis could be performed. AS&E was selected because of general familiarity with the HEAO-B mirror and low computer costs (an overhead item at AS&E).

2.4.3 Ball Aerospace Systems Division

BASD (formerly BBRC) performed a number of studies reported in Ref. 2 and summarized in Section 10. The principal thrust of the work was to trade the Image Dissector Tube (IDT) aspect sensor against solid state alternatives. On-going IR&D results at BASD were utilized in support of these studies. BASD was selected on the basis of obvious benefit to SAO from IR&D activities and the fact that BASD has the most NASA supported experience with IDT fixed head trackers. From the start the IDT did not look attractive to either SAO or MSFC system engineers for the AXAF fine sensor application, but since it represented exsisting technology it did deserve serious consideration. BASD has an on-going vested interest in IDT sensors (Shuttle) which we felt would tend to produce as favorable an evaluation of the IDT sensor as would be objectively possible. Nevertheless, BASD concluded that the IDT is not appropriate to the AXAF application.

2.5 Future Work

Recommended future work is a continuation of the work reported herein. A Study Plan for the next extension has been prepared and is being submitted under separate cover in the context of contract renewal activities.

2.6 Other Activities

In addition to work reported here, SAO supported other activities relative to the AXAF program. Engineering work was done in response to questions raised by the AXAF Science Working Group. Presentations of representative work at SAO were prepared and made by SAO scientists and engineers to the Group. Additionally, SAO participated in the preparation of Reference 3 and prepared and made presentations to NASA Headquarters personnel.

SAO was also participant in the study group establishing the required modifications to the present MSFC test facility in order to accommodate the AXAF.

3.0 OPTICAL DESIGN STUDIES*

3.1 General

A number of candidate mirror designs for the Advanced X-ray Astrophysics Facility (AXAF) have been studied. The approximate size of the optics is limited by the available spacecraft and by engineering constraints; the latter limits are obtained partially through the preliminary mechanical calculations which have been performed, and partially from the conservative desire not to depart excessively from our experience with the HEAO-B mirrors. The candidate designs studied thus span relatively small ranges (typically of order ±25% about a base design) of the parameters which define a mirror.

3.2 Baseline Optical Design

The Baseline Optical Design is a Wolter Type I Mirror configured as shown in Figure 3-1 and as defined in Table 3-1. The mirror system consists of 6 nested parabola-hyperbola pairs, an outer optical diameter of 1.2 meters, a focal length of 33 feet, segment lengths (parabola and hyperbola) of 33 inches, and an optical surface separation sufficient to avoid vignetting rays within 20 arc minutes of the optical axis and allowing 1.5 inches for mirror walls. This results in grazing angles for the inner and outer mirrors of about 27 and 51 arc minutes respectively. The inner mirror grazing angle thus is suitable for the 7-8 keV region, whereas the outer mirror is optimum at about 3 keV. A larger diameter outer mirror would be useful for lower energies, but 1.2 m was chosen as a reasonable extension of the HEAO-B value of 0.6 meters. Similarly, a nest of 6 pairs

*The principal portion of this section is extracted from a private communication from L. Van Speybroeck of SAO to W. Kraushaar and is included in the SWG minutes of March 1968.

FIGURE 3-1

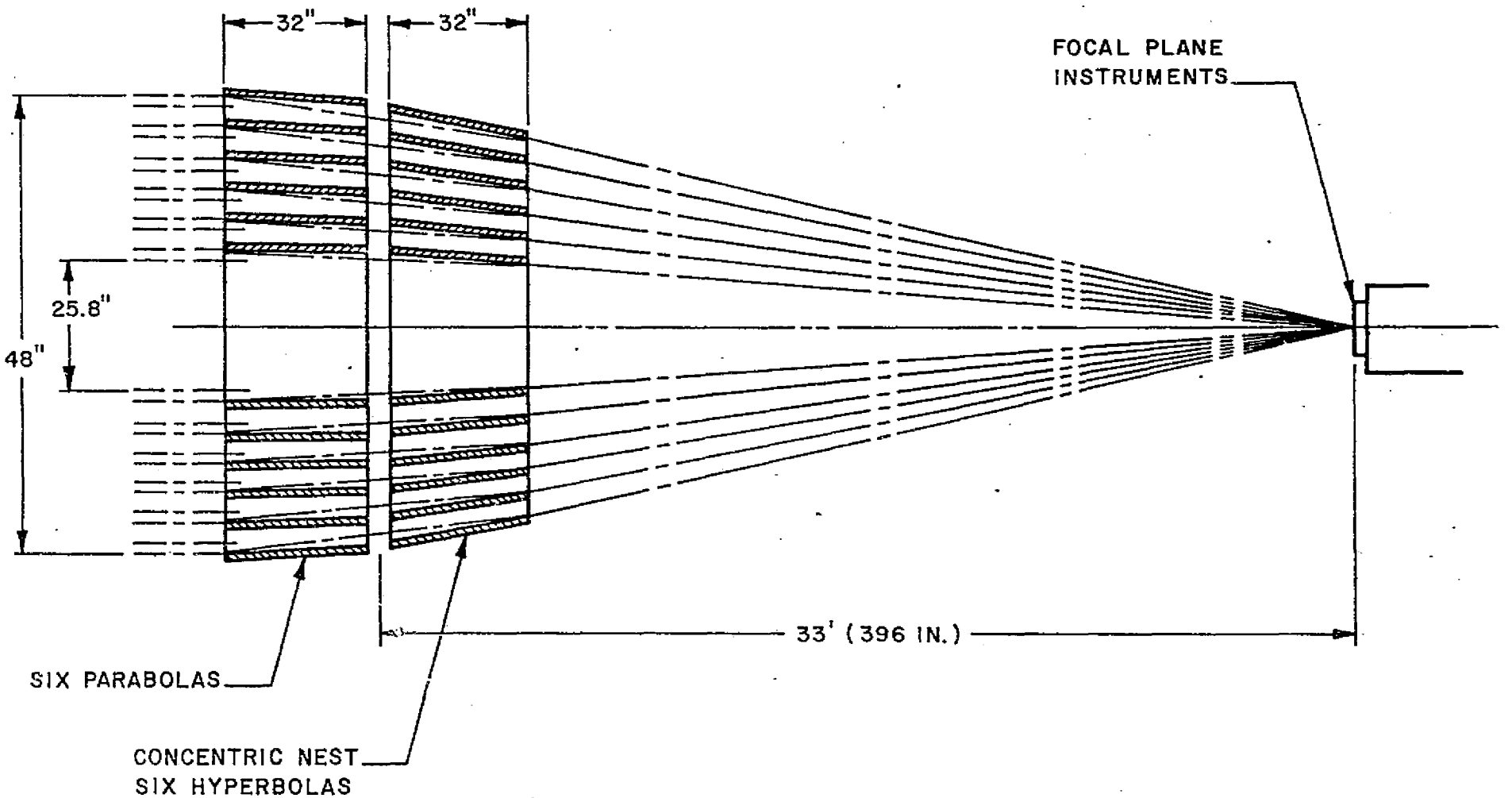

X-RAY MIRROR ASSEMBLY

BASELINE DESIGN CONCEPT – WOLTER TYPE I

TABLE 3-1

BASELINE OPTICAL DESIGN
HIGH RESOLUTION MIRROR ASSEMBLY

BASE DESIGN

No. Of Elements:	6 Nested Parabola-Hyperbola Pairs
Outer Diameter:	1.2 Meter Nominal
Focal Length:	33 Feet (10.06 m)
Segment Length:	32 Inches (.84 m)
Max. Thickness	1.5 Inches (3.81 cm)
Optical Separation:	20 Arc-Min From Axis Without Vignetting
Inner Mirror Grazing Angle:	~ 27 Arc-Min
Outer Mirror Grazing Angle:	~ 51 Arc-Min
Resolution:	0.5 Arc-Sec (Goal)

is a modest extension of the 4 pair HEAO-B design. The focal length of 33 feet was somewhat less than we originally thought could be accomodated, but is about the maximum length which is presently allowed. The segment length of 33 inches is about 50% larger than that of HEAO-B, and was made relatively shorter (compared to the diameter ratio of 2) to improve resolution off-axis. The clear field half-angle of 20 arc minutes is adequate to include the better part of the field, and actually has no effect on the final design. Finally, the wall thickness allowance of 1.5 inches was based on HEAO-B experience, and seems reasonable after preliminary mechanical calculations, but must be subjected to further engineering analysis.

3.3 Effective Area Related To Energy

The effective area in the few keV region has been emphasized while still obtaining a useful response at the energy of the Kα line of single electron ion. The baseline design is based on these critiera. It is suitable for planning purposes at this stage of the program. The design has not, however, been "fine-tuned" to optimize a specific performance criterion. The final design will include modifications for both mechanical requirements as these become known quantitatively, and minor variations which will slightly improve performance.

The mirrors which have been studied are all two-surface figures of revolution for fundamental reasons. The minimum number of reflections is desired because of reflection and scattering losses, and two is the minimum number of surfaces which will form an image over an extended field at the small grazing angles required for efficient X-ray reflection.

The effective area for such mirrors is approximately proportional to the product of the reflection efficiency squared,

the grazing angle squared, the focal length, and the segment length. The efficiency enters twice because of the two surfaces (the grazing angles at both surfaces, and therefore the efficiencies, are approximately the same because this also maximizes the collecting area for a given amount of surface to be polished). The projected area is approximately proportional to the segment length times the grazing angle, and to the radius, which is proportional to the focal length times the grazing angle, thus accounting for the remaining factors. It is useful, therefore, to examine the product (efficiency x grazing angle) squared; this is shown for the energy range 2-9 keV in Figures 3-2 and 3-3 for nickel and gold respectively. Nickel was chosen as the most suitable surface material in the mid-atomic number region, which yields superior reflection efficiencies in the few keV region. gold was selected to represent the high atomic number materials, which give better reflection efficiencies at higher energies, but it is probable that platinum will be substituted for gold in the final mirror because of superior evaporation properties.

There is an optimum angle for any energy; the effective area is limited by the grazing angle for small angles, and by the reflection efficiency for larger angles. The theoretical approximate optimum and half power angles for some wavelengths are given in Table 3-2.

Thus, to maximize the effective area for a fixed focal length in the energy range 3 to 7 keV it is useful to have grazing angles between about 25 and 60 arc-min. Scattering, which is less for smaller grazing angles, decreases the values of the optimum angles.

3.4 Mirror Parametric Studies

Using computerized ray tracing techniques developed at

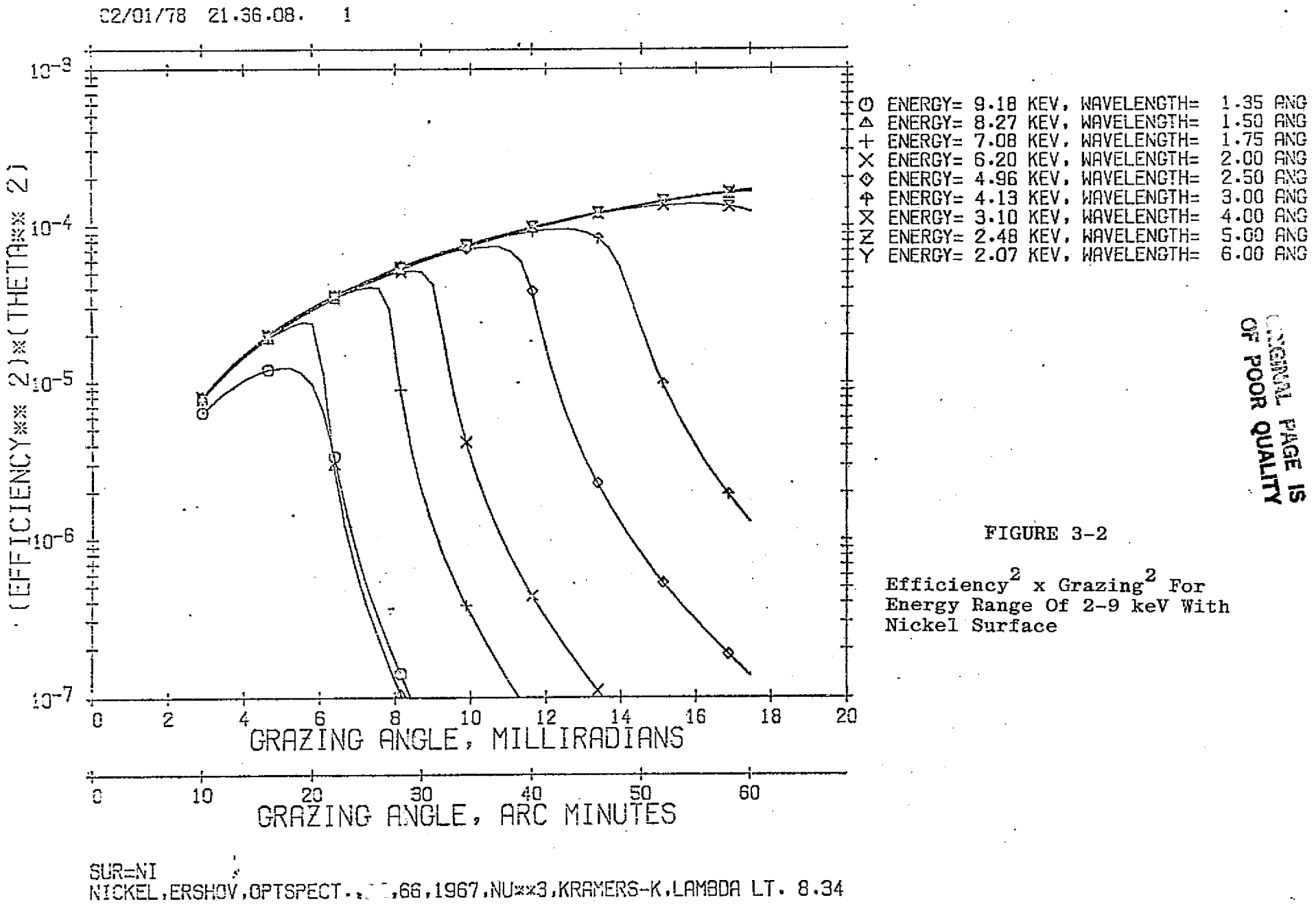

FIGURE 3-2

Efficiency^2 x Grazing^2 For Energy Range Of 2-9 keV With Nickel Surface

ORIGINAL PAGE IS OF POOR QUALITY

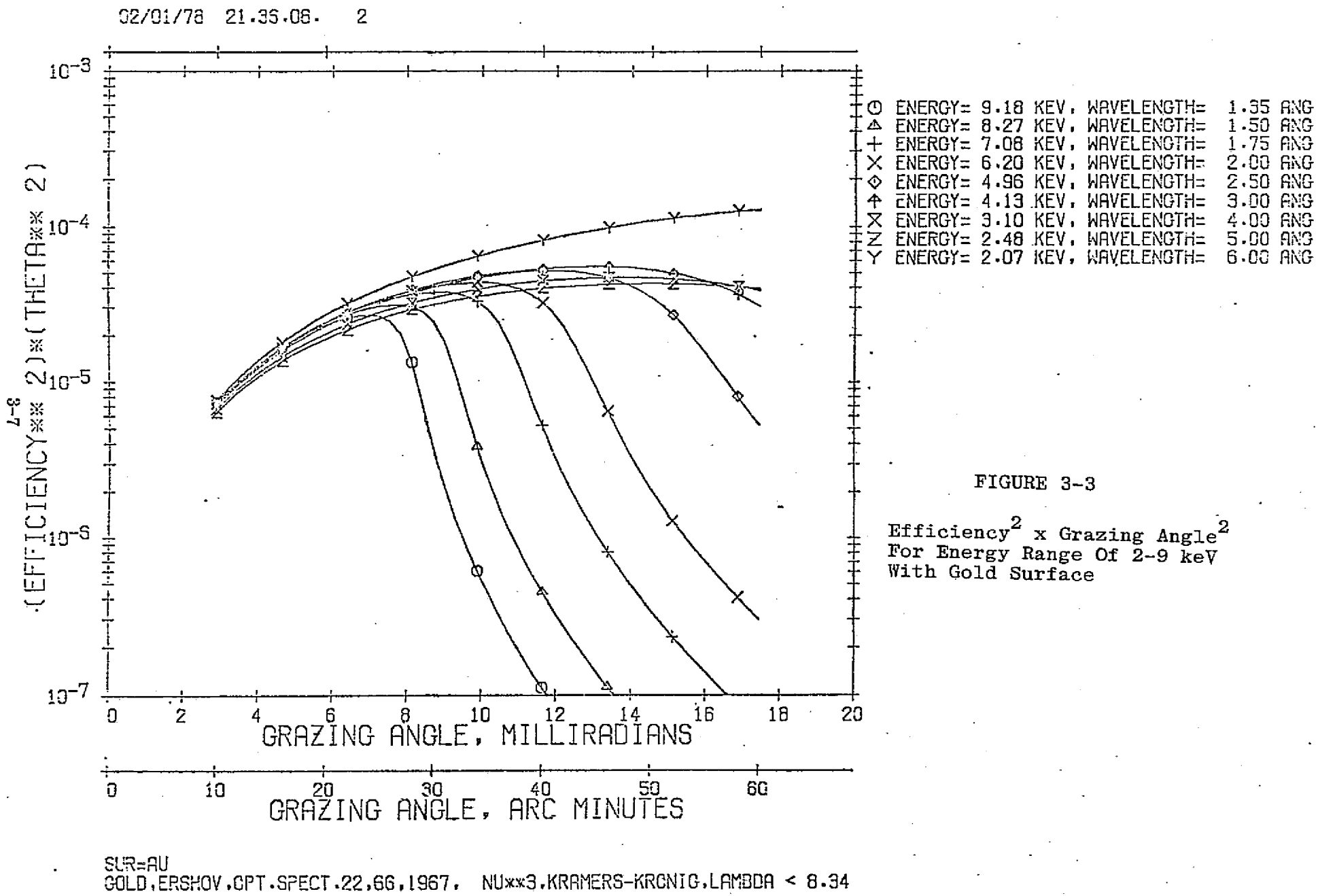

FIGURE 3-3

Efficiency^2 x Grazing Angle^2
For Energy Range Of 2-9 keV
With Gold Surface

TABLE 3-2

FOR EACH ENERGY THERE IS AN OPTIMUM GRAZING ANGLE

ANGLES, ARC-MINUTES

(A)	E (keV)	Ni θ1/2,low	Ni θmax	Ni θ1/2,high	Au θ1/2,low	Au θmax	Au θ1/2,high
1.5	8.27	12	19	21	15	26	31
1.75	7.09	16	25	30	17	30	37
2.0	6.20	18	29	35	19	34	42
2.5	4.96	22	36	40	21	40	52
3.0	4.13	26	42	48	23	45	61
4.0	3.10	31	55	65	22	47	70
5.0	2.48	37	66	81	22	49	80
6.0	2.07	41	76	96	34	66	90

SAO, the mirror parameters including surface material, radius, focal length, segment length and allowable wall thickness (which affects the radial spacing of elements) were varied around the baseline design. The effects of these variations are shown in graphs and discussed herein. The graphs describe each mirror system by a mirror geometric identifier using only the first two significant digits of the design quantities in these very mixed units, thus a 1.2 meter outer optical diameter mirror having a 33 ft. focal length, a 39 inch segment length, 20 arc-minute clearance angle, and 1.5 inch wall thickness allowance would be called 1233392015 in the graphs.

3.4.1 Effects Of Surface Material

A comparison of the properties of nickel and gold shows the following:

1. Gold is markedly superior for energies greater than an upper limit (Eu) which depends upon angle, but is always less than the nickel K-edge at about 8 keV.

2. Nickel is markedly superior for energies between Eu and the gold M edges (Em, Au) at about 2.3 keV. For the mirrors described in Fig. 3-4, Eu ≈ 5 keV.

3. Gold is somewhat superior between Em, Au and the nickel L edges (Eℓ, Ni) at about 1 keV.

4. Nickel is somewhat superior below Eℓ, Ni.

The above comparison suggests that a mirror utilizing a high atomic number surface on its inner surfaces to obtain high energy response, and an intermediate atomic number material on

FIGURE 3-4

Effect Of Surface Materials

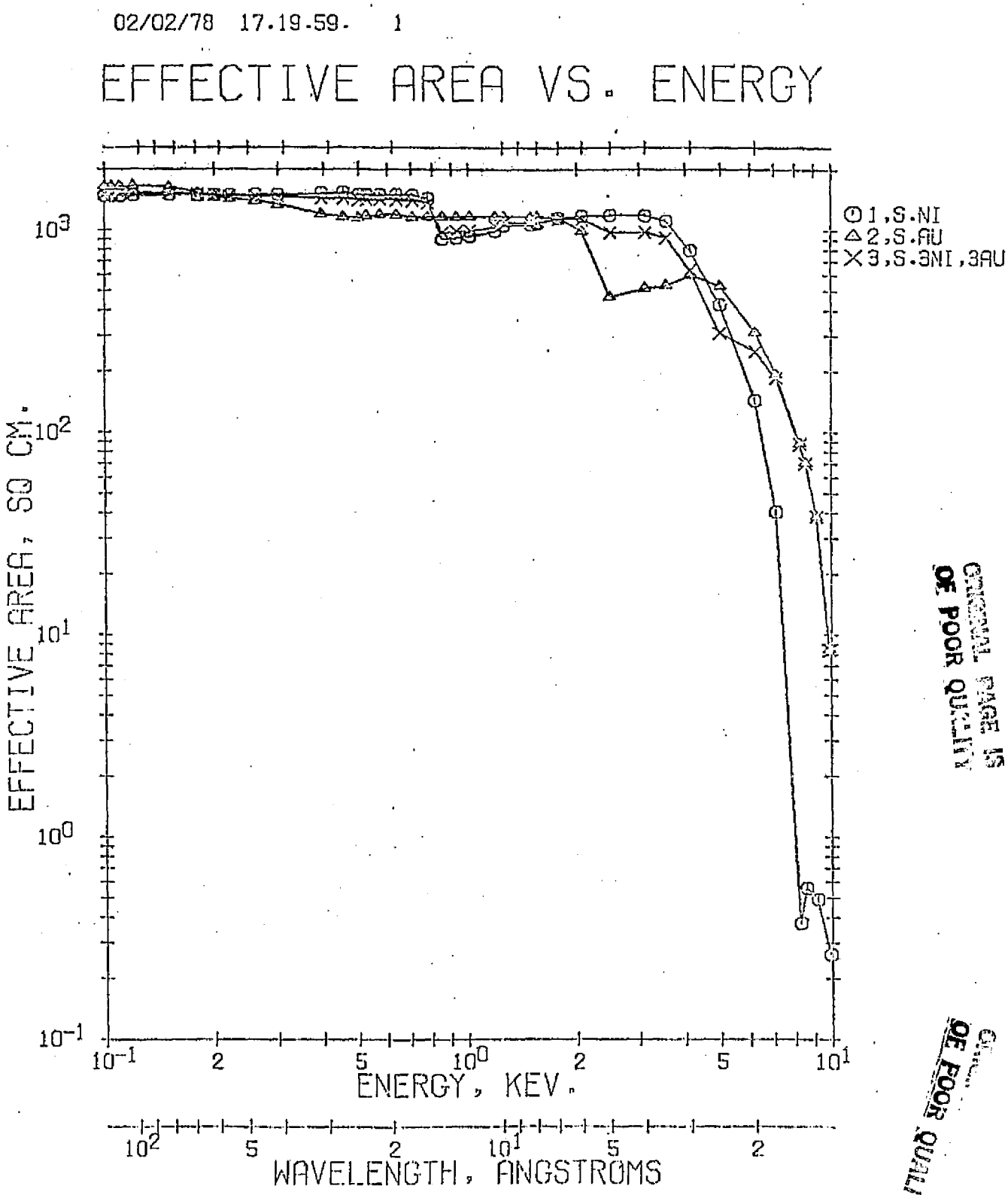

COM TERMS
MDES.1233332015,APT.=1233332015
M 1-6

ORIGINAL PAGE IS OF POOR QUALITY

its outer surfaces to maximize response at other energies might be superior to a mirror coated entirely with one or the other material. The effective area in the iron K-α energy region for gold surfaces having grazing angles larger than 37 arc minutes is less than half that obtained at the optimum angle, and so there is little loss at higher energies if the surfaces having grazing angles larger than this value are nickel. Similarly, there is little loss at lower energies if surfaces having grazing angles of less than 37 arc-minutes are gold.

The baseline design has grazing angles of approximately 27, 32, 36, 41, 46 and 51 arc-minutes, and so for this design the optimum choice of surface materials for many applications is gold or platinum on the inner three and nickel on the outer three. The effects of choosing this mixture vs. all gold or all nickel is shown in Figure 3-4; in most energy regions the mixture gives approximately the same area as the better of the two single material choices. The actual mixture eventually will be chosen by integrating the candidate mirror responses with typical source spectra, but at this point in the program it is reasonable to base planning on the properties of assemblies having 3 inner surfaces of gold or platinum and 3 outer surfaces of nickel. All subsequent comparisons in this preliminary analysis are based upon this choice.

3.4.2 Effect Of Focal Length Variations

The effects of decreasing the focal length to 28 feet and increasing it to 39 feet while other design parameters are held fixed are shown in Figure 3-5. In general, increasing the focal length decreases typical grazing angles, and therefore decreases the effective area at lower energies and increases it at higher energies. There is a negligible effect on mirror resolution.

FIGURE 3-5

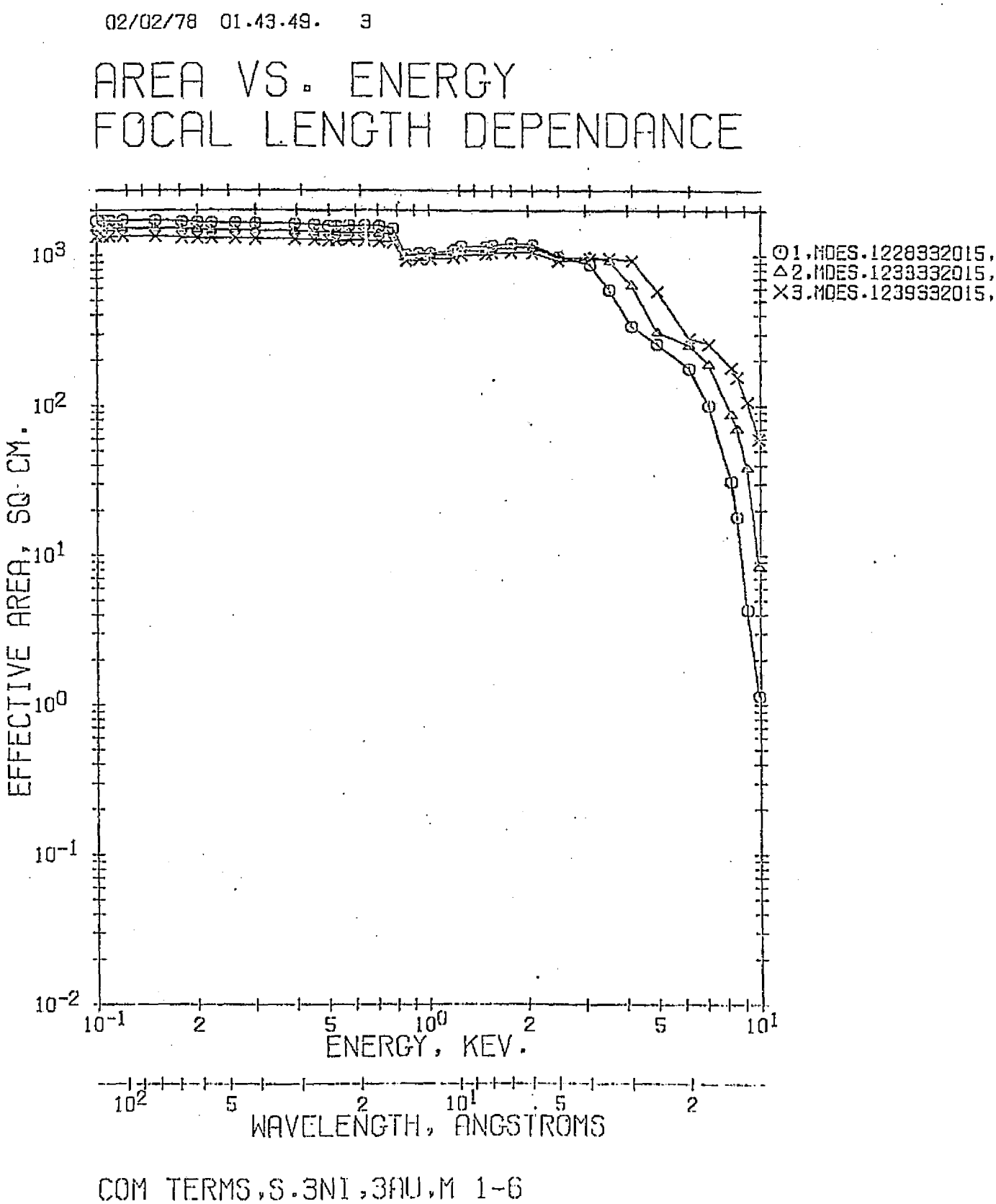
02/02/78 01.43.49. 3
AREA VS. ENERGY
FOCAL LENGTH DEPENDANCE
EFFECTIVE AREA, SQ CM.
ENERGY, KEV.
WAVELENGTH, ANGSTROMS
1.MOES.1228332015,
2.MOES.1233332015,
3.MOES.1239332015,
COM TERMS,S.3NI,3AU,M 1-6

1. Shorter (28 ft) focal length. This results in 10% or less increase in effective area for E < 3 keV. It results in a loss of 46% of the area at 7 keV, and 54% of the area at 8 keV. It also will cause a loss of angular resolution for many detectors because of the smaller focal plane scale. It is definitely an undesirable direction of design modifications.

2. Longer (39 ft) focal length. This results in 10% or less decrease in effective area below 3 keV, a 37% increase as 7 keV, and a 100% increase at 8 keV. It also would increase the focal plane scale. We should consider increasing the focal length if permitted by later vehicle designs.

3.4.3 Effect Of Radius Variations

The effect of varying the radius along is shown in Figure 3-6. This is, unfortunately, a misleading representation of the effects of varying the radius because it assumes that other parameters would remain fixed, whereas in fact, if the radius increased, the mirror spacing would also be increased to avoid the indicated loss at higher energies. The figure indicates that going to 1.5 meters from 1.2 would increase the effective area by about 50% at lower energies, and would drastically decrease the area at higher energies. In fact, by increasing the mirror spacing the same area would be essentially retained at higher energies but a gain of only 30% would be obtained at lower energies.

Decreasing the radius to 1 meter causes a loss of about 30% of the area below about 3 keV and does not substantially improve the area until E ≃ 7.5 keV; this gain at higher energies

FIGURE 3-6

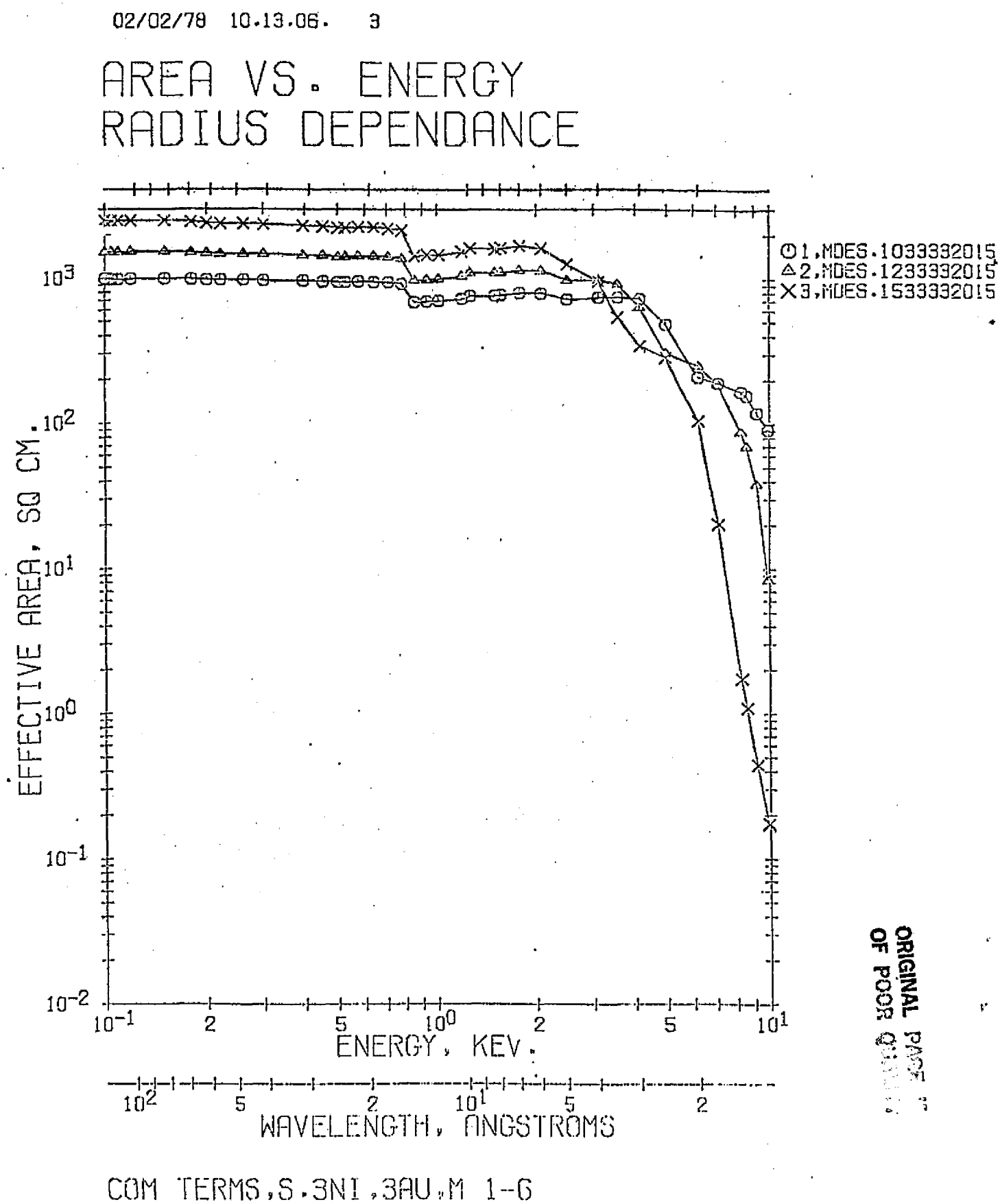

ORIGINAL PAGE IS
OF POOR QUALITY

also is an illusion, for if an increase in the area at E > 7.5 keV is required it can be accomplished by increasing the spacing of the nominal design.

There is about 25% resolution change for either of the radii considered, the smaller radius resulting in better resolution. These effects are shown in Figure 3-7.

Summary. Increase in outer radius and mirror spacing will improve mirror performance and should be considered in the context of cost and vehicle constraints.

3.4.4 Effect Of Segment Length Variation

Effective area and resolution both are approximately proportional to segment length; the effects are shown in Figures 3-8 and 3-9 for segment lengths of 27, 33 and 39 inches. There also are mechanical limits to segment length which are not known quantitatively at this time.

The eventual segment length probably will be near that of the baseline design. The aft diameter of the inner hyperboloid of the baseline design is 23 inches, and the polishing and support properties of mirrors much longer than 1-1/2 diameters are not favorable.

3.4.5 Effect Of Element Separation (Wall Thickness)

The effect of varying element separation is shown in Figure 3-10 for allowed wall thicknesses of 1.0, 1.5, and 2.0 inches. There is a negligible effect upon angular resolution.

FIGURE 3-7

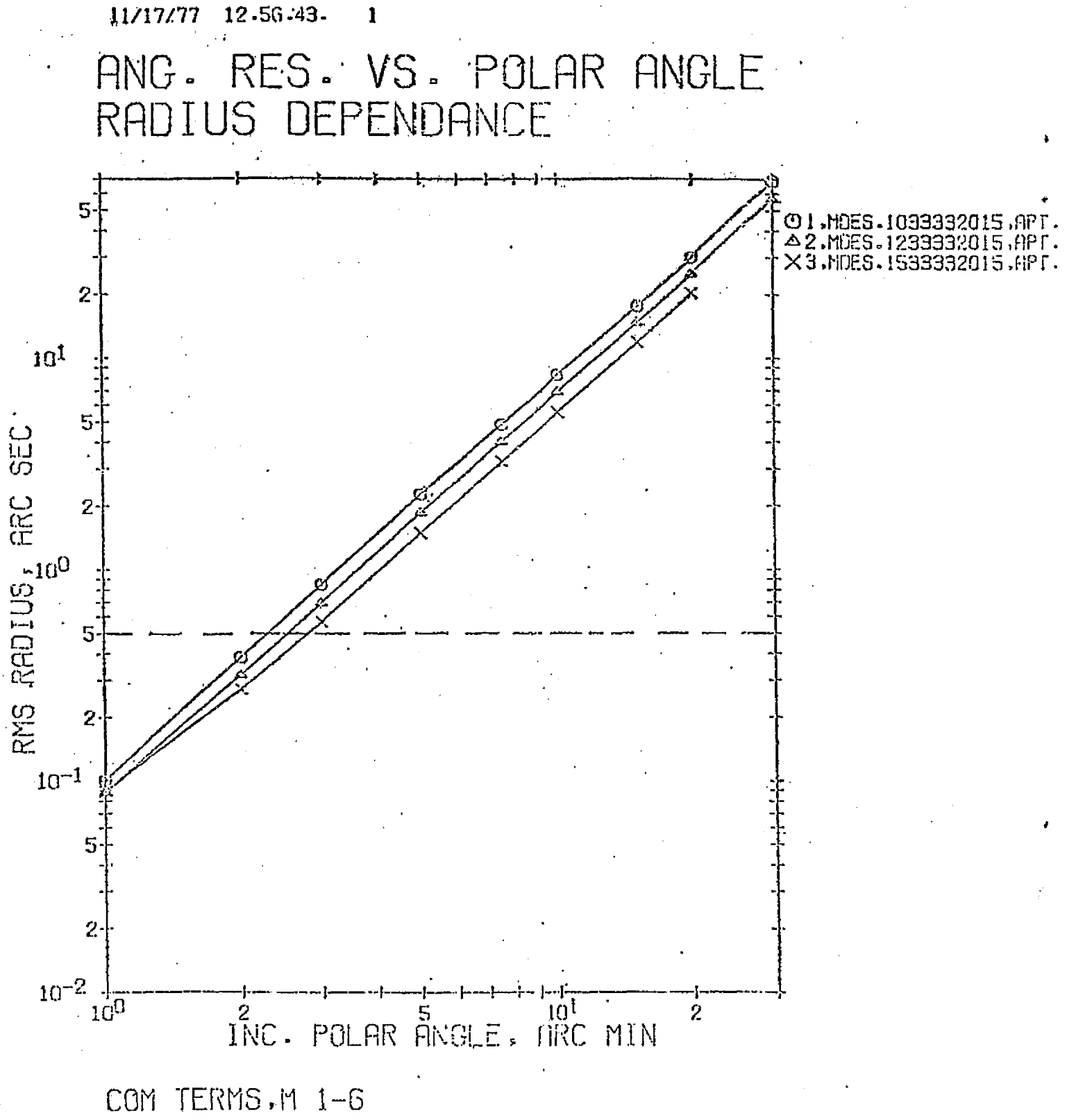
11/17/77 12.56.43. 1
ANG. RES. VS. POLAR ANGLE
RADIUS DEPENDANCE
1.MDES.1033332015.APT.
2.MDES.1233332015.APT.
3.MDES.1533332015.APT.
RMS RADIUS, ARC SEC
INC. POLAR ANGLE, ARC MIN
COM TERMS.M 1-6

FIGURE 3-8

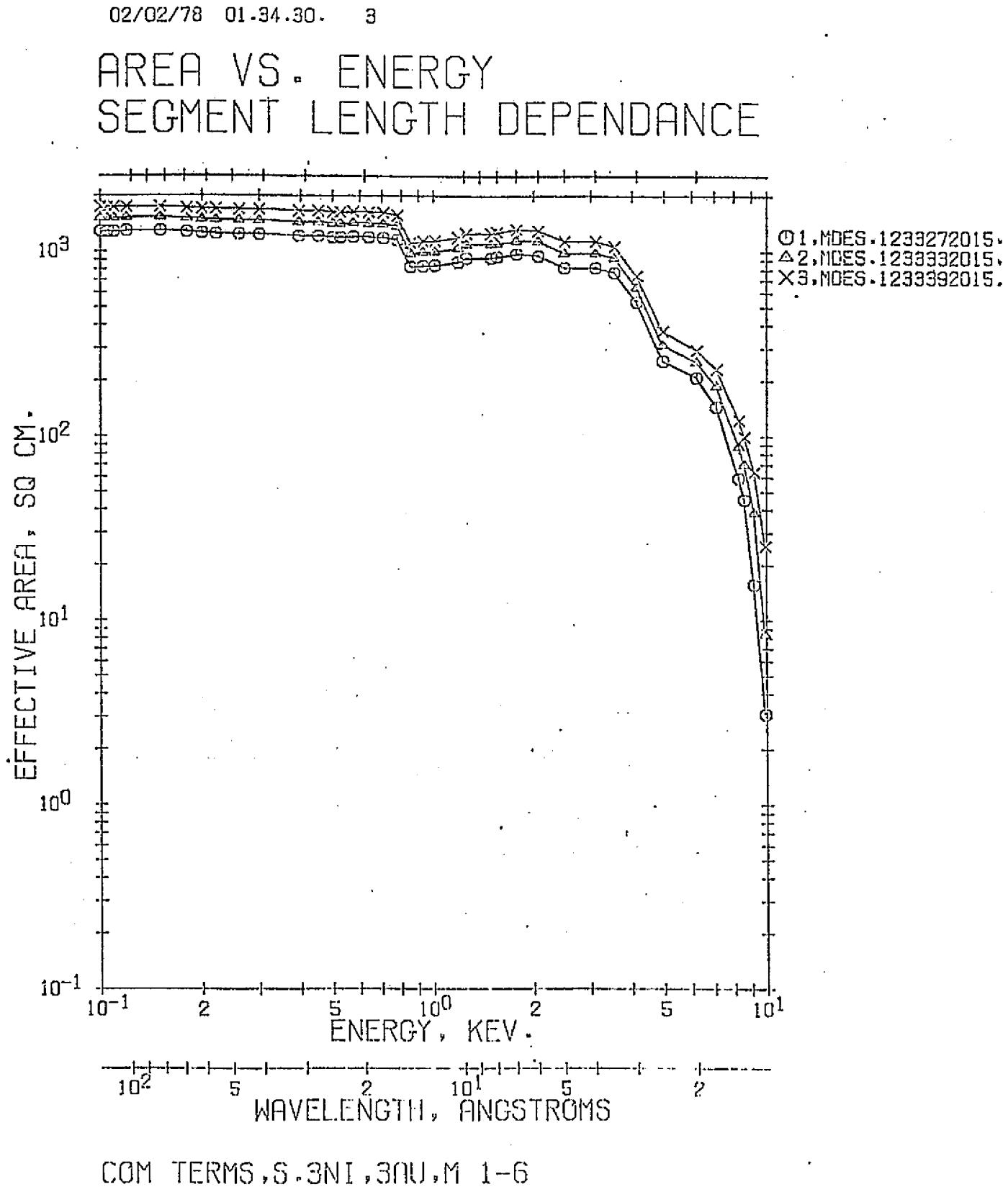
02/02/78 01.34.30. 3
AREA VS. ENERGY
SEGMENT LENGTH DEPENDANCE
1.MDES.1233272015.
2.MDES.1233332015.
3.MDES.1233392015.
EFFECTIVE AREA, SQ CM.
ENERGY, KEV.
WAVELENGTH, ANGSTROMS
COM TERMS,S.3NI,3AU,M 1-6

FIGURE 3-9

ORIGINAL PAGE IS
OF POOR QUALITY

11/17/77 13.05.20. 1

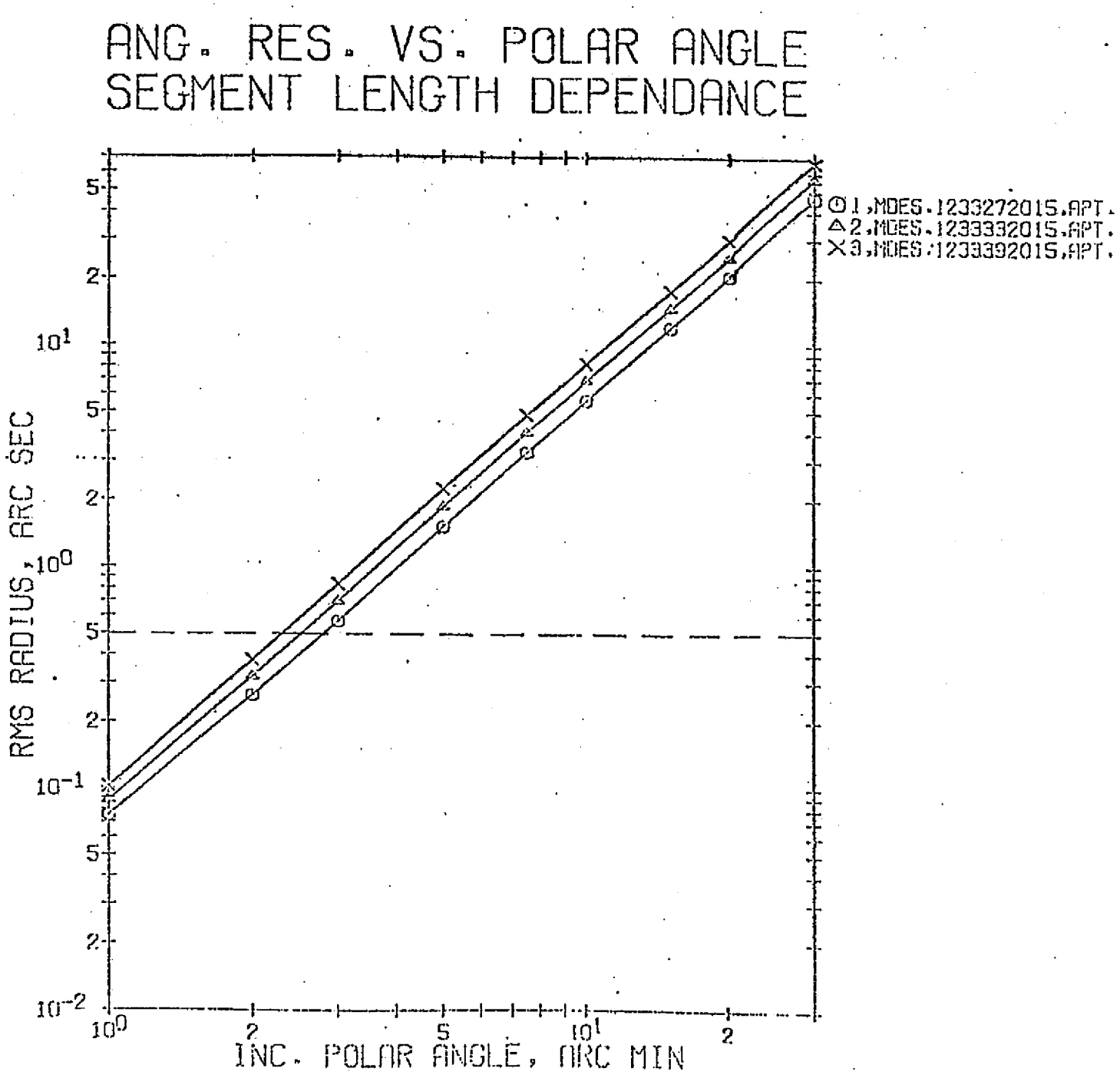

COM TERMS,M 1-6

FIGURE 3-10

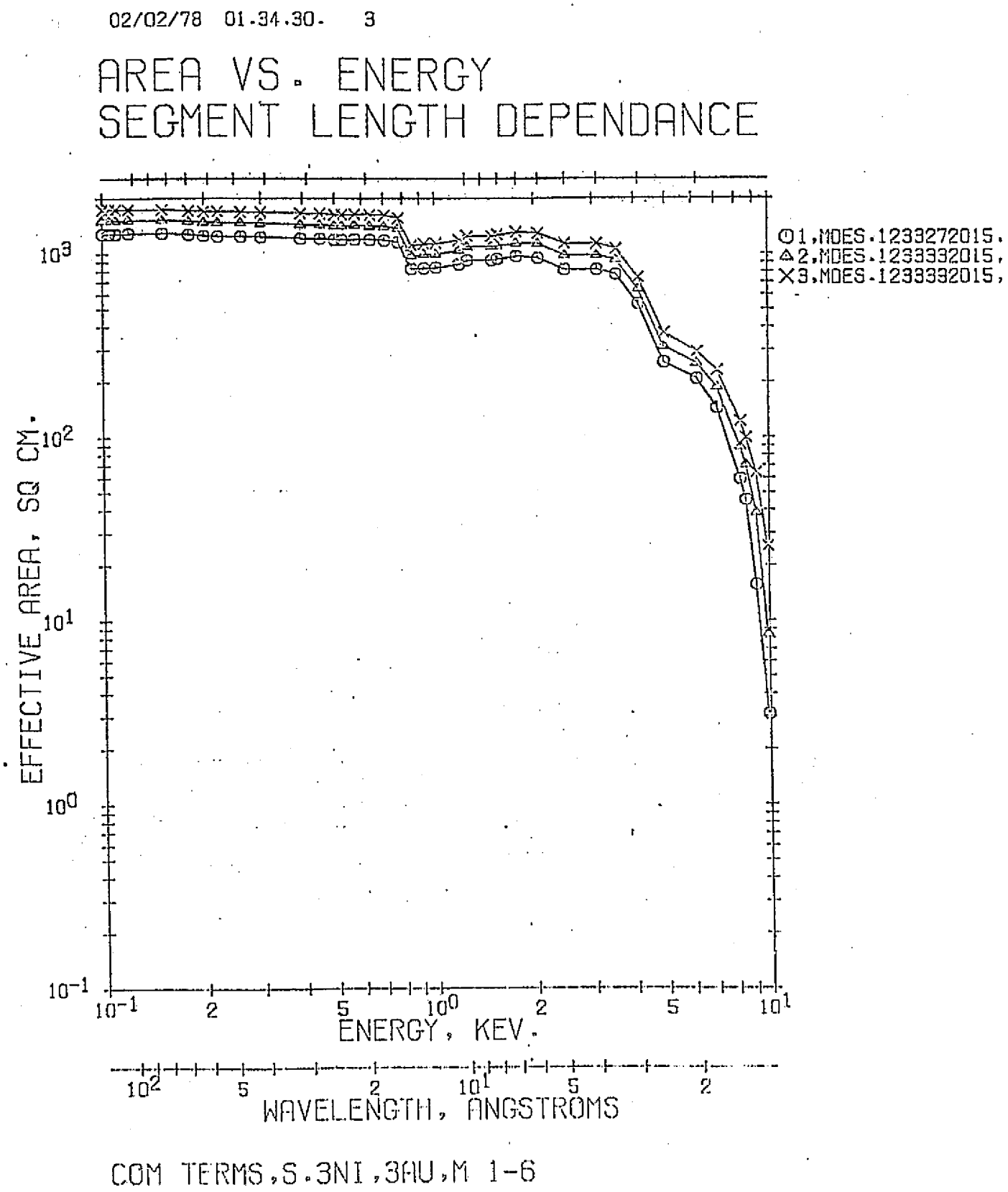
02/02/78 01.34.30. 3
AREA VS. ENERGY
SEGMENT LENGTH DEPENDANCE
⊙1,MOES.1233272015.
△2,MOES.1233332015.
×3,MOES.1233332015.
EFFECTIVE AREA, SQ CM.
ENERGY, KEV.
WAVELENGTH, ANGSTROMS
COM TERMS,S.3NI,3AU,M 1-6

The effects on area are:

1. Larger separation. This results in about a 10% loss below 4 keV, a 10% gain between 4 and 7 keV, and a 46% gain at 8 keV.

2. Smaller separation. This results in about a 10% gain below 4 keV, a 34% loss at 7 keV, and an 80% loss at 8 keV. The mirror also would be more difficult to fabricate.

Summary. The element spacing should not be decreased. There is no reason to increase it from baseline radius and focal length except for possible structural or manufacturing reasons.

3.5 Baseline Off-Axis Properties

The effective areas vs. energy at incident angles of 0, 10, 20, and 30 arc minutes are shown in Figure 3-11. The half-power angle is smaller for the higher energies because these rays are reflected from the inner surfaces; the half power angles are about 27 arc-minutes at low energies, and about 12 arc-minutes at the highest energies.

The rms blur circle radii for flat and optimally curved focal planes are shown in Figure 3-12. The image distribution is not completely described by the rms radius; in fact, the FWHM of the central peak varies quite slowly with incident polar angle but the fraction of the power within the FWHM decreases with angle. The practical consequence of this is that small but bright features can be recognized as such even for large incident angles.

The changes to be considered to the baseline design

FIGURE 3-11

Baseline Off-Axis Response

02/03/78 15.51.04. 1

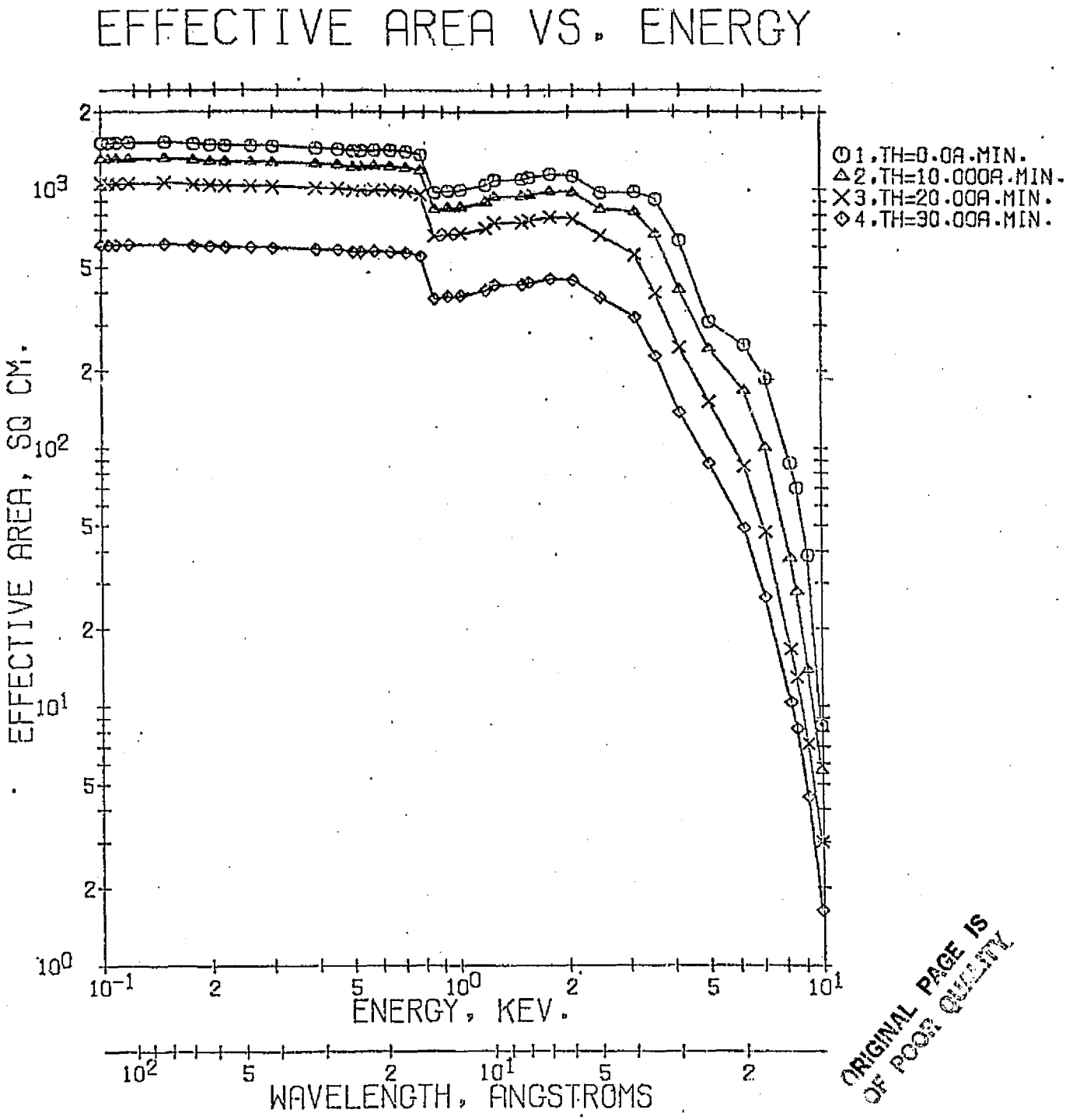

ORIGINAL PAGE IS OF POOR QUALITY

COM TERMS
MDES.1233332015,APT.=1233332015
S.3NI,3AU,M 1-6,DS=INF,PHI=0.0DEG.

FIGURE 3-12
Baseline Off-Axis Response

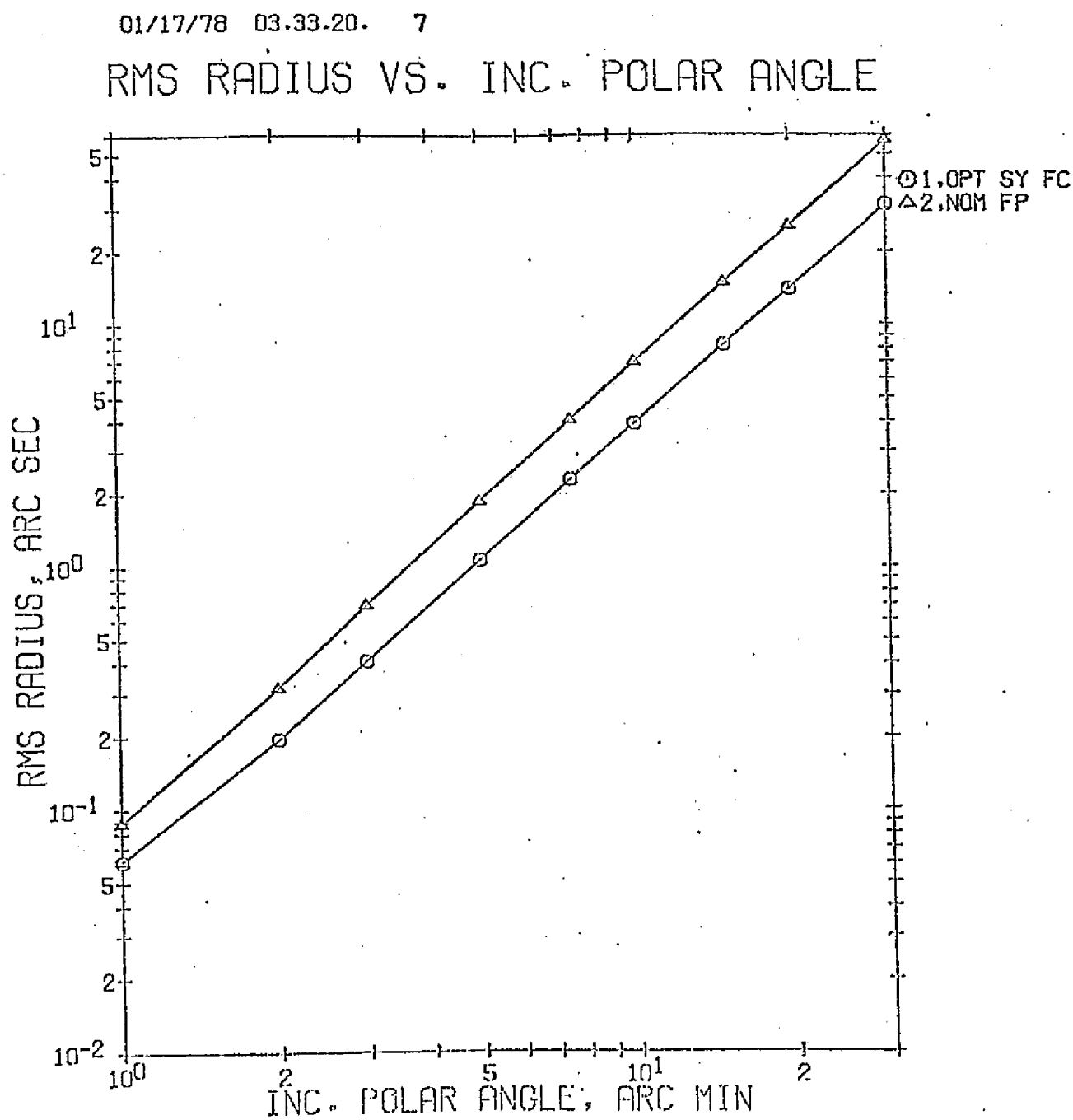

COM TERMS
MDES.1233332015,APT.=1233332015
M 1-6

largely depend upon the ultimate vehicle and fiscal constraints. It would be useful to increase the focal length (to > 33 feet) and the radius of the outer mirrors (to > 1.2 meters). The inner mirror radius should stay fixed, or possibly be decreased slightly. The segment length should be increased if permitted by mirror stiffness requirements.

3.6 Scattering Effects

The Beckmann model of the scattering distribution was extended to the two reflection conical geometry typical of X-ray telescopes assuming a gaussian auto-correlation function. The fit to HEAO-B data, using measured values of roughness and an estimated value of 0.05 mm for the correlation length, agreed qualitatively, although not exactly, with the scattering which was observed. The model will be improved by making a more realistic approximation to the auto-correlation function, but can be used in its present form to indicate the scale of scattering effects.

The results (Figures 3-13 to 3-15) show that a 15Å surface, which we consider a reasonable expectation, will have less than 24% loss from the central image for E < 2 keV, but only about 20% remaining in the central image at 7 keV. The angular scale of the scattering is small, however, and for most experiments much of the energy is not lost; for example, about 50% of the energy at 7 keV will be within 10 arc-seconds.

The scattering will be decreased for smaller grazing angles, thus favoring changes in design towards longer focal lengths and smaller radii.

FIGURE 3-13

Scattering Effects For:

Effective Area in Image Center
RMS Roughness = 0, 10, 15, 20A
Correlation Length = 0.05 MM.

ORIGINAL PAGE IS OF POOR QUALITY

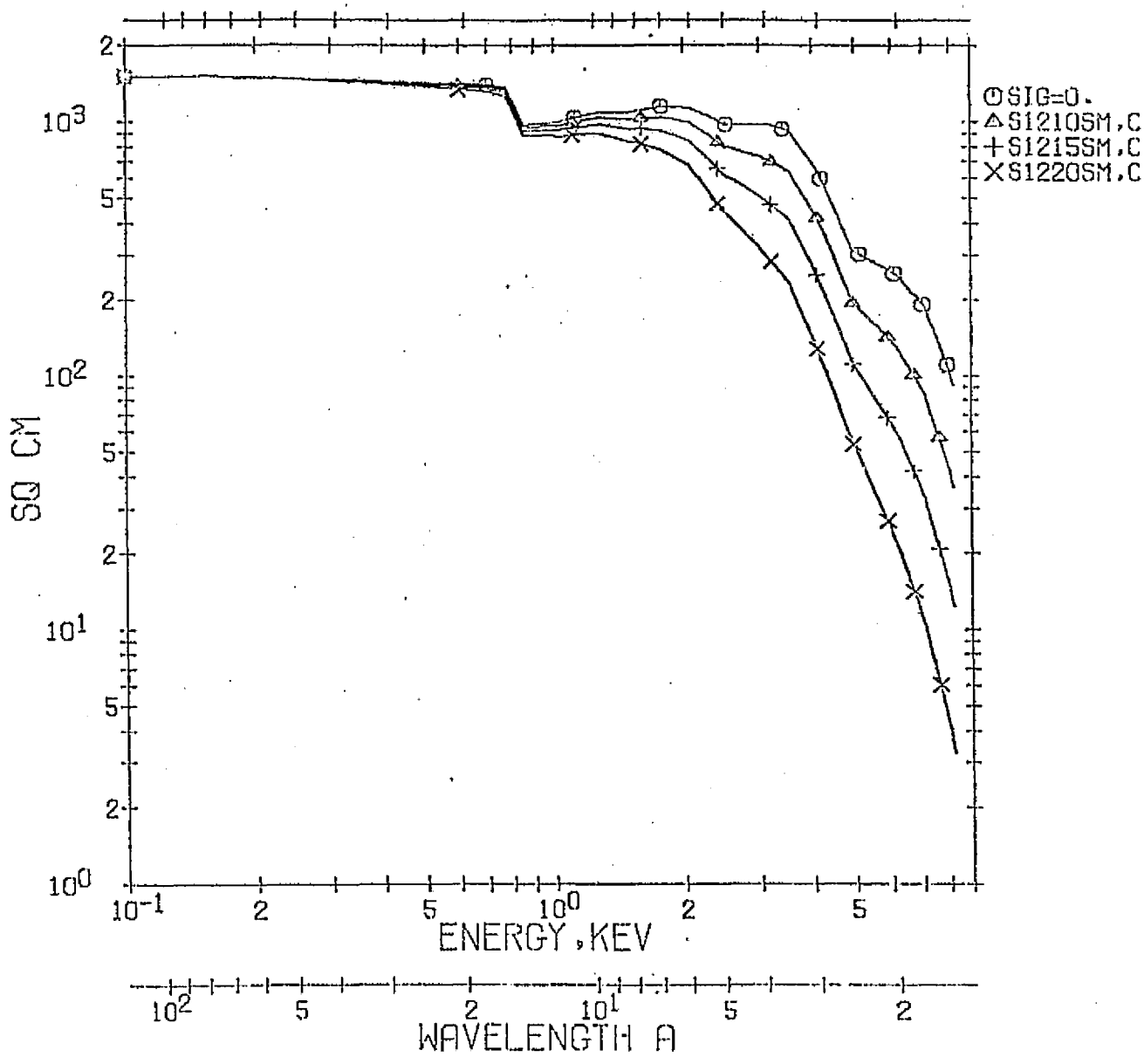

MIRROR
1233332015,3NI,3AU

FIGURE 3-14

Scattering Effects For:

Effective Area in 10 ARC SEC Radius
RMS Roughness = 0, 10, 15, 20A
Correlation Length = 0.05 MM.

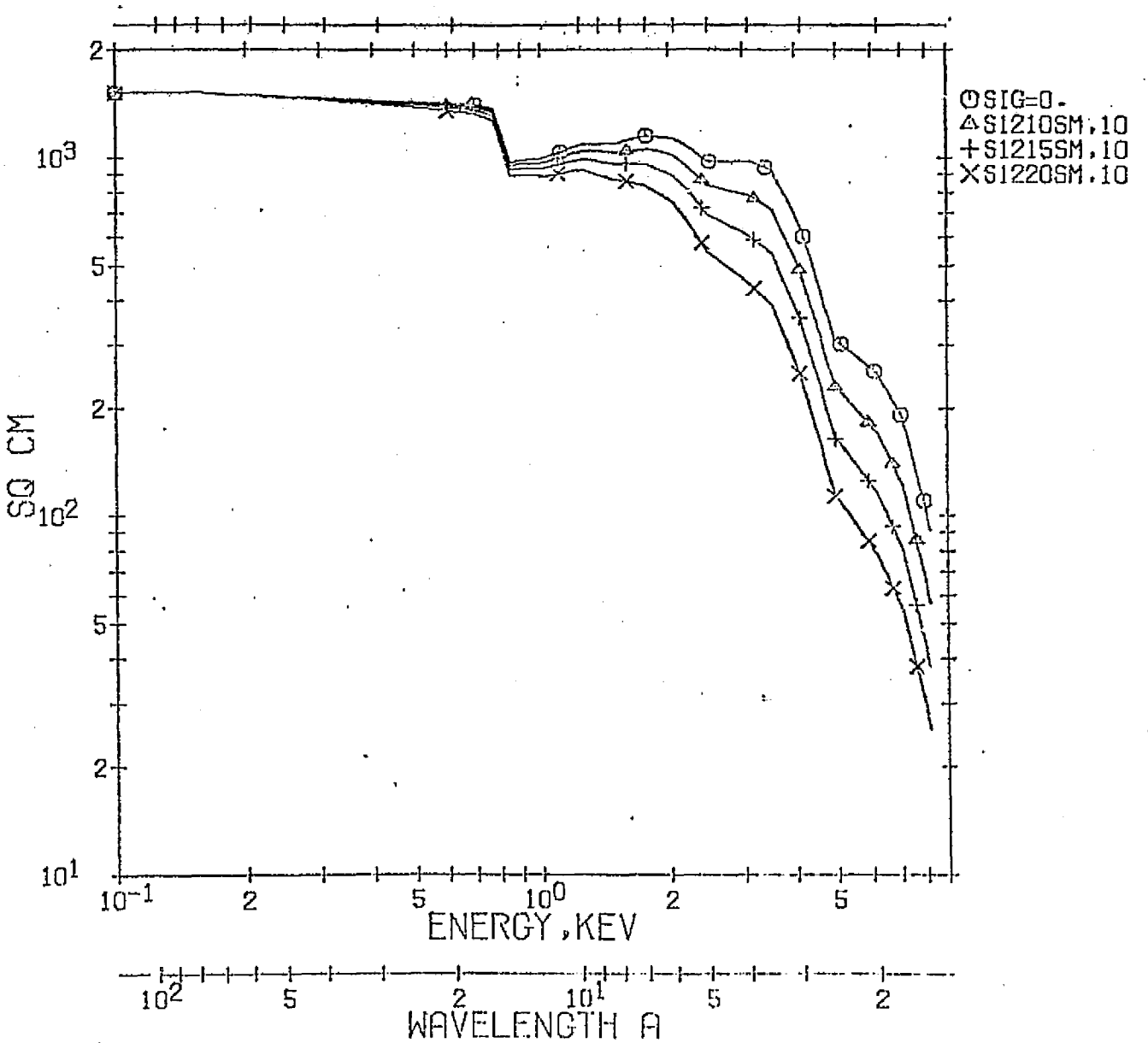

MIRROR
1233332015,3NI,3AU

FIGURE 3-15

Scattering Effects For:

Effective Area in 10 ARC SEC Radius

RMS Roughness = 0, 10, 15, 20A

Correlation Length = 0.1 MM.

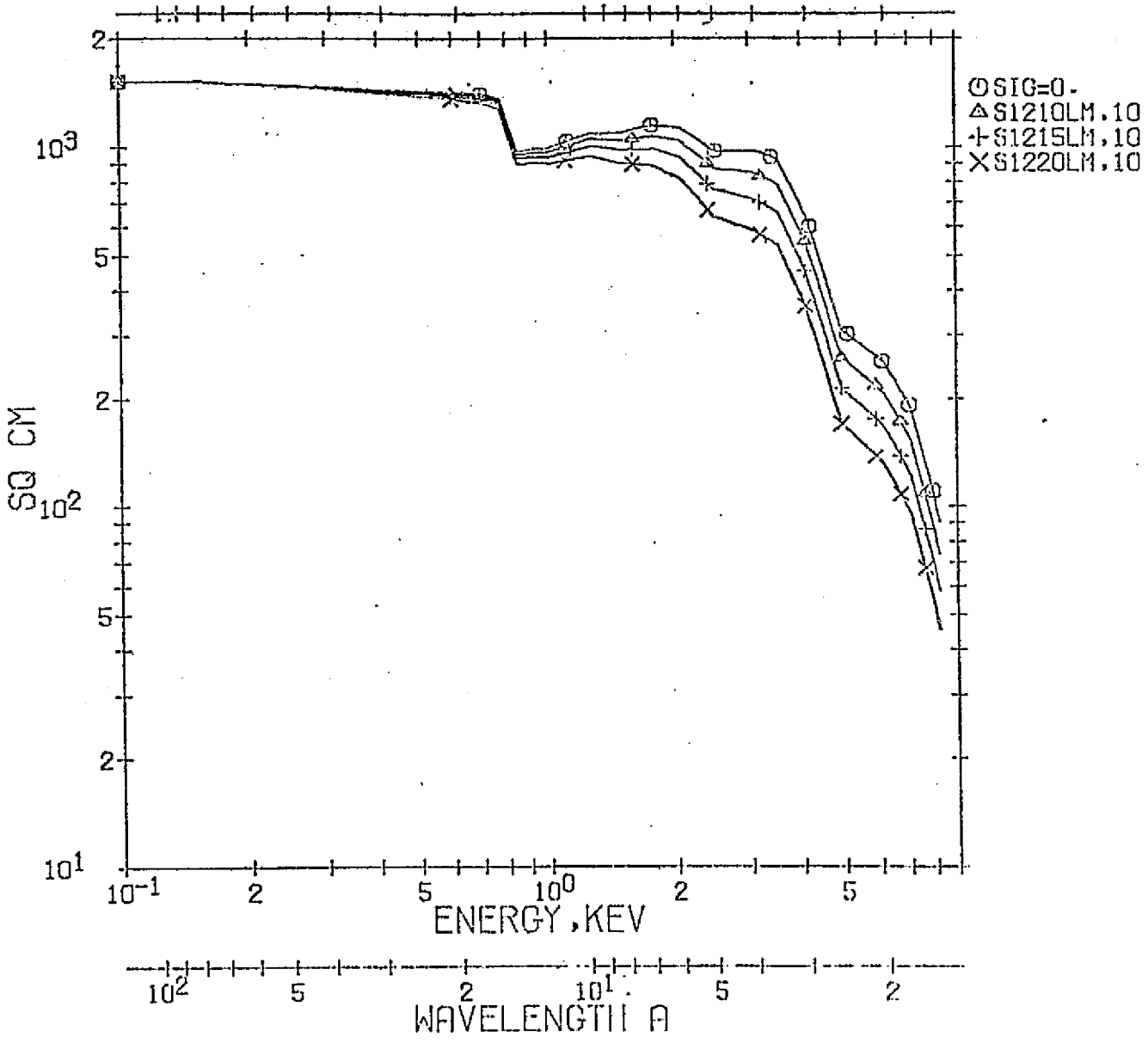

MIRROR
1233332015,3NI,3AU

4.0 MIRROR SUPPORT CONCEPTS

4.1 General

The success of the HEAO-2 mirror concept in terms of optical/X-ray test, mechanical and thermal test, and subsequent on-orbit performance provides an excellent basis for the development of the AXAF mirror assembly design. It also creates a temptation to merely "scale up" the HEAO design directly and concentrate on other studies. This is not as straight forward as it appears initially when both the improved resolution and increased size of AXAF with respect to HEAO-2 are considered. The size differences are shown graphically in Figures 4-1 and 4-2.

There are four principal criteria to be considered. These are:

1. Will the mirror survive mechanical and thermal loads during launch, re-entry, relaunch and orbital operations and maintain its alignment.

2. Can the mirror performance be tested horizontally with X-rays in a meaningful way.

3. Is the design such that support fixturing during alignment, assembly, and horizontal test permits reliable prediction of 0 g performance.

4. Does the design permit assembly and alignment to the desired degree.

In this section two basic concepts are examined which illustrate the two general classes of mirror assembly systems that have been or are being studied. It is important to recognize the conceptual difference. In the Cantilevered Support Cylinder (see Figure 4-3a) the front and rear mirror elements are cantilevered from a

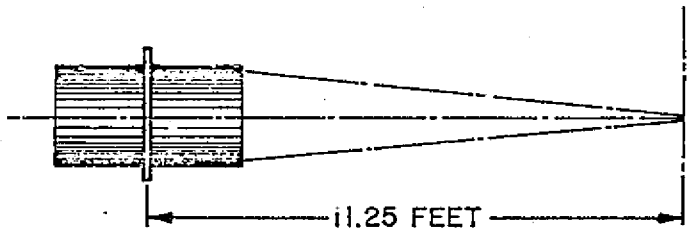

HEAO-B

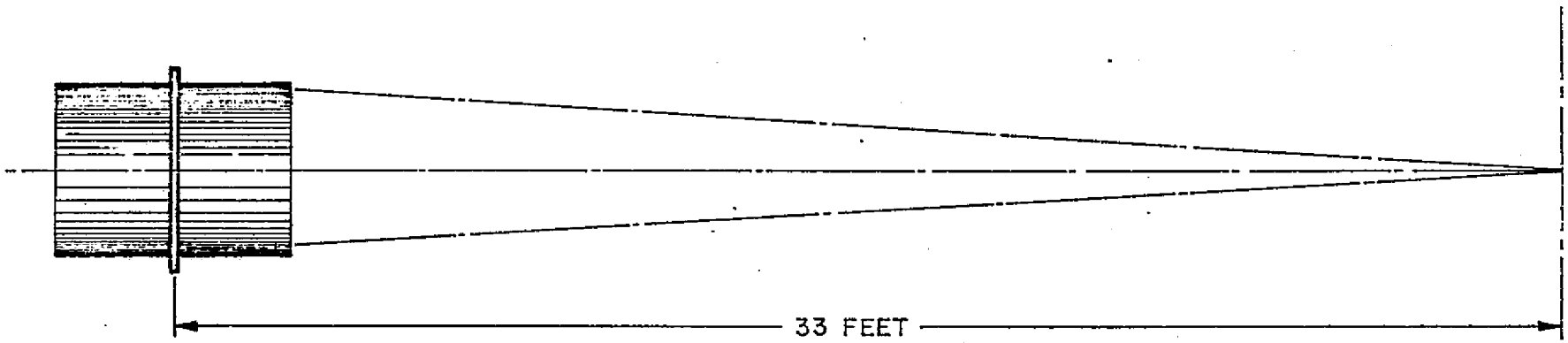

AXAF

FIGURE 4-1

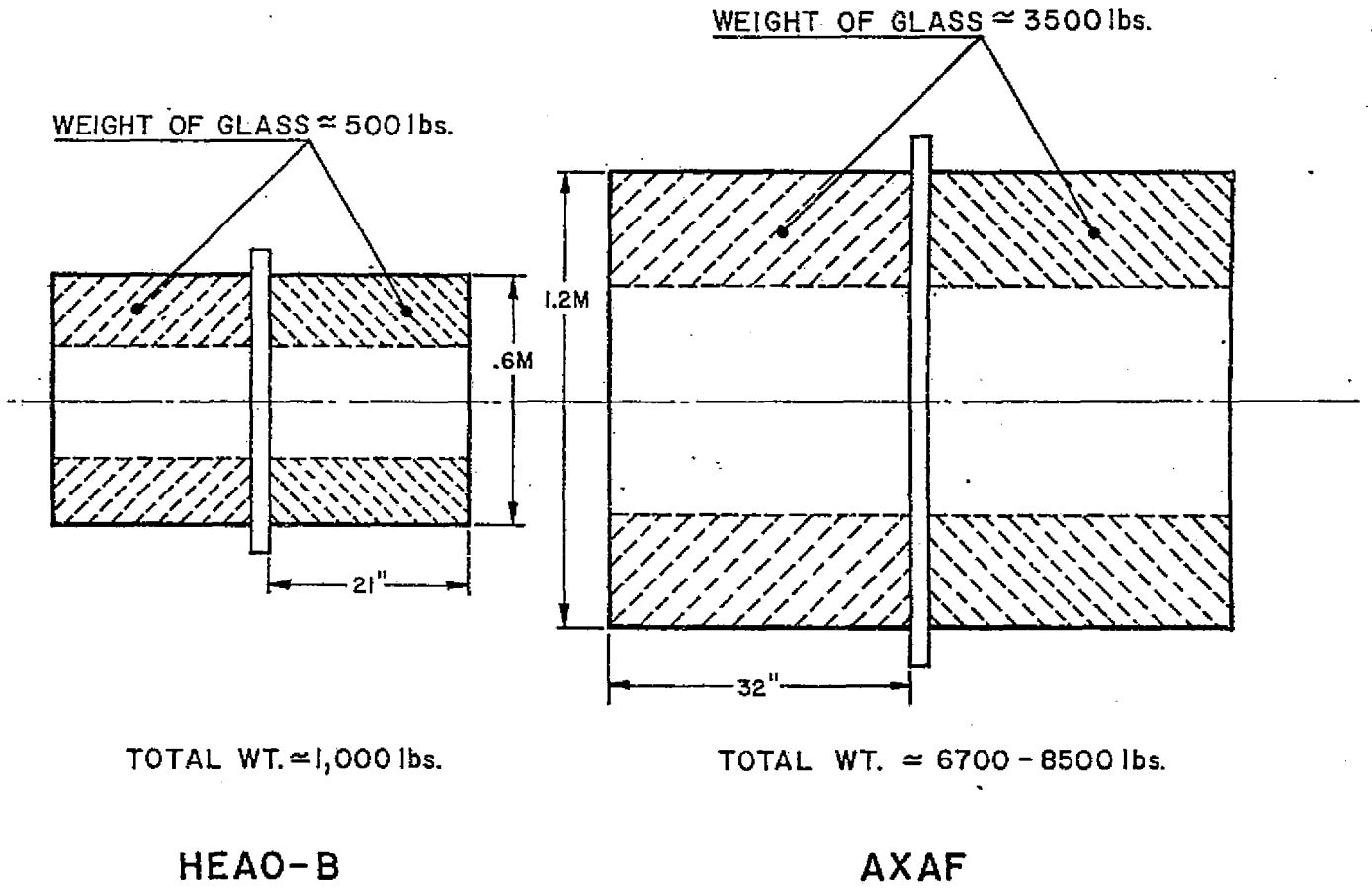

FIGURE 4-2

ORIGINAL PAGE IS OF POOR QUALITY

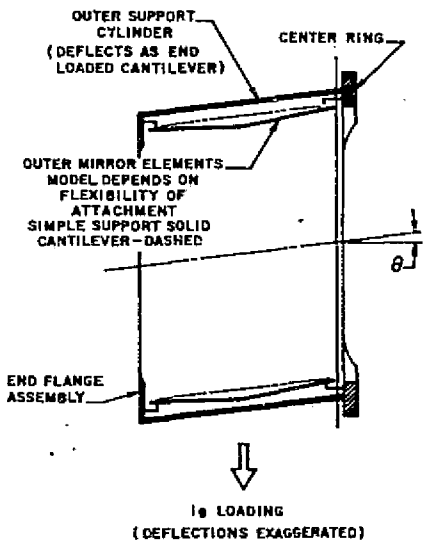

FIGURE 4-3a
Cantilevered Support Cylinder

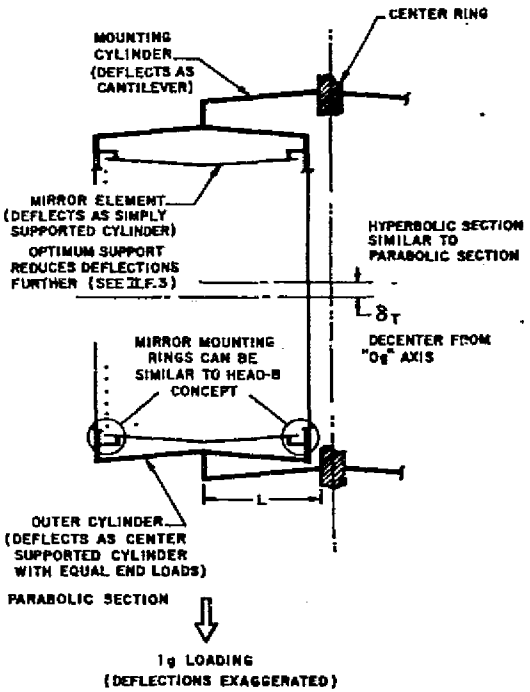

FIGURE 4-3b
Center Supported Cylinder

ORIGINAL PAGE IS OF POOR QUALITY

center support/alignment ring which is also an integral part of the mirror assembly. In the Center Supported Cylinder concept (see Figure 4-3b) the front and rear mirrors are, in effect, contained in separate cylindrical assemblies whose relative alignment is maintained by the mounting cylinder and the center ring. In terms of ease of assembly and initial alignment, the Cantilever Support Cylinder appears greatly superior. However, in the other areas it is less desirable, particularly with regard to criteria 2 and 3 above. The status at present is that means of reducing the disadvantages of the Cantilevered system are being examined in parallel with studies as to how a non-cantilevered mirror assembly would be aligned at assembly. Additionally, problems common to either concept are being studied.

4.2 Cantilever Support Cylinder Concept

4.2.1 1 g Global Deflections

One half of a cantilevered mirror assembly is shown in Figure 4-3a with the horizontal 1 g deflections greatly exaggerated. When a typical system is analyzed it turns out that most of the mirror assembly strength is due to the glass elements which support not only their own weight but that of the end aperture flange assemblies.

If the mirror is unsupported in the horizontal position during test, the 1 g forces produce a deformation that is predominantely due to shear and which results in an equivalent slope change θ (see Figure 4-3a). The value of θ will be order 0.5 arc-sec for feasible configurations. This deflection produces a degradation in on-axis resolution as shown in Figure 4-4 which is seen to be significant.

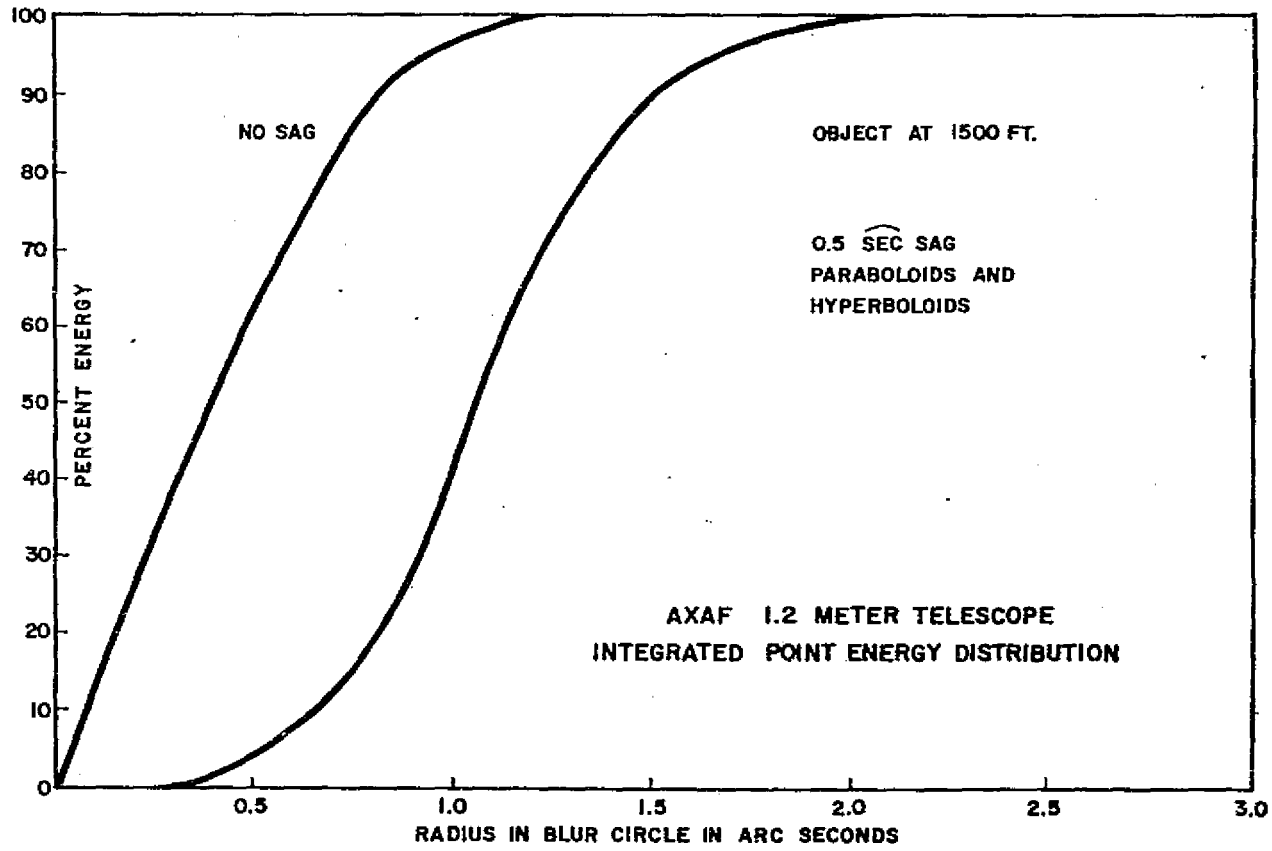

FIGURE 4-4
Effect Of Cantilever Sag

4.2.2 Compensating Support Difficulties

The argument can be made that the ends of the mirror assembly could be supported during horizontal test in such a way that the "0 g" condition is simulated at least with regard to eliminating the cantilever "sag". This must be done by the appropriate application of force and not by measured displacement. The displacements involved are less than 10^{-4} inches and simply cannot be maintained in ambient air even if they could be established. A "first order" force correction is possible if one can design a reliable means of applying the required forces to the mirror assembly ends through the optical bench (at least in the case of the rear mirror) without distorting the mirror assembly-optical bench interface.

The correction obtained will be as good as the analysis of the mirror assembly is accurate. The nature of the system makes accurate modeling difficult. The mirror elements which are the principal structural members are neither simply supported, pinned, or pure cantilevers. Consequently, exceedingly fine grid finite elements analysis is required and even then, the model is sensitive to the assigned mechanical properties of the various materials and, in particular, the bonding epoxy.

4.2.3 Minimization of 1 g Sag

Regardless of the outer cylinder stiffness to mirror and mirror flange loads which can be varied by dimensional changes, the support cylinder should deflect less under its own weight than do the individual glass elements.

The deflection due to self-weight is proportional to the density ρ and inversely proportional to g (torsional modulus) of

the material assuming shear to be the predominant deflection mechanism. The shear deflection is not affected by change in wall thickness.

Ratios of ρ/g for some different materials are:

material	ρ/g	
fused silica	1.75×10^{-8}	
invar	3.62×10^{-8}	(more than glass)
graphite epoxy	1.45×10^{-8}	(less than glass)
beryllium	$.4 \times 10^{-8}$	(less than glass)

The lower limit on deflection is the deflection of the support cylinder due to its own weight. For graphite epoxy this is about 0.2 arc-sec and for beryllium about 0.05 arc-seconds. Beryllium offers some potential improvement over graphite epoxy.

However, in order to make the beryllium support cylinder carry about 75% of the load, its wall thickness must be almost 3 inches thick. The weight of two such cylinders will be about 2400 pounds and a severe thermal mismatch between the glass elements and the outer cylinder will have to be accommodated by flexures of some sort. Cost impact can be considered significant, but has not be assessed to date.

4.2.4 Conclusions

The use of the cantilever concept is certainly not precluded and may, in fact, be ultimately required to assure assembly/alignment feasibility. However, unless a thick beryllium cylinder is used, some support will be necessary to permit meaningful determination of the AXAF mirror performance in X-rays during test.

4.3 Center Support Cylinder

4.3.1 General

Given the potential problems associated with the cantilevered support cylinder, it is appropriate to examine alternative approaches. This is being done on the context of the ground rules in Table 4-1. One basic concept which appears to satisfy these ground rules is the Center Support Cylinder of Figure 4-3a.

The front and rear mirror sets are, when assembled and aligned, each separate subassemblies enclosed in an outer support cylinder which is, in turn, connected to the center ring by means of a cantilevered mounting cylinder.

The significant difference is that the only global slope change is due to the beam or bending rotation of the mounting cylinder and not to the larger shear induced slope. Also, the transfer or flow of loads is much better defined and more accurate modeling and analysis results. Each mirror element is supported near its end. It supports only its own weight. The load is carried out through the end flanges to the support cylinder which is loaded in a well-defined way. The principal deflection mechanism is still shear which because of the balanced design produces only translation from the 0 g optical axis.

The following subsections examine the deflection which determines concept performance and feasibility. Analysis is mainly based upon handbook formulas.

4.3.2 Deformation Of Mounting Cylinder

The mounting cylinder deflects by a combination of bending and shear as shown in Figure 4-5. The principal slope

TABLE 4-1

GROUND RULES

Each individual mirror element supports only its own weight in a 1 g field.

The support concept introduces minimum slope (rotation) changes due to 1 g deflections.

Transfer of loads is well-defined.

Use of Invar is not precluded.

Decentering effects due to 1 g are small and controllable.

Total system is sufficiently stiff with high resonant frequencies.

Stresses in main mounting ring are decoupled from mirror elements.

Concept is feasible in terms of alignment considerations and environmental requirements.

ORIGINAL PAGE IS
OF POOR QUALITY

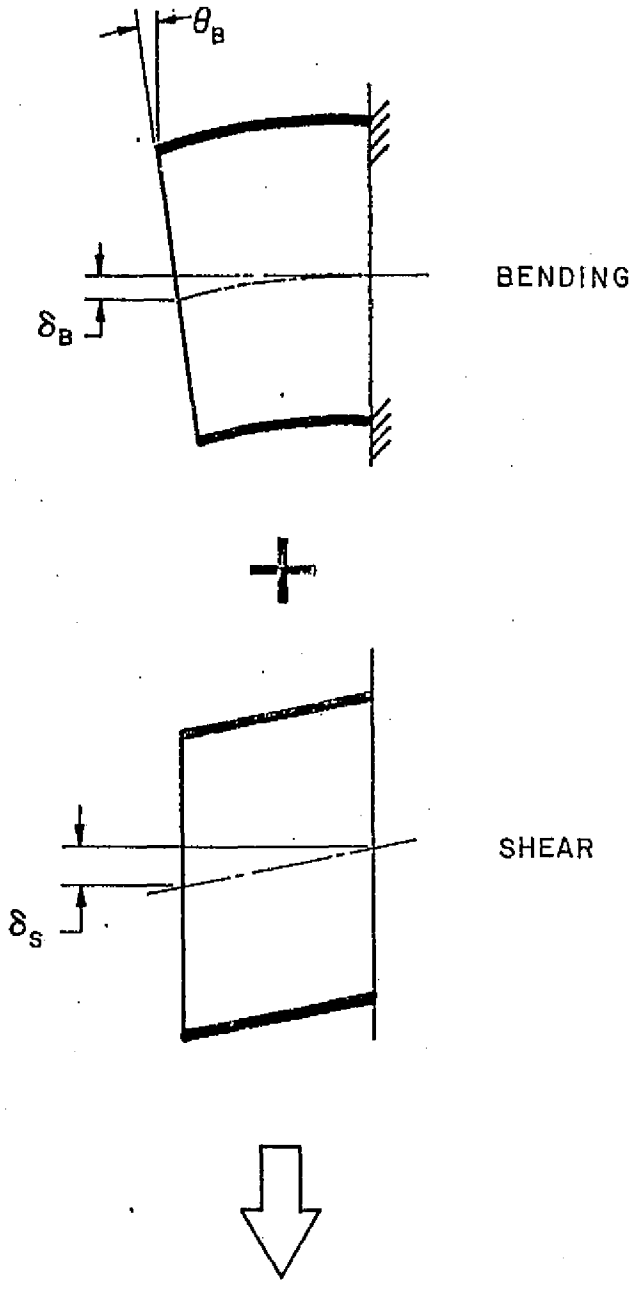

TOTAL DECENTER $\delta_T = \delta_B + \delta_S$

ROTATION θ_B

FIGURE 4-5
Deflection Modes

error is due to bending rotation. The value of θ_B is given by:

$$\theta_B = \frac{PL^2}{2EI} + \frac{WL^2}{GEI} \qquad \text{Eq. 4.1}$$

where P = weight of mirror assembly = 3,317 pounds
E = Young's modulus
I = sectional moment
W = uniformly distributed total weight of cylinder
D_o = outer diameter of cylinder = 76 inches

Values of θ_B for representative wall thicknesses and materials are shown in Figure 4-6. The preferred material would appear to be beryllium. Wall thicknesses of less than 0.25 inch are acceptable and result in slope errors on the order of .03 to .05 arc-seconds. The thermal mismatch problem of the cantilever case does not exist here because the mounting cylinder is free to expand and contract. Uniform changes in temperature will produce de-focus or vertex changes which will be negligible (2.2 x 10^{-4} inches/degree F.). However, the rotational effect of thermal "hot-dogging" due to a 1°F radial gradient is of order 0.2 arc-sec indicating a need for good thermal control.

The decentering is approximated by:

$$\delta_T = \delta_B + \delta_S \qquad \text{Eq. 4.2}$$

where $$\delta_B = \frac{PL^3}{3EI} + \frac{WL^3}{8EI} \qquad \text{Eq. 4.3}$$

and $$\delta_S = \frac{PL}{AG} + \frac{\rho L^2}{G} \qquad \text{Eq. 4.4}$$

Taking the diamter of the cylinder as 76 inches, representative

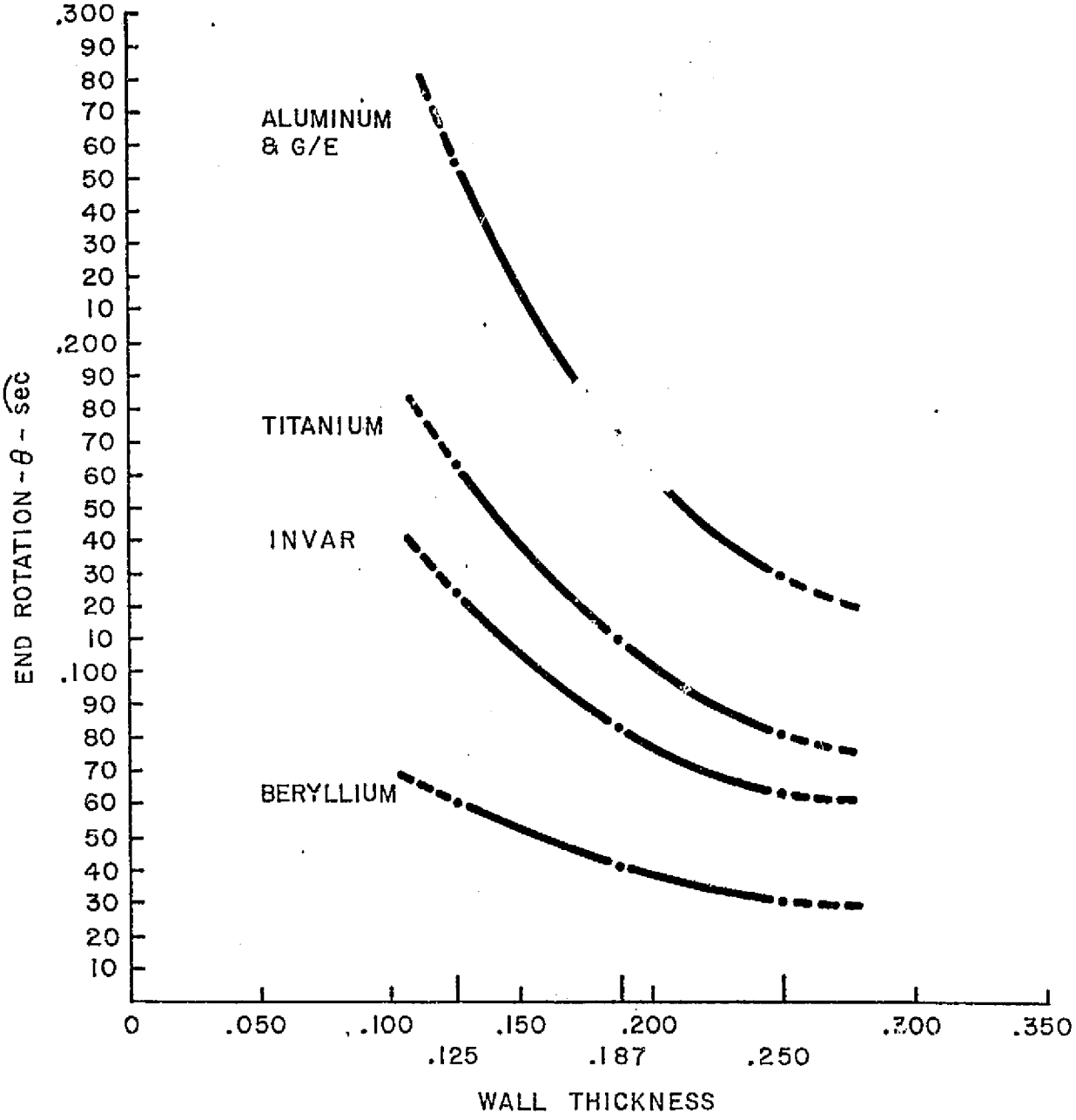

FIGURE 4-6
Mounting Cylinder Rotation

deflections are shown in Figure 4-7. Decentering can be limited to .0005 inches or less. Note that if beryllium is used to minimize rotation, the resultant decentering is less than .0002 inches which corresponds to 0.1 arc-sec. in the focal plane. Clearly the differential decentering between front and rear assemblies is insignificant.

4.3.3 Deformation Of Support Cylinder

The support cylinder is a key element in the system concept. It provides a symmetrical load path to the mirror elements and their mounting rings. It is somewhat flexible and therefore attenuates strains induced in the mounting cylinder.

Rotation of the ends is negligible. Typical decentering is shown in Figure 4-8. The differential decentering between the front and rear sections can be controlled by design to very small values.

4.3.4 Deformation Of Mirror Mounting Rings

Calculation of mirror mounting ring decentering depends upon design details. Using simplified analysis for a worst case configuration where the mirror elements are supported 8 inches from each end, the deflections are as shown in Fig. 4-9. Maximum decenter is of order 14 μ inches for .1 inch thick rings and differential decentering is more like 8 μ inches.

4.3.5 Conclusion

The approach offers the potential of significantly im-

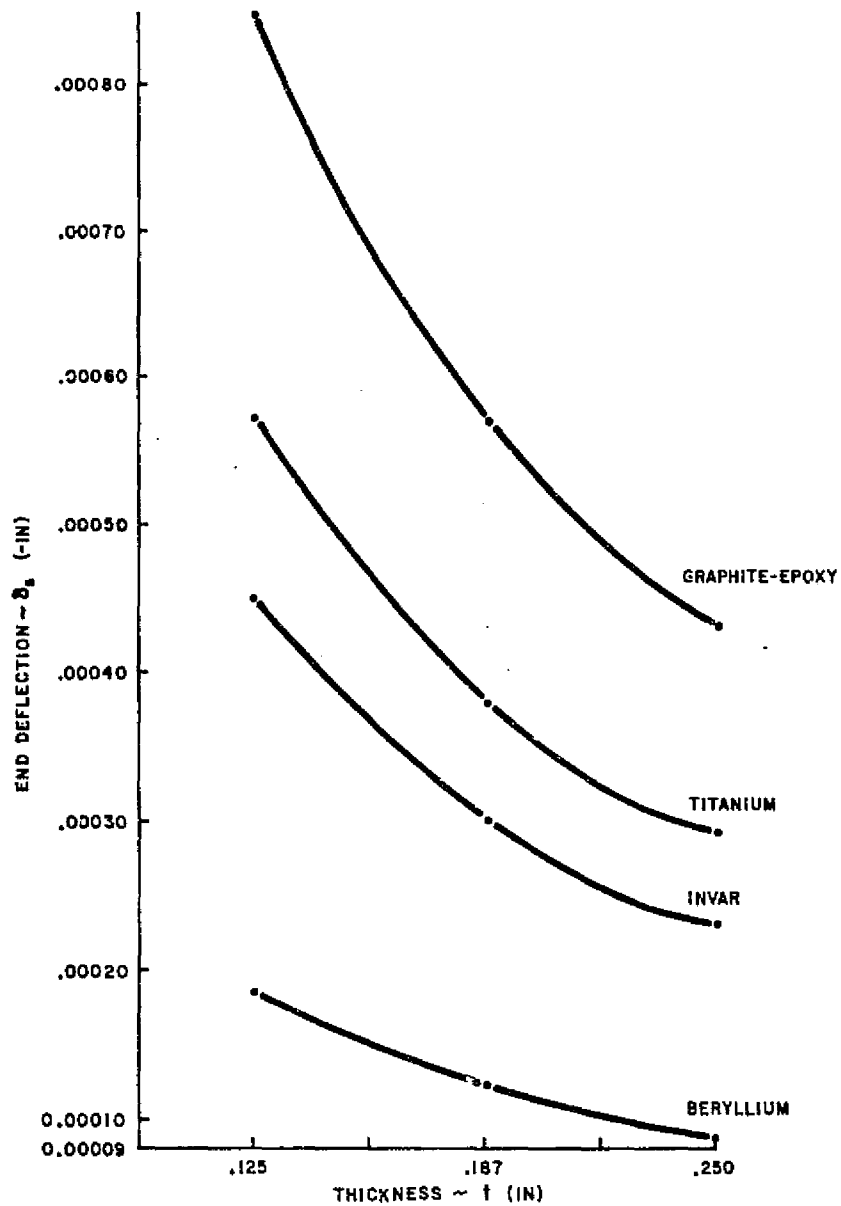

FIGURE 4-7
Mounting Cylinder Decentering

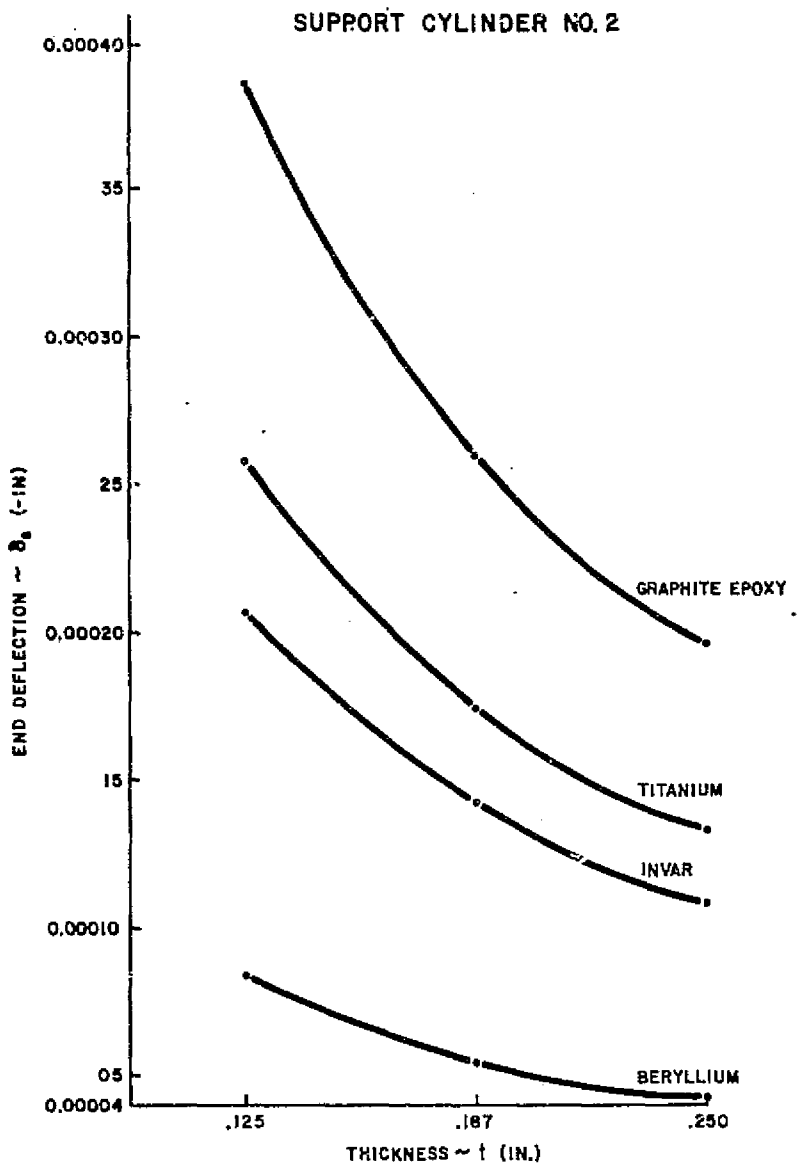

FIGURE 4-8
Support Cylinder Decentering

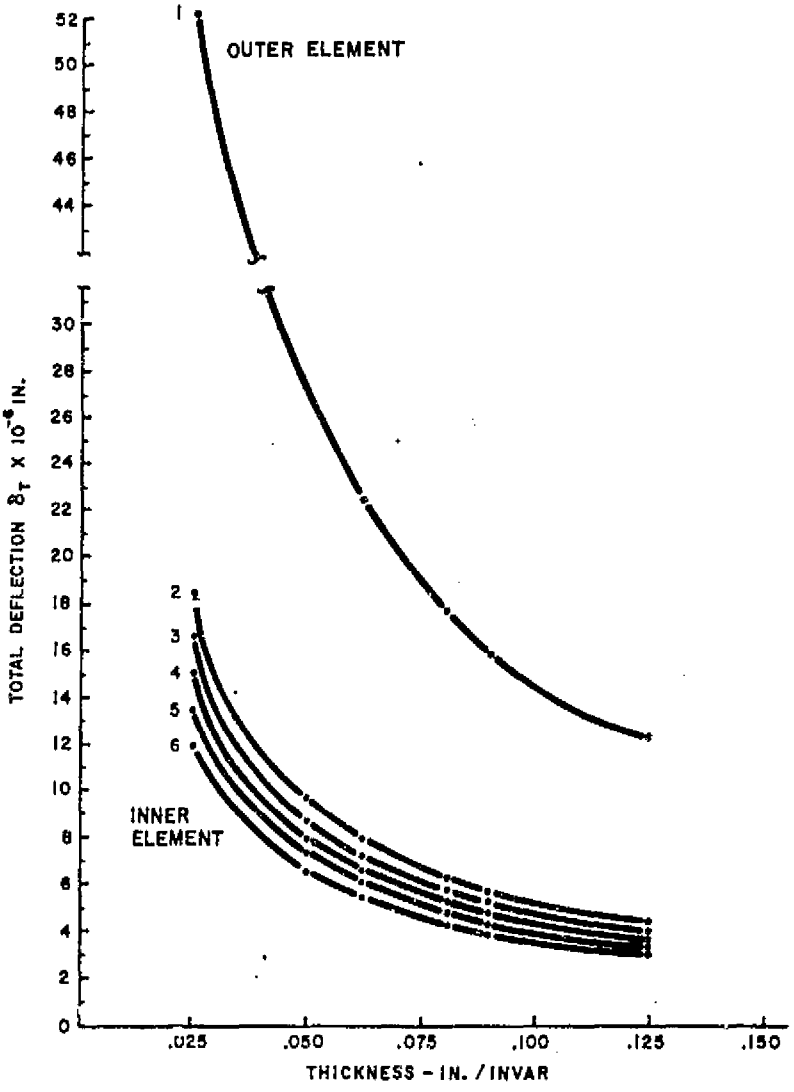

FIGURE 4-9

Mounting Ring Deflection

proved prelaunch testing with minimal 1 g induced rotation and acceptable decentering without compensating support. While the stability of alignment should be comparable to the cantilever approach, initial mirror build up and alignment appears to be significantly more complicated.

4.4 Thermal Gradient Effects Trade

It is important to recognize that a trade exists between minimizing 1 g slope errors and minimizing equivalent slope errors induced by thermal "hot-dogging". Thermal effects are minimized by using graphite epoxy support cylinders in the cantilever case and graphite epoxy mounting cylinders in the center supported cylinder case rather than beryllium cylinders. However, the corresponding 1 g slope errors are of order 0.5 arc-sec for the cantilever case and 0.13 arc-sec for the center supported cylinder case. Invar could be used in the center supported cylinder configuration if the resultant magnetic effects were not too great.

The trade is clearly tied to the thermal control of the mirror. Gradients should be significantly less than $1^{\circ}F$ across the mirror diameter when the thermal control system is operating. During test, however, this might not be the case.

In any event, it is apparent that a better trade exists with the center supported cylinder approach than with the cantilever approach.

4.5 Work In Progress

Two mirror assembly configurations are being analyzed

in some detail for mechanical and thermal stability*. One concept is a cantilever design and the other is an extension of the center supported cylinder concept. Both employ the graphite epoxy sleeve method of glass element support described in Section 5.

The key question at present is how does one go about assembling and aligning a center supported cylinder mirror and what tooling, support fixturing, etc. is required. The general problem is being examined by SAO.

---

*Part of this work is being performed under subcontract to American Science & Engineering.

5.0 MIRROR WEIGHT ESTIMATES

5.1 General

Work performed at MSFC prior to SAO start relative to general structural, inertial, and attitude control considerations assumed a total mirror assembly weight of 11,000 pounds. It was therefore important to verify this number as early as possible in the program which precluded a detailed design and weight calculation. However, work on both optical design and mirror support concept studies proceeded at a sufficiently rapid rate to quickly establish reasonable limits on mirror assembly weight at 6,700 to 8,500 pounds which lie well below the assumed value of 11,000 pounds. Consequently, all conclusions affected by mirror assembly weight can be considered to be conservative.

5.2 Weight Of Glass

The weight of the mirror glass elements is of course a function of thickness. Thickness will be determined almost entirely by handling, manufacturing, and test considerations and not by mechanical strength requirements. Values on the order of 0.7 to 1.0 inches are probably typical of finished thicknesses. Fig. 5-1 shows the weight of the glass in various optical designs as a function of glass thickness. The weight can be seen to lie between 3,000 and 3,500 pounds for the "most probable" baseline design.

5.3 Structure Weight

The weight of the structure depends upon design and material selection. Using the center supported cylinder concept

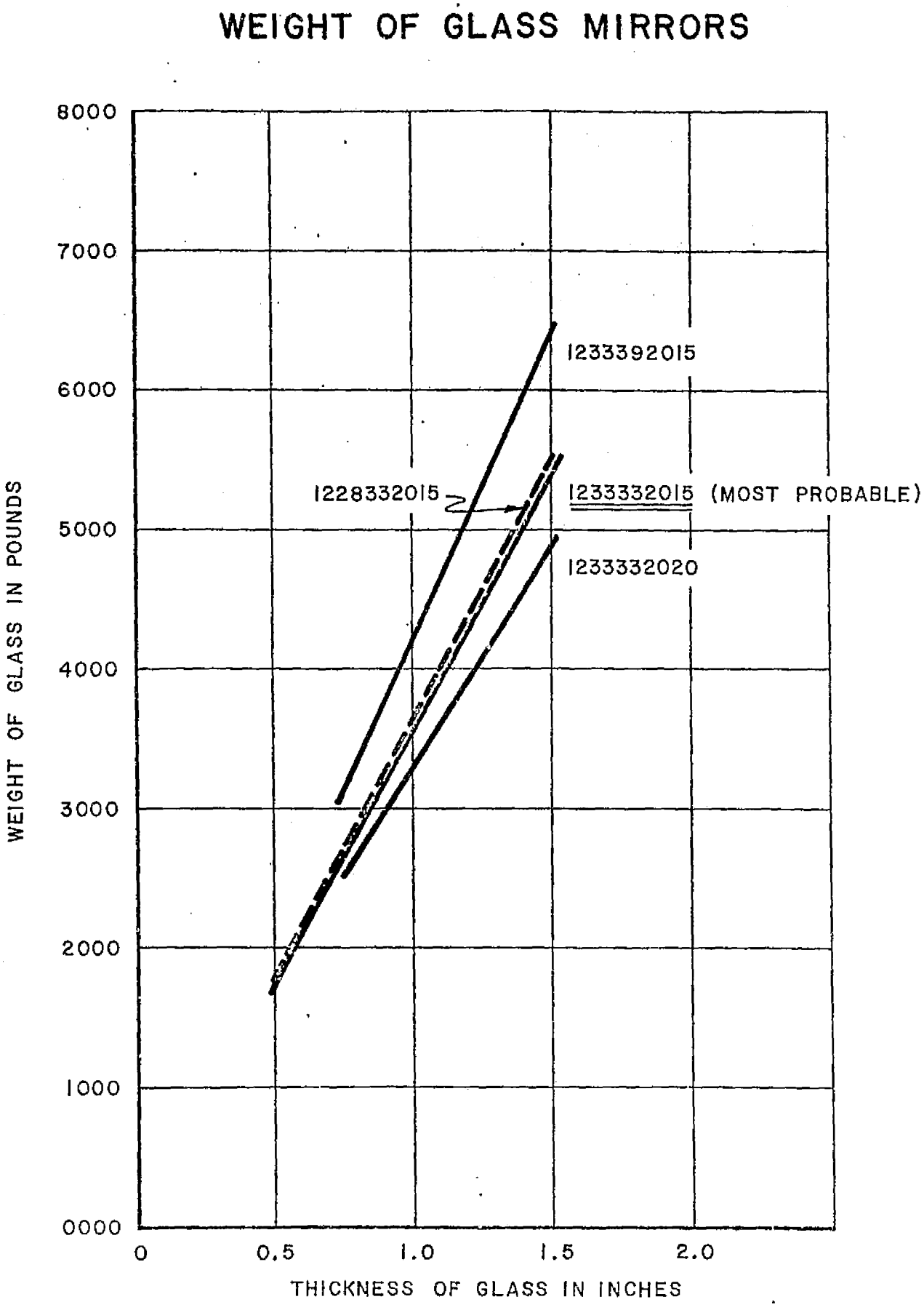
WEIGHT OF GLASS MIRRORS
8000
7000
6000
5000
4000
3000
2000
1000
0000
WEIGHT OF GLASS IN POUNDS
0
0.5
1.0
1.5
2.0
THICKNESS OF GLASS IN INCHES
1233392015
1228332015
1233332015 (MOST PROBABLE)
1233332020

FIGURE 5-1

as typical of an elaborate design the weight for a structurally sound assembly was calculated at 3,700 to 4,500 pounds depending upon the amount of Invar used.

6.0 1 G EFFECTS ON MIRROR ELEMENTS

6.1 Comment

Regardless of how the mirror support system is implemented and supported during horizontal test (assuming the cantilever concept is supported if it is used) there is an irremovable deflection of each element with respect to its support that is due to the weight of the element itself. These effects have been examined. These studies have also identified a mirror element support concept that offers some potential improvement over attachment to comparatively stiff rings near the ends of the glass elements.

The basic deflection calculations were performed by AS&E and are discussed in some detail in Ref. 1. The key results are included here for continuity and clarity.

6.2 Deflections Vs. Support Plane

Using approximate analysis SAO examined the effect of support plane location and established that significant reduction in both maximum displacement and slope errors resulted from moving the plane of element support from the ends to a distance about 25% of the total length in from the ends as shown in Fig. 6-1.

Detailed analysis using BOSOR modeling was performed at AS&E for the 48 inch diameter outer element and the 24 inch diameter inner element for various glass thicknesses and support plane locations. One such analysis is shown in Fig. 6-2 where slope is considered. The curves behave qualitatively as expected in that the maximum slope error decreases as the support plane is moved towards the center (8 inches is L/4 point). However, the

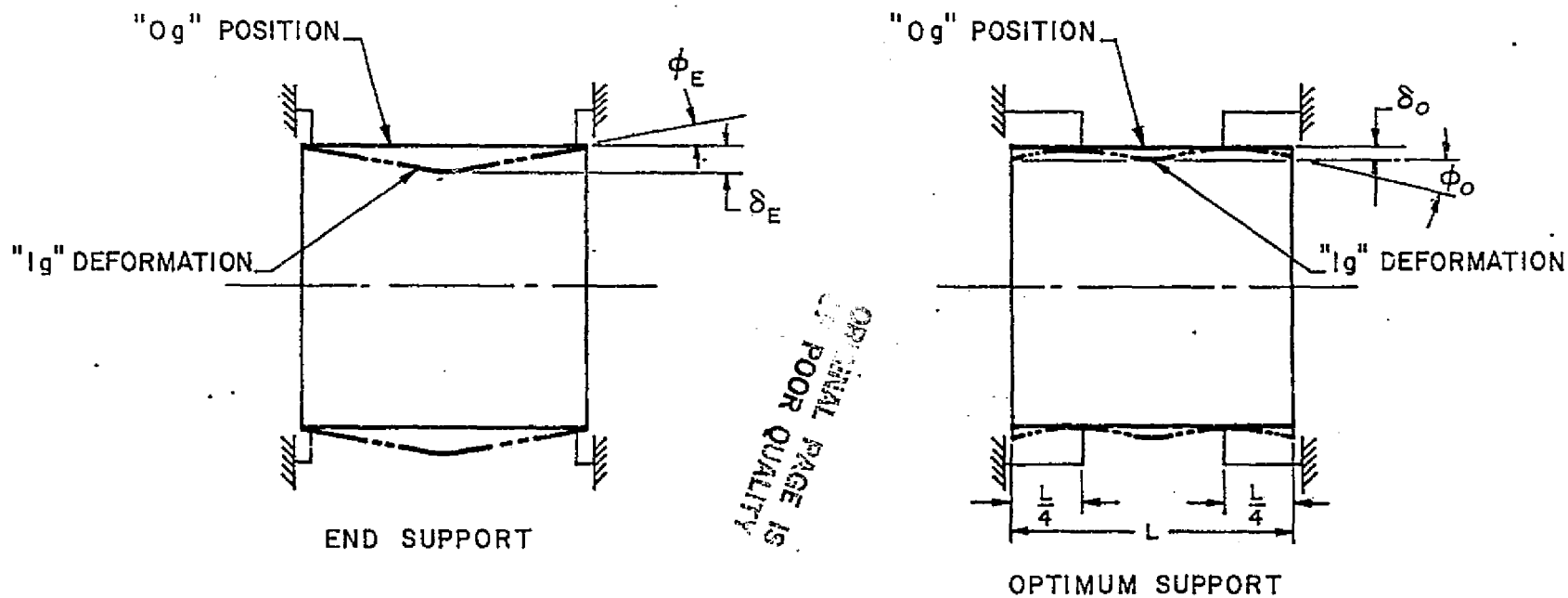

$$\phi_E > \phi_o$$

$$\delta_E > \delta_o$$

FIGURE 6-1
Support Plane Locations

ORIGINAL PAGE IS OF POOR QUALITY

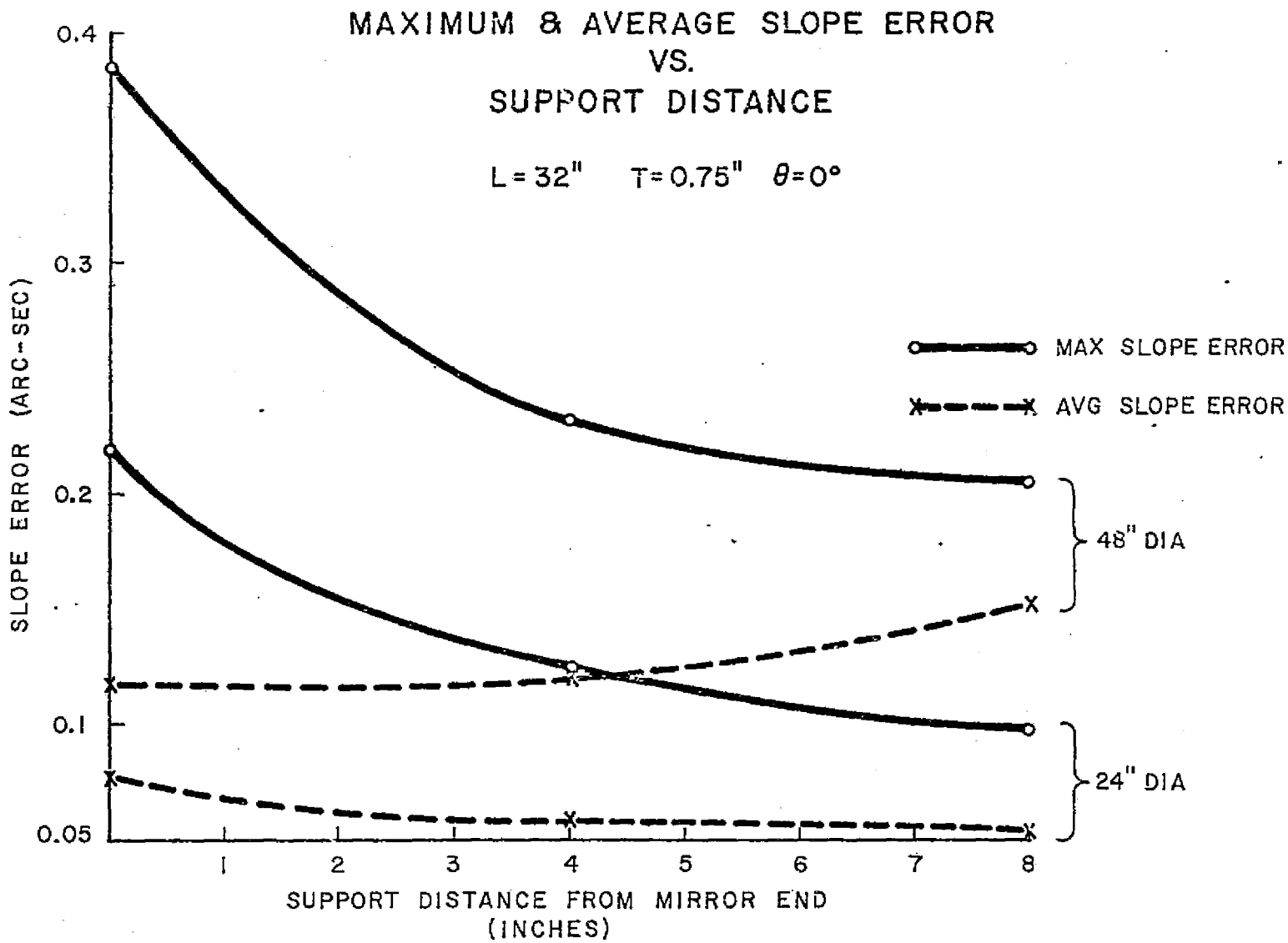
MAXIMUM & AVERAGE SLOPE ERROR
VS.
SUPPORT DISTANCE
L = 32" T = 0.75" θ = 0°
SLOPE ERROR (ARC-SEC)
0.4
0.3
0.2
0.1
0.05
1
2
3
4
5
6
7
8
SUPPORT DISTANCE FROM MIRROR END
(INCHES)
MAX SLOPE ERROR
AVG SLOPE ERROR
48" DIA
24" DIA

FIGURE 6-2

average slope error for the larger element increases as the support point is moved towards the L/4 point.

Ray trace analysis was performed at SAO to determine the geometric response of the outer (48") element pair when distorted as calculated. The results are shown in Fig. 6-3 and indicated that the best performance occurs when the elements are supported at their ends and not at the L/4 point. Two facts emerge. First, the effect of the 1 g distortions is comparable to the scattering effect of an assumed "best effort" surface roughness of 0.1 arc-sec rms.

Second, average slope error is a better criterion for performance comparisons than is maximum slope error.

Decentering and departure from roundness were found to be negligible.

Another useful output of the AS&E work was a comparison between deflections in right cylindrical elements and tapered cylindrical elements. Results differed only by a few per cent at most. Consequently, the use of right cylinder approximations to the various mirror elements which greatly simplifies finite element modeling is appropriate.

6.3 Sleeve Support Concept

AS&E examined various means by which the attachment plane could conveniently be varied. The concept of Fig. 6-4 emerged. When the total assembly was analyzed, an interaction between the G/E* sleeve and the glass element was identified which for thinner sections produces a compensating moment in the glass that cancels the effect of the 1 g deformations. This is shown

*Graphite-epoxy.

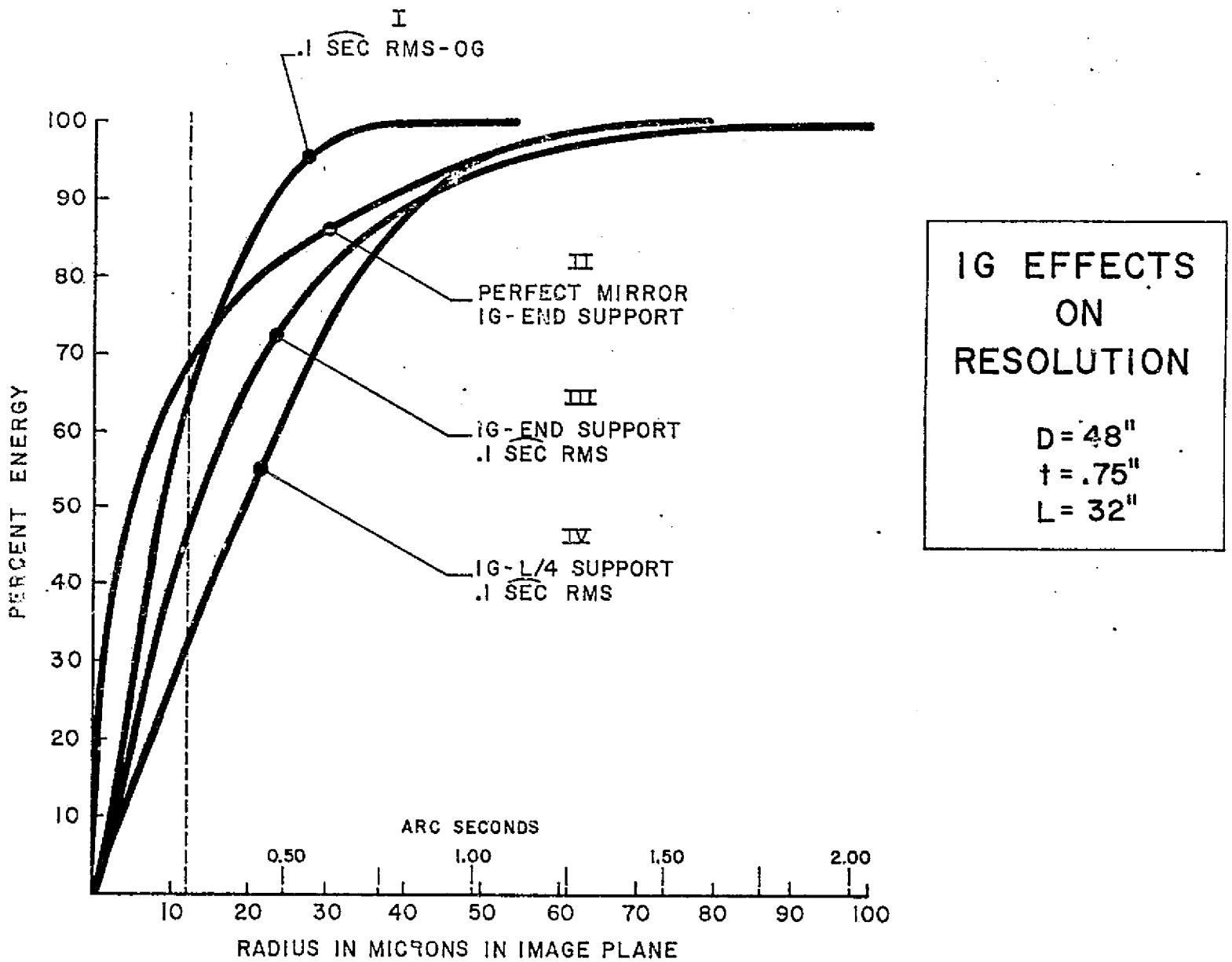

FIGURE 6-3

Resolution vs Support Plane Location (Outer Element)

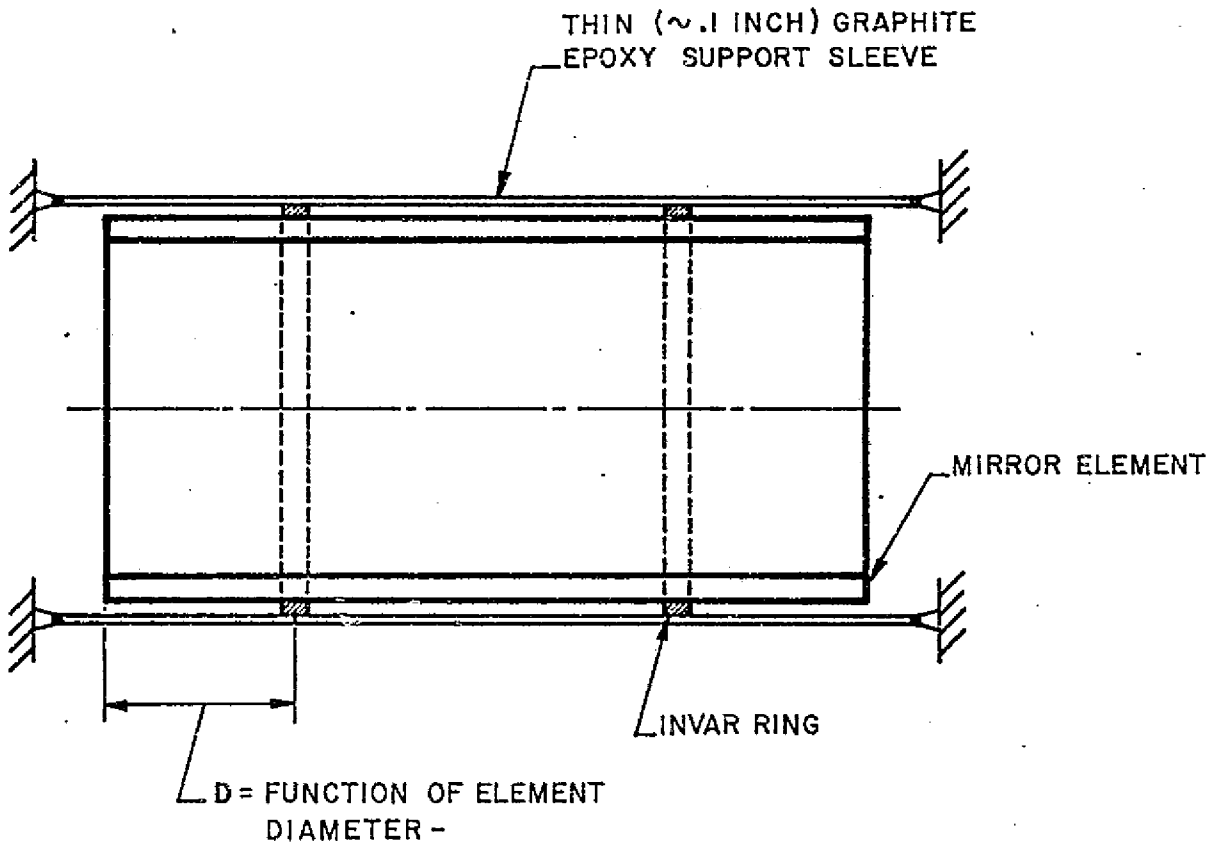

FIGURE 6-4

SUPPORT SLEEVE CONCEPT

in Fig. 6-5. The maximum slope error is .031 arc-sec. The entire assembly translates radically producing a "de-centering" of about 50 μ inches. Differential de-centering can be made negligible by design.

No claim is made for the concept other than the first order elimination of mirror element deflections due to their own weight. It is, however, obvious that the G/E sleeve offers isolation between the mirror element and the rest of the mirror structure which can possibly be utilized to advantage. AS&E is examining two mirror assembly concepts, both of which exploit the G/E sleeve concept. The G/E sleeve also provides a thermal control surface in close proximity to the mirror element which can potentially be utilized to simplify and/or improve mirror thermal control.

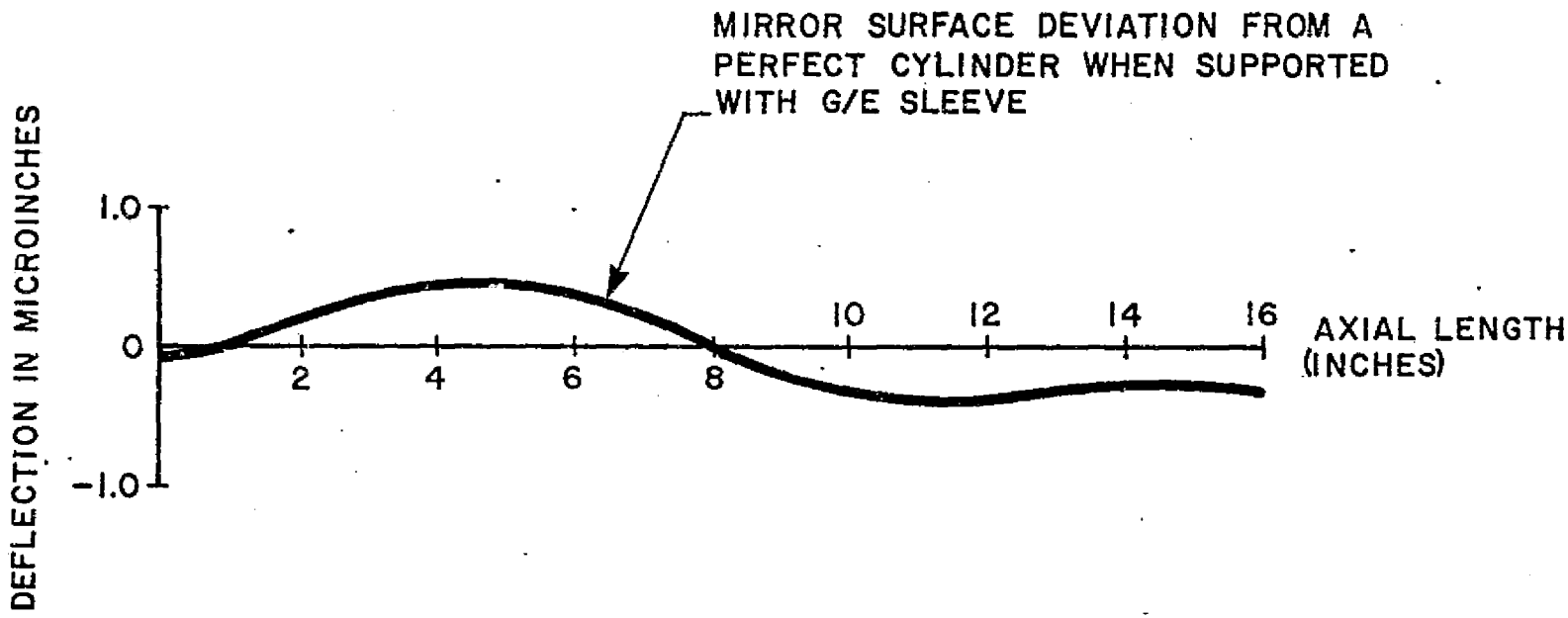

EFFECT OF G/E CYL. - INVAR RING SUPPORT ON MIRROR DEFLECTION T = 0.1 INCH

FIGURE 6-5

7.0 MIRROR ASSEMBLY RESONANT FREQUENCIES

7.1 General

Some preliminary analysis of mirror assembly resonant frequencies has been performed using both approximate and finite element methods. This is viewed as a continuing activity in support of conceptual and detailed design activities. The mirror assembly must not only withstand the launch and re-entry mechanical loads but it must exhibit natural resonant frequencies well above the attitude control system bandwidth and maximum reaction wheel unbalance frequences.

The principal concern at present relates to the axial mode (parallel to the optical axis) where the large mass of the mirror assembly is opposed by comparatively little stiffness.

7.2 Mirror Element Resonant Frequencies

Analysis of mirror element natural frequencies has been carried out. A technical memo is in preparation detailing the results. The frequencies range from about 500 Hz up to about 800 Hz.

7.3 Lateral Assembly Frequencies

Lateral mode natural frequencies have been calculated for candidate configurations and found to be well above 100 Hz. A value of 150 Hz seems feasible.

7.4 Axial Assembly Frequencies

The weakness of the system in the axial direction re-

sults in low natural frequencies. Although the periphery of the center support ring is fixed to the optical bench, the weight of the glass plus flange plates acts against the end plates and/or center ring which are largely open to provide maximum telescope effective area.

Detailed analysis is in process, but preliminary hand calculations indicate frequencies to be in the range of 30 to 60 Hz unless additional stiffening is added. The objective of the analysis is to identfy requirements, constraints, and/or auxiliary structure which will ensure a natural frequency above 100 Hz.

8.0 OPTICAL BENCH CONSIDERATIONS

8.1 General

The twin goals of 0.5 arc-sec telescope resolution and post facto aspect determination to better than 1 arc-sec require the so-called optical bench to be considered together with the mirror assembly, the aspect determination system, and the focal plane assembly as an integrated X-ray Telescope Assembly (XTA) system.

Optical bench studies to date have emphasized allowable thermal and mechanical deformations. The results indicate that the required static tolerances can be met with realizable configurations.

Additionally, qualitative concerns relative to dynamic response considerations have been identified and indicate the need to examine the dynamics of all candidate configurations.

8.2 Model For Optical Bench Studies

System performance studies of the optical bench are based on a simplified model that is compatible with preceeding and parallel MSFC studies and the temperature control concept that is currently preferred (see Section 9.0). The model is shown in Fig. 8-1. The bench is defined as being cylindrical having an equivalent right cylinder diameter D and a wall thickness t.

8.3 Sources Of Error From Bench Deformations

The optical bench deforms from static and dynamic

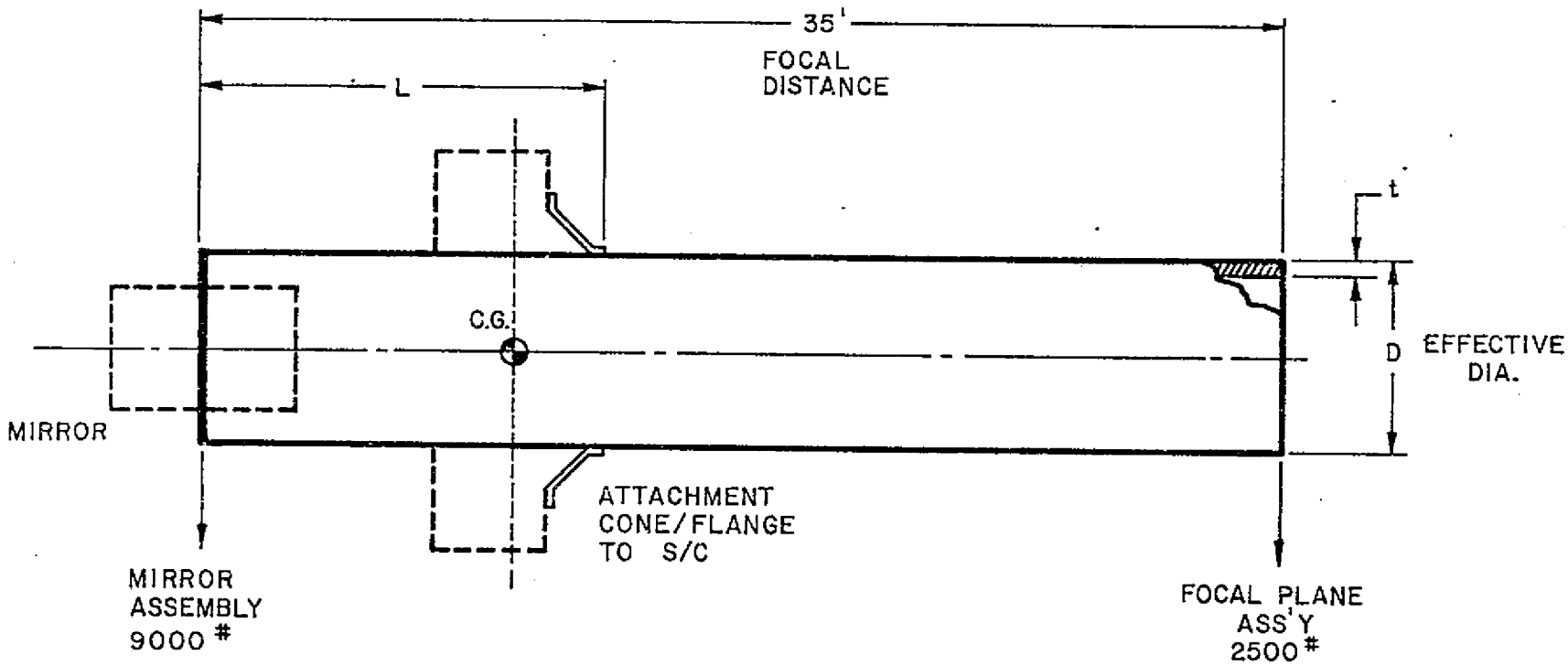

FIGURE 8-1

Simplified Optical Bench Model

mechanical loads, from thermal gradients, and from uniform changes in absolute temperature. The deformations, however they are caused, result in three principal areas of concern:

1. change in optical axis length from mirror to instrument image plane (de-focusing)

2. displacement of image in instrument image plane (de-centering)

3. degradation of resolution due to mirror rotation (de-focusing)

8.4 Focal Length Changes (De-focus)

8.4.1 Sources Of Focal Length Change (ΔFL)

There are potentially several sources of change in focal length (ΔFL) due to bench deformation. These are:

1. curvature of bench due to thermal gradients (hot-dogging) and mechanical loads (chord is significantly shorter than arc)

2. change in bench length due to uniform temperature changes

3. change in bench length due to expansion/contraction from moisture absorption/outgassing (if any)

4. de-focus of off-axis points due to instrument plane rotation in a plane containing the optical axis

5. change in length due to vertical loads (if assembled, aligned, tested vertically)

8.4.2 Allowable Effect Values

Allowable values of the various effects have been determined in the context of an acceptable value of $\Delta FL = \pm .002$ inches. This corresponds to a broadening of a point image by about .12 arc-seconds.

8.4.2.1 Bench Curvature

The difference between arc and chord length has been examined as a function of equivalent deflection as shown in Fig. 8-2. Circular curvature has been assumed. Equivalent deflections in excess of 0.5 inches can be accommodated. Actual deflections from typical system configurations will be less than 0.1 inches in the special case of 1 g horizontal test and less than .010 inches in orbit.

8.4.2.2 Image Plane Rotation

Rotation of the image plane changes the off-axis focal length as shown in Fig. 8-3. The maximum FOV is about 20 arc-minutes which represents the radial displacement of 2.3 inches shown. The resolution of the mirror measured in a plane this far off-axis is comparatively poor being something on the order of 20 arc-seconds. This means a much great ΔFL can actually be allowed before a detectable effect on the off-axis image occurs. However, it turns out that no ΔFL problem due to this effect exists. Taking an allowable value of $\Delta FL = .004$ inches, the allowable value of ϕ becomes:

$$\phi = \tan^{-1} \frac{\Delta FL}{2.3} = \tan^{-1} \frac{.004}{2.3} \simeq 6 \text{ arc-min}$$

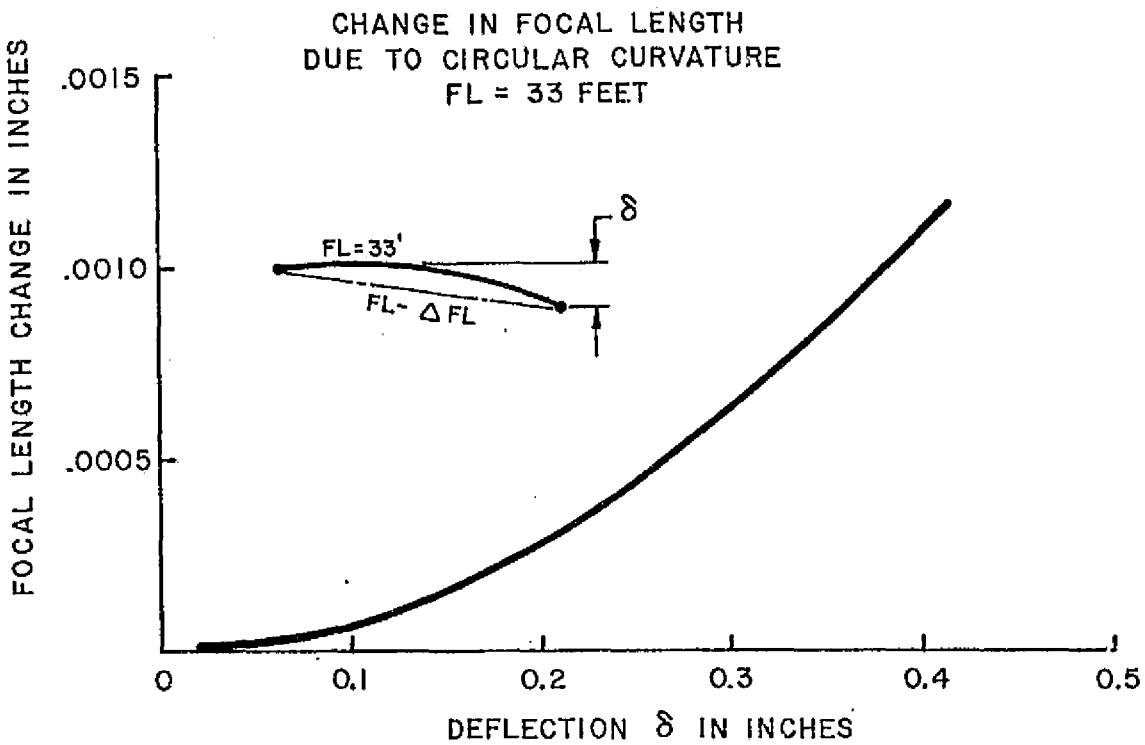

FIGURE 8-2

Bench Curvature Effect On Focal Length

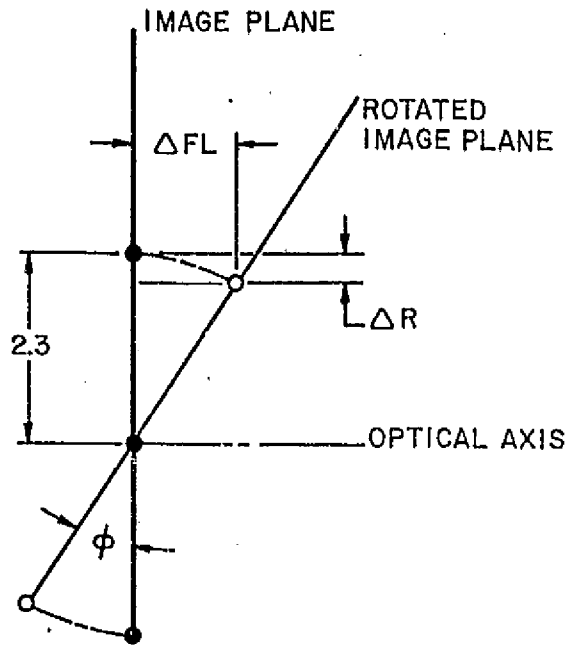

FIGURE 8-3

Rotation Effects On Image Plane

This will not be approached in realistic designs as shown in following sections.

8.4.2.3 Conclusion

The principal source of ΔFL errors will be due to thermal expansion of the bench. Setting the allowable expansion/contraction equal to .002, the resultant coefficient of thermal expansion must be less than:

$$\alpha = \frac{.002}{33x12 \cdot \Delta T} = \frac{5x10^{-6}}{\Delta T}$$

where ΔT is the change in temperature.

What emerges is that if ΔT is less than $\pm 1^{o}F$ either graphite epoxy or titanium can be used. Increasing the allowable value of ΔFL to ±.004 permits the use of a wide variety of materials including beryllium, most ferrous metals and even aluminum with slightly tighter temperature control.

The key point is that if G/E is used, its exact coefficient is not at all critical as long as it is low. This reduces the requirement for controlling the optical bench temperature (although control of the optical bench temperature appears highly desirable when mirror assembly temperature control is considered - see Section 9.0).

8.5 Decentering Changes (ΔR)

8.5.1 Sources Of ΔR Errors

Decentering errors (ΔR) are displacements of the image

plane points in the plane, i.e. orthogonal to the optical axis. These effects are due to curvature or displacement effects in the bench and to rotation of the image plane (see Fig. 8-3).

Two classes of ΔR effects are defined. These are so-called "slow" variations which can be tracked with a fiducial system and "fast" variations which cannot. We arbitrarily have set design limits at:

$$\Delta R_{slow} \leq \pm .010 \text{ inches } (\sim 5 \text{ arc-sec})^*$$

$$\Delta R_{fast} \geq \pm .0002 \text{ inches } (\sim 0.1 \text{ arc-sec})$$

The principal source of slow ΔR variations in orbit are thermal gradients. This ΔR_{slow} parameter is used to set a limit on allowable thermal "hot-dogging". This constraint of $\pm .010$ inches is satisfied by G/E in reasonable diamters.

ΔR_{fast} effects are due to mechanical vibrations induced by interaction with the attitude control system and system unbalances.

From Fig. 8-3 the rotational effect is:

$$\Delta R = 2.3\ (1 - \cos \phi) \text{ from which}$$

$$\phi = \cos^{-1} \left(1 - \frac{\Delta R}{2.3}\right)$$

Taking $\Delta R = .010$ for the "slow" case

$$\phi_{slow} \leq 5.3^{\circ}$$

---

*In previous presentations this was taken as .002 inches (1 arc-sec). No need for such a tight specification has been supported to date hence the relaxation.

For the "fast" case

$\phi_{fast} \leq 45.3$ arc-minutes

Both of these are large values that would not be approached in any realistic design.

8.6 Horizontal Testing Considerations

8.6.1 General

When the AXAF is mounted horizontally in the X-ray test facility, 1 g forces will produce significant deflections in the bench which in combination with other deformations occurring in the mirror assembly *per se* will degrade the total apparent performance of the XTA. It is important that these effects be understood and desirable that they be minimized wherever possible.

8.6.2 Support Concept

The support concept is shown schematically in Fig. 8-4. Here "L" is as shown in Fig. 8-1 and is therefore the same point of attachment as used in the bench/support module interface. This dimension is selected such that the deflections at each end of the bench are equal, i.e. $\delta_M = \delta_I$. Consequently, even though δ_M and δ_I are comparatively large (see Section 8.7), the differential displacement is small. Reasonably accurate alignment, bore sighting, etc. is thus possible.

Secondly, the mirror assembly is mounted so that end rotation is about a nodal axis. This approach eliminates decentering due to rotation. It does not compensate for degradation

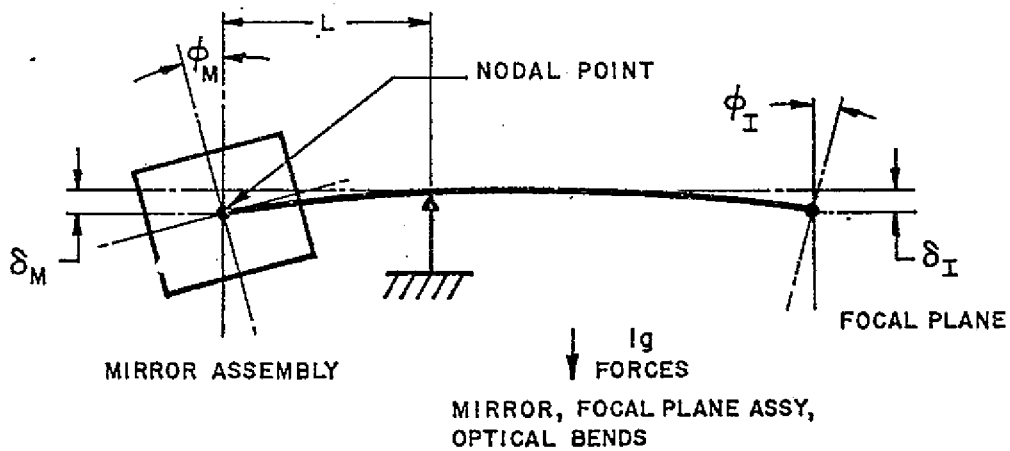

FIGURE 8-4

Support Concept

ORIGINAL PAGE IS
OF POOR QUALITY

of resolution. However, the effect of tilt on resolution is not too great during test given that significant degradation already is caused by the finite distance to the X-ray test source. Relative effects are shown in Fig. 8-5.

8.7 Typical Deformations

We have examined typical deformations due to horizontal static loads and thermal hot-dogging due to circumferential gradients. Figures 8-6 and 8-7 show static deflection and end rotation (focal plane end) for G/E benches of various equivalent diameter and wall thickness. A wall thickness of .187 is considered reasonable. The deflections are within ΔFL constraints and the differential deflections are within ΔR constraints. End rotation is much less than that allowed by conservative ΔFL considerations.

Thermal gradient induced hot-dogging is examined in Fig. 8-8. End rotation is well within limits for G/E benches almost regardless of gradient. The $\Delta R \leq .010$ inch constraint is equivalent to rotations of 10 arc-seconds or less. Since D will certainly be greater than 3.0 feet, no stringent limit on gradients exist at least with regard to optical bench deformation.

8.8 Ground Testing Dynamic Considerations

The optical bench system acts as a distributed mass-spring system. When supported for horizontal test it can be considered as two end loaded cantilevers (neglecting the attach flange).

Because of the optimum support location to compensate 1 g effects, the two cantilevers have fundamental natural fre-

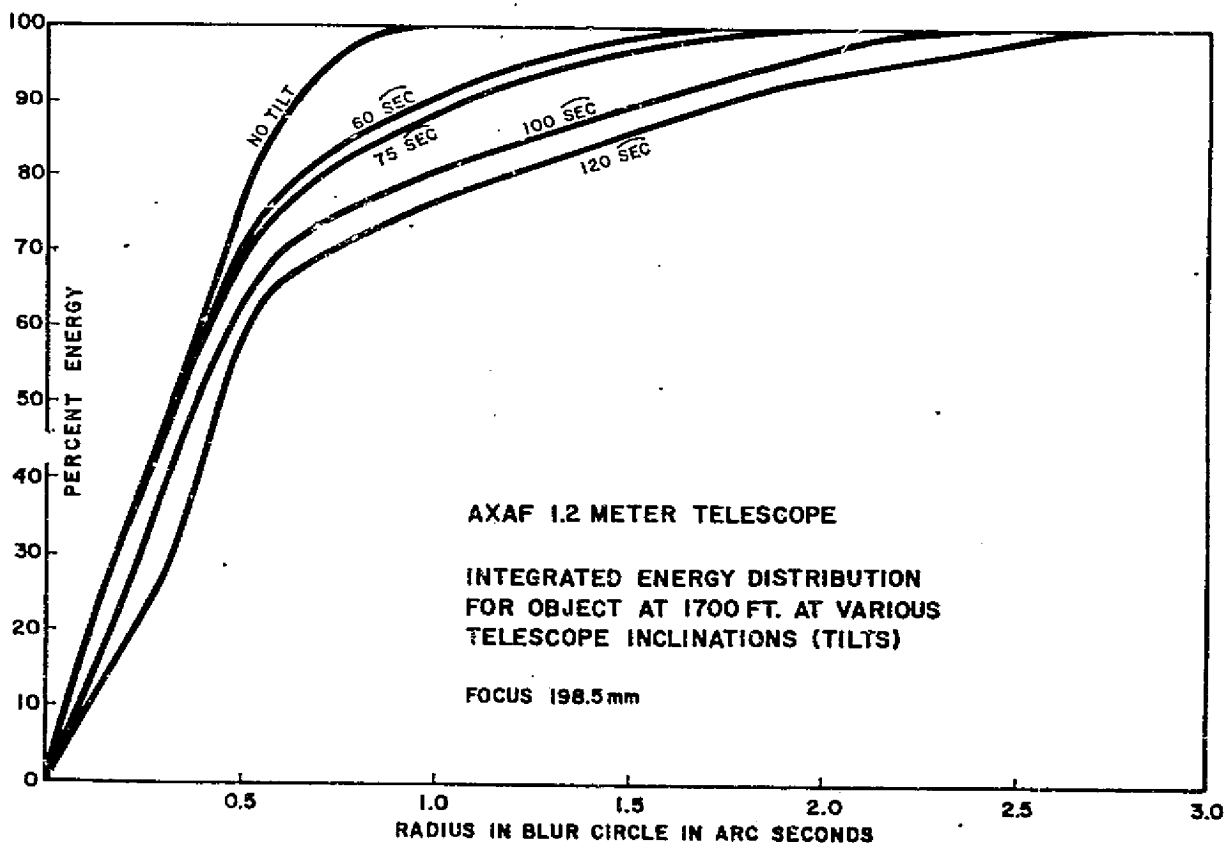

FIGURE 8-5

Effect Of Rotation About Node

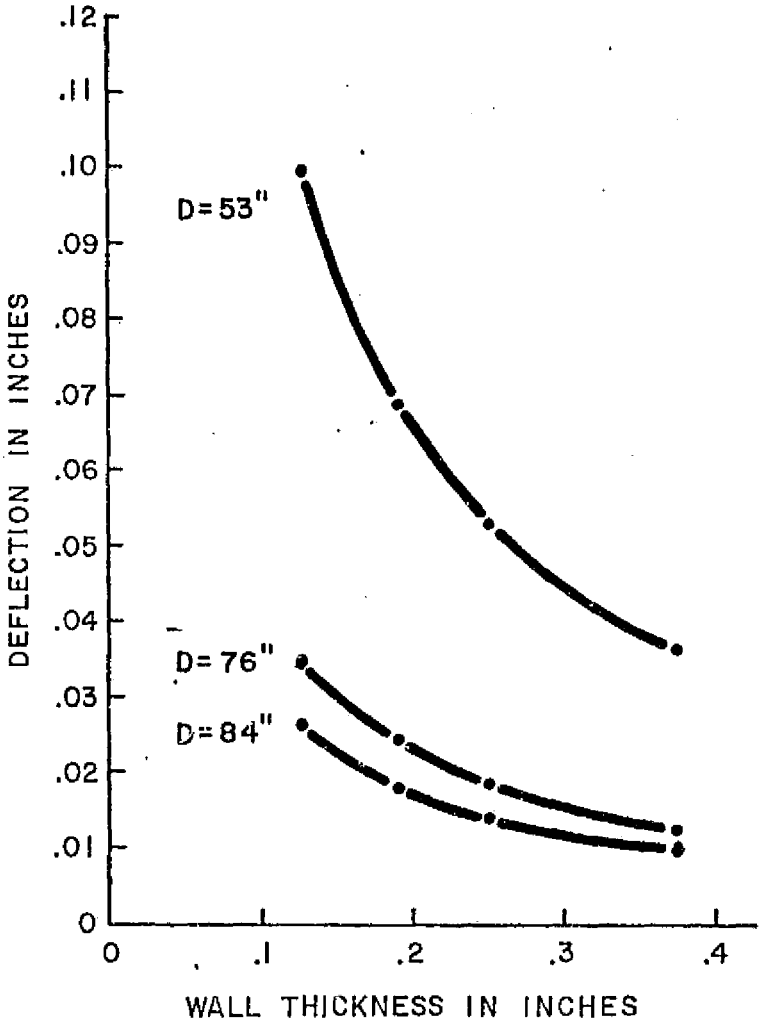

FIGURE 8-6

1 g Static Deflection

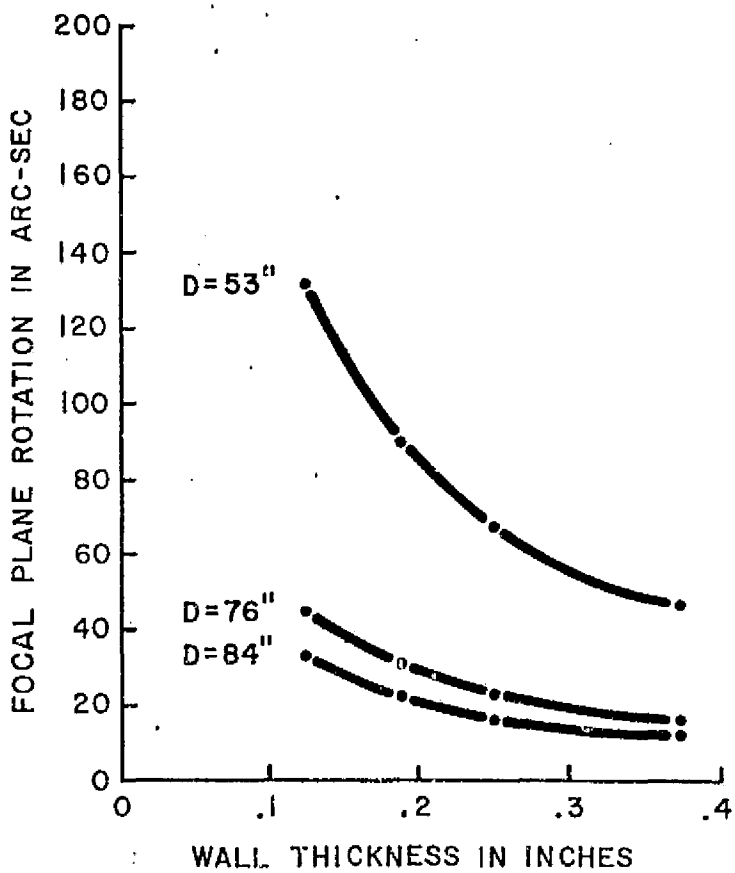

MATERIAL = GRAPHITE EPOXY
$\rho = .06\ \#/in^3$
$E = 16 \times 10^6$ psi

FIGURE 8-7

1 g Static Rotation

ORIGINAL PAGE IS
POOR QUALITY

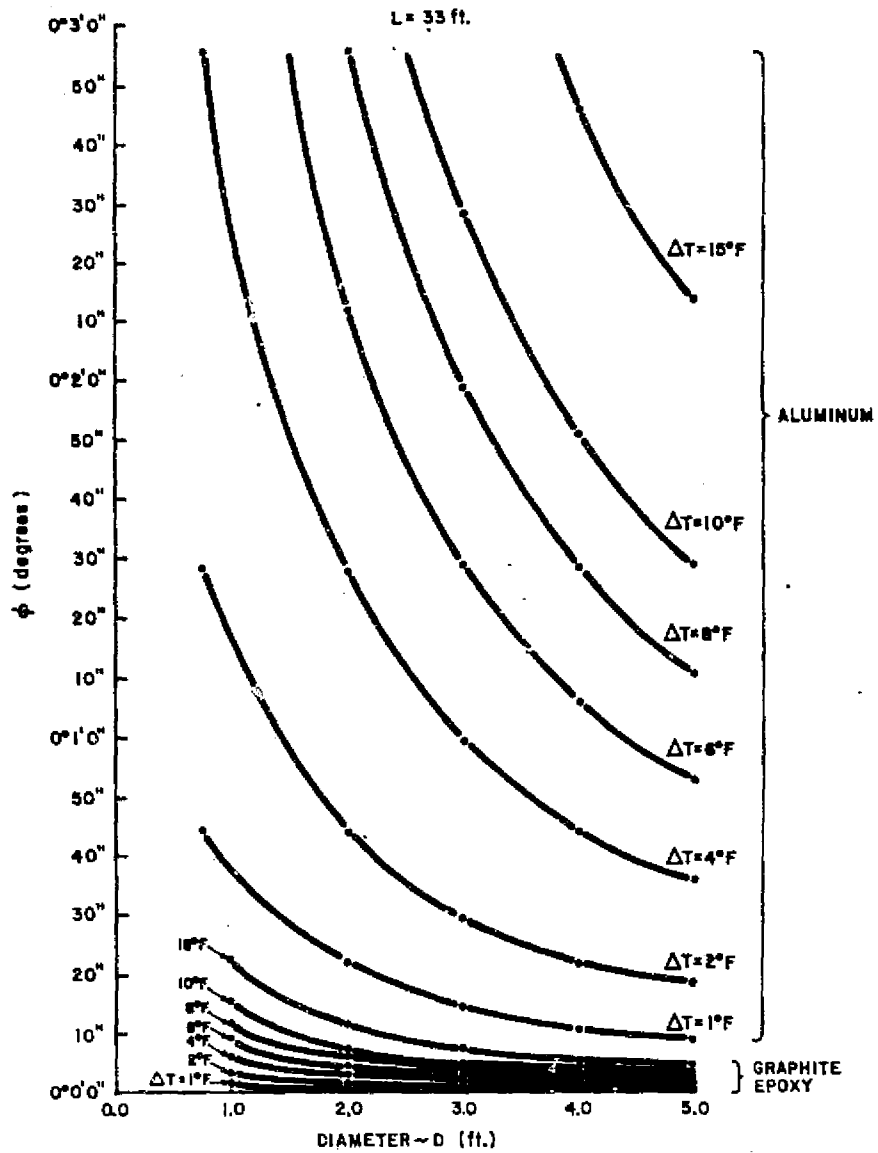

FIGURE 8-8

Hot-Dog Effects

quencies that are approximately equal. When the effect of the flange is included, resonances in the range of 15 Hz can be expected. With 1% damping, accelerations of the support must be less than 10^{-4} g to keep ΔR errors to about 0.1 arc-sec.

Vehicular traffic, rotating machinery, and possibly building and ground motion are potential sources of excitation. Study of the magnitude of the problem and some measurement of MSFC test facility vibrations appears appropriate.

9.0 TEMPERATURE CONTROL OF MIRROR ASSEMBLY

9.1 General

Temperature control of the mirror assembly is required in the fine sense to maintain optical figure and alignment tolerances and in the coarse sense to preclude excessive local stress levels due to differential thermal expansions.

At the outset of the SAO activity it was recognized that the mirror substrate material would not be selected until later in the program (certainly not before the completion of the optical technology flat program) and that a variety of optical bench structure concepts could be expected to emerge as various aerospace and optical houses begin to put forth their own ideas. Consequently, the initial emphasis has been on establishing insight and constraints that can be (and now are being) applied to more specific situations.

9.2 Thermal Control Concept Model

The basic concept examined is shown in Fig. 9-1. The objective is to establish a benign thermal environment for the mirror assembly and to isolate the X-ray Telescope Assembly from the outer S/C thermal shroud and the system support module. In the figure "active" is taken to mean either controlled heaters or variable surface properties (louvres, etc). Emphasis to date has been on the use of heaters alone to establish isothermal surfaces.

e concept is based upon:

1. Maintaining the mirror assembly at the same temperature at which manufacture, optical test, and

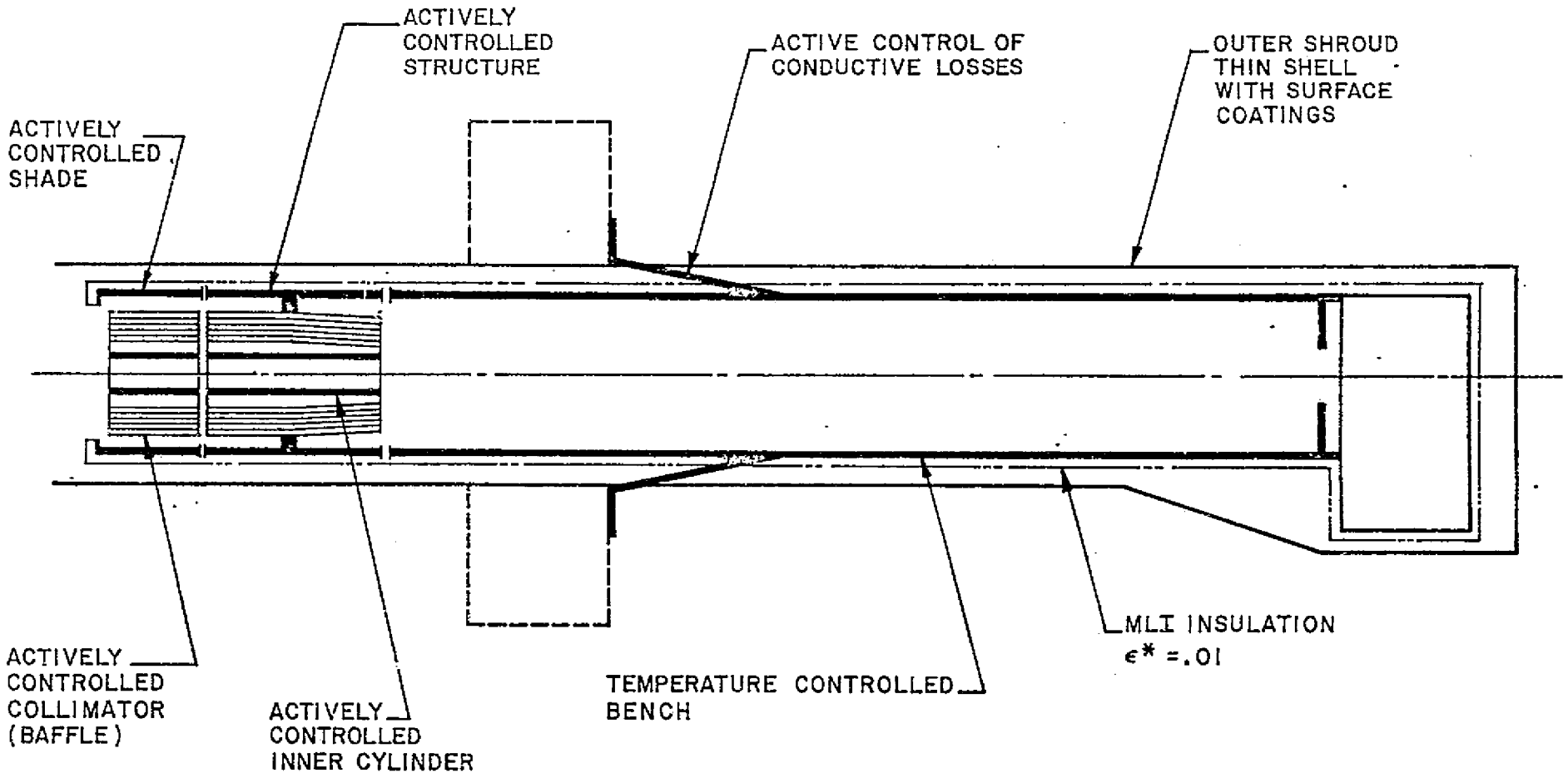

SIMPLIFIED THERMAL CONTROL CONCEPT

FIGURE 9-1

initial alignment takes place.

2. Isolation of the optical bench, front shade, etc. from the S/C outer thermal shroud with sufficient MLI to obtain an effective emissivity of .01 (1-2 inches of MLI) to control radiational transfer from the bench to the cold running shroud.

3. Control of the optical bench temperature by means of controlled temperature zones. Zonal organization is TBD and depends upon sensitivity and specific design details.

4. Control of bench and support directly around mirror assembly by controlled heaters. Heaters will not be placed on glass, but could be placed on G/E support sleeves if concept is utilized.

5. Control of inner thermal cylinder temperature with controlled heaters.

6. Control of shade temperature with controlled heaters.

7. Control of front thermal collimator/baffle temperature with controlled heaters.

8. Control of conductive losses through mounting flange (or equivalent structure) by active control (possibly heaters) if S/C runs colder than bench for all configurations.

9.3 Need For Optical Bench Control

The requirement for control of the optical bench temperature along its entire length is not of itself firmly established as a general requirement. There are three issues, however, that

must be recognized in any thermal design.

First, the distortions induced in the bench due to gradients and uniform temperature changes must meet the constraints of Section 8. In general, it appears that if G/E is used a great deal of latitude will exist and control of bench distortions will not be a major problem.

Second, the thermal equivalent of the temperature controlled optical bench as seen by the mirror could at least in principal be obtained by using a temperature controlled thermal baffle/collimator such as used on the front. However, all strawman AXAF configurations must allow for the placement of objective gratings which when "closed" are in close proximity to the rear (inner) surface of the mirror as well as spectral filters. These scientific requirements would cause the thermal baffle to be placed at least 1.5 feet away from mirror rear surface. The feasibility of a thermally effective baffle that does not "shadow" either directly reflected or, if the gratings are used, dispersed rays over the useful field of view of the AXAF requires study. This activity will be carried out by SAO in the next phase to resolve the issue.

Finally, the design of a wide variety of instruments over the life of the AXAF will be greatly simplified by the standard, uniform environment as will the prelaunch testing thereof. Although Fig. 9-1 does not show the bench establishing the focal plane environment except for the front assembly, the detailed design certainly could be extended to accomplish this.

In summary, if a cylindrical optical bench as recommended by MSFC is implemented it should be controlled over its entire length. Preliminary analysis indicates that a truss structure

will probably require the thermal equivalent of the total length cylinder (a separate controlled shroud) although much further study now in progress at SAO is necessary to resolve these issues.

9.4 Control Surface Effects

Regardless of the final design details it is important to understand the effects of the various "control" surfaces on maintaining uniform temperatures in the mirror assembly. Temperature distributions resulting from radiative transfer have been examined for a number of cases*. The model used is shown in Fig. 9-2. Eight axial nodes were established along each mirror element. Azimuthal symmetry is assumed. Results are shown in Figs. 9-3 through 9-7. The conclusion follows that all viewed surfaces must be controlled.

9.5 Baffle Studies

The thermal baffle length used in the analysis above was taken at 32 inches. The next step was to examine the effect of the baffle configuration on mirror assembly temperature gradients while holding all other control surfaces constant at 20°F. The results are shown on Figures 9-8 through 9-21.

Review of these results indicated that a 24 inch baffle will probably be acceptable. A more refined model of the 24 inch baffle was run with the results shown in Figs. 9-22 through 9-25. The aperture losses are shown in Fig. 9-26 for what are considered to be limiting values of ε.

---

*This work has been performed under SAO subcontract to Ernst, Armand, and Botti Associates.

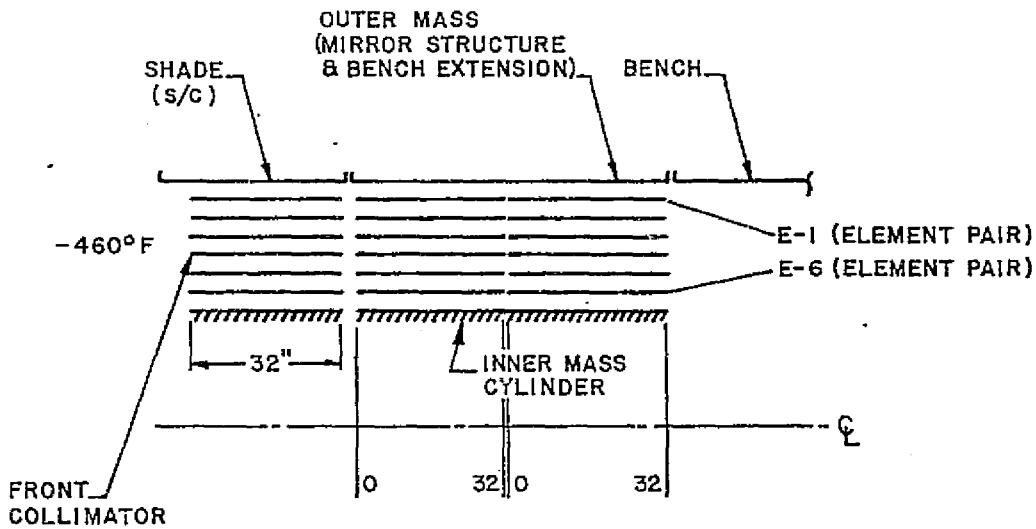

FIGURE 9-2

Model For Baffle Studies

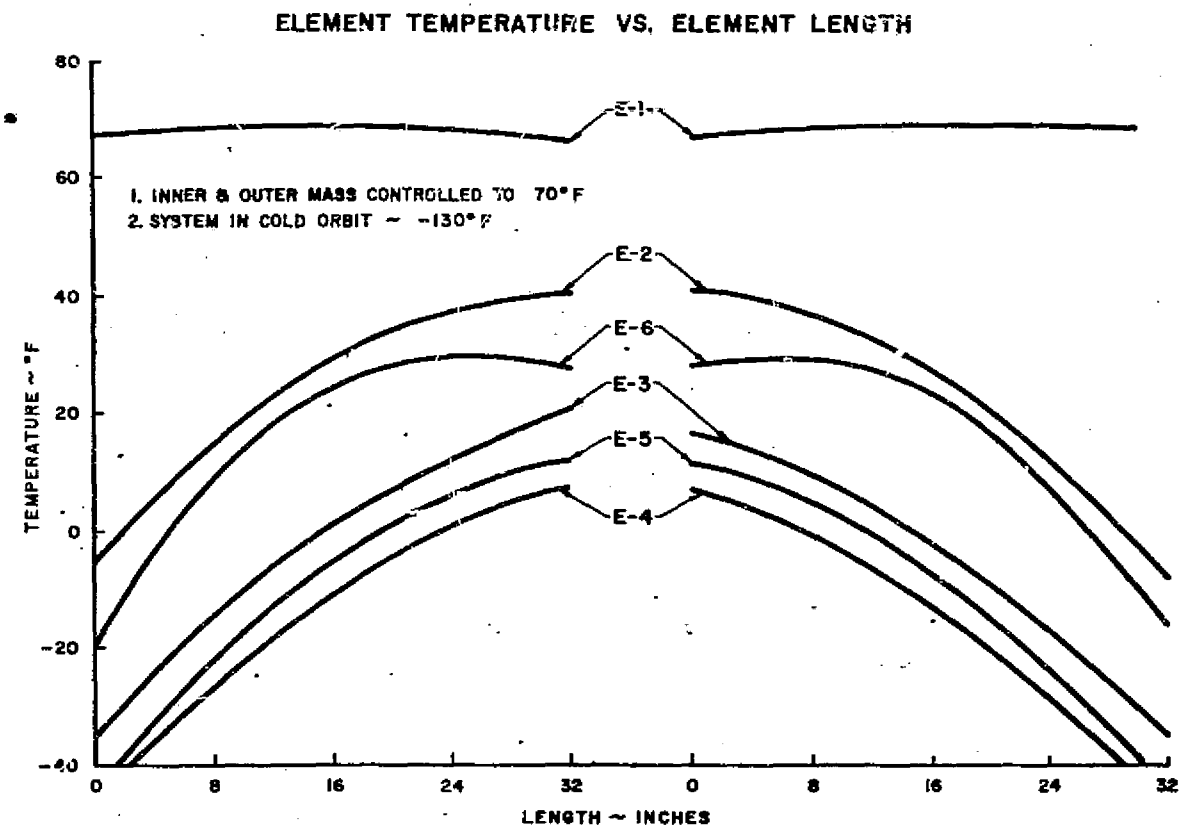
ELEMENT TEMPERATURE VS. ELEMENT LENGTH
1. INNER & OUTER MASS CONTROLLED TO 70°F
2. SYSTEM IN COLD ORBIT ~ -130°F
E-1
E-2
E-6
E-3
E-5
E-4
TEMPERATURE ~ °F
80
60
40
20
0
-20
-40
0
8
16
24
32
0
8
16
24
32
LENGTH ~ INCHES

FIGURE 9-3

C-2

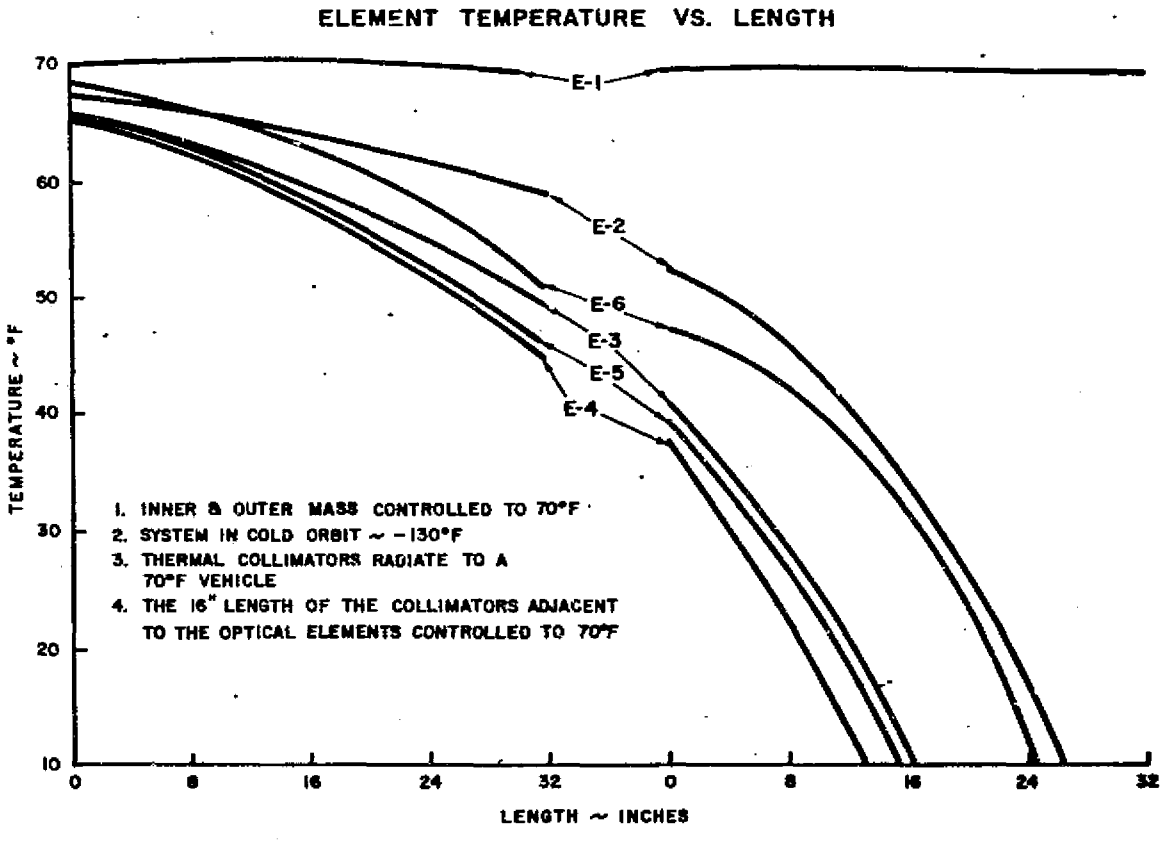
ELEMENT TEMPERATURE VS. LENGTH
TEMPERATURE ~ °F
70
60
50
40
30
20
10
E-1
E-2
E-6
E-3
E-5
E-4
1. INNER & OUTER MASS CONTROLLED TO 70°F
2. SYSTEM IN COLD ORBIT ~ -130°F
3. THERMAL COLLIMATORS RADIATE TO A 70°F VEHICLE
4. THE 16" LENGTH OF THE COLLIMATORS ADJACENT TO THE OPTICAL ELEMENTS CONTROLLED TO 70°F
0
8
16
24
32
0
8
16
24
32
LENGTH ~ INCHES

FIGURE 9-4

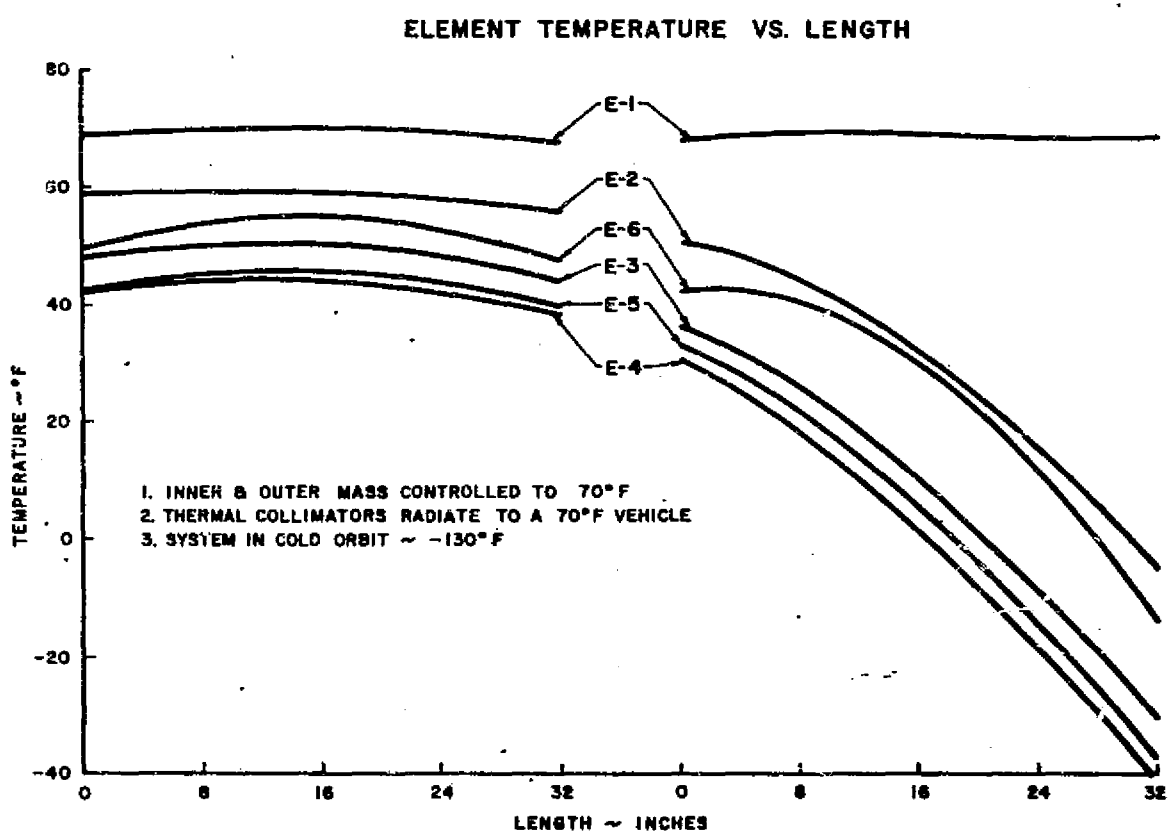
ELEMENT TEMPERATURE VS. LENGTH
TEMPERATURE ~ °F
80
60
40
20
0
-20
-40
E-1
E-2
E-6
E-3
E-5
E-4
1. INNER & OUTER MASS CONTROLLED TO 70°F
2. THERMAL COLLIMATORS RADIATE TO A 70°F VEHICLE
3. SYSTEM IN COLD ORBIT ~ -130°F
0
8
16
24
32
0
8
16
24
32
LENGTH ~ INCHES

FIGURE 9-5

ELEMENT TEMPERATURE VS. LENGTH

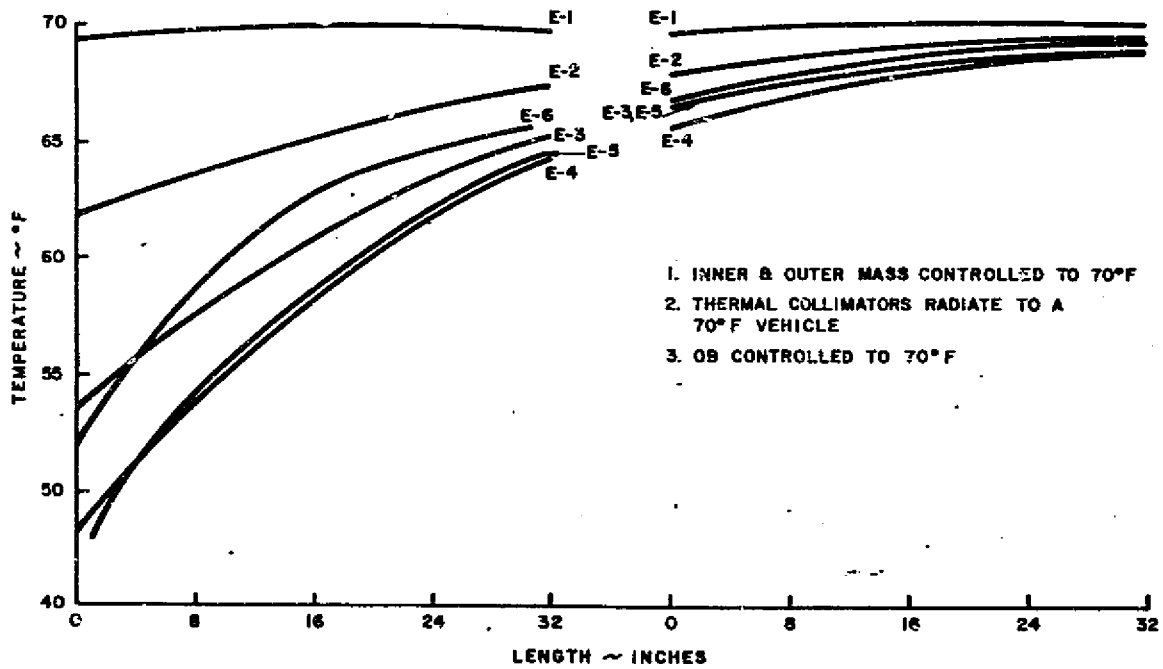

FIGURE 9-6

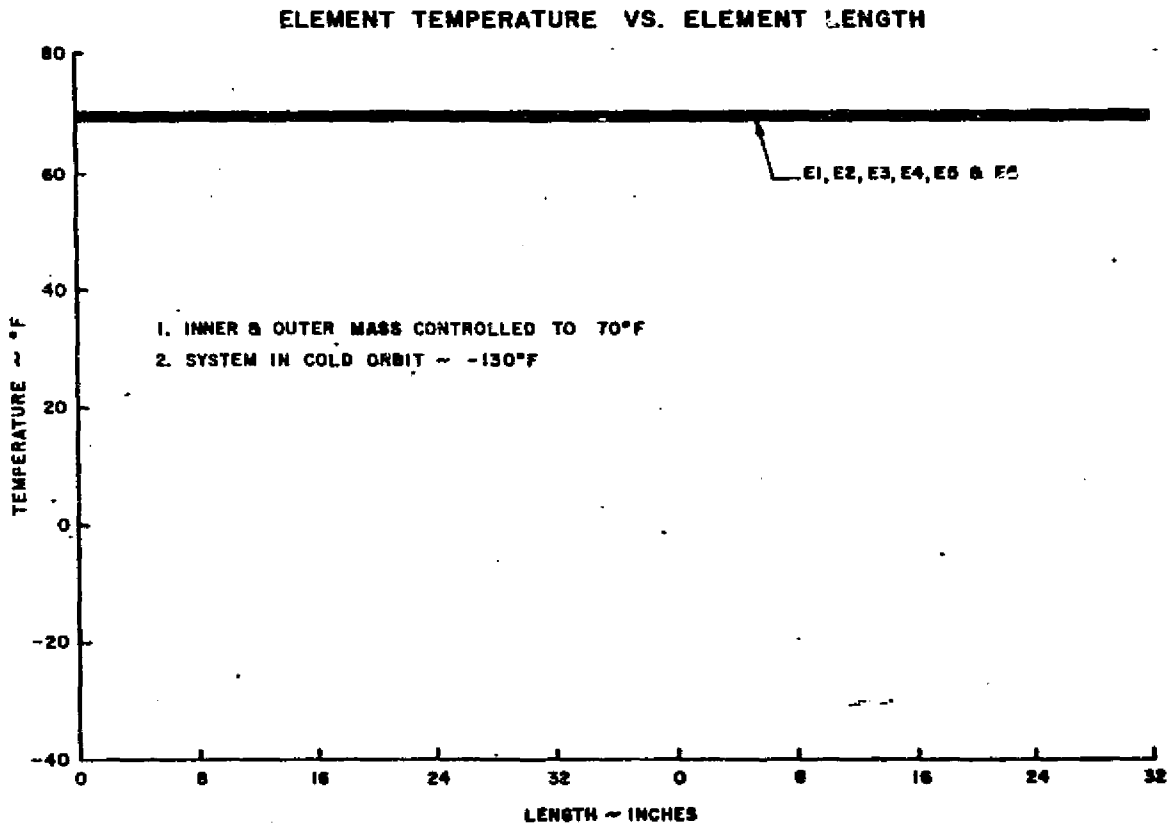
ELEMENT TEMPERATURE VS. ELEMENT LENGTH
80
60
40
20
0
-20
-40
TEMPERATURE ~ °F
E1, E2, E3, E4, E5 & E6
1. INNER & OUTER MASS CONTROLLED TO 70°F
2. SYSTEM IN COLD ORBIT ~ -130°F
0
8
16
24
32
0
8
16
24
32
LENGTH ~ INCHES

FIGURE 9-7

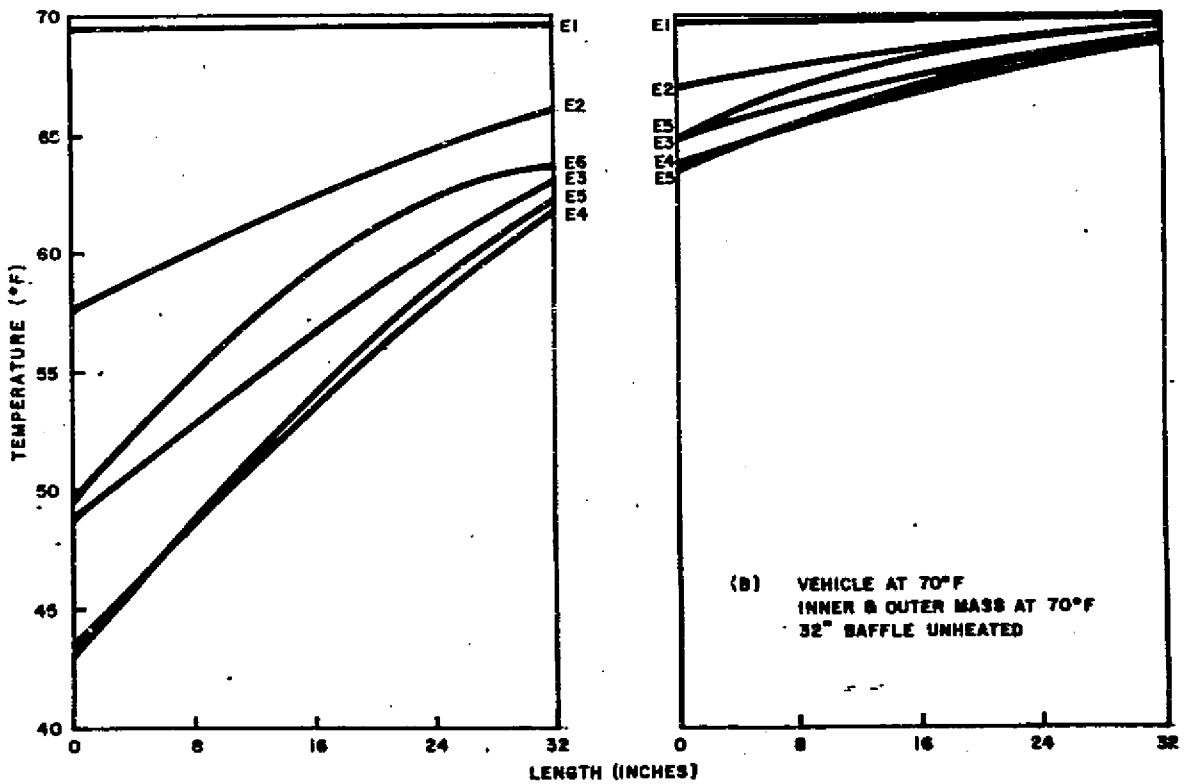

ELEMENT TEMPERATURE VS. ELEMENT LENGTH

FIGURE 9-8

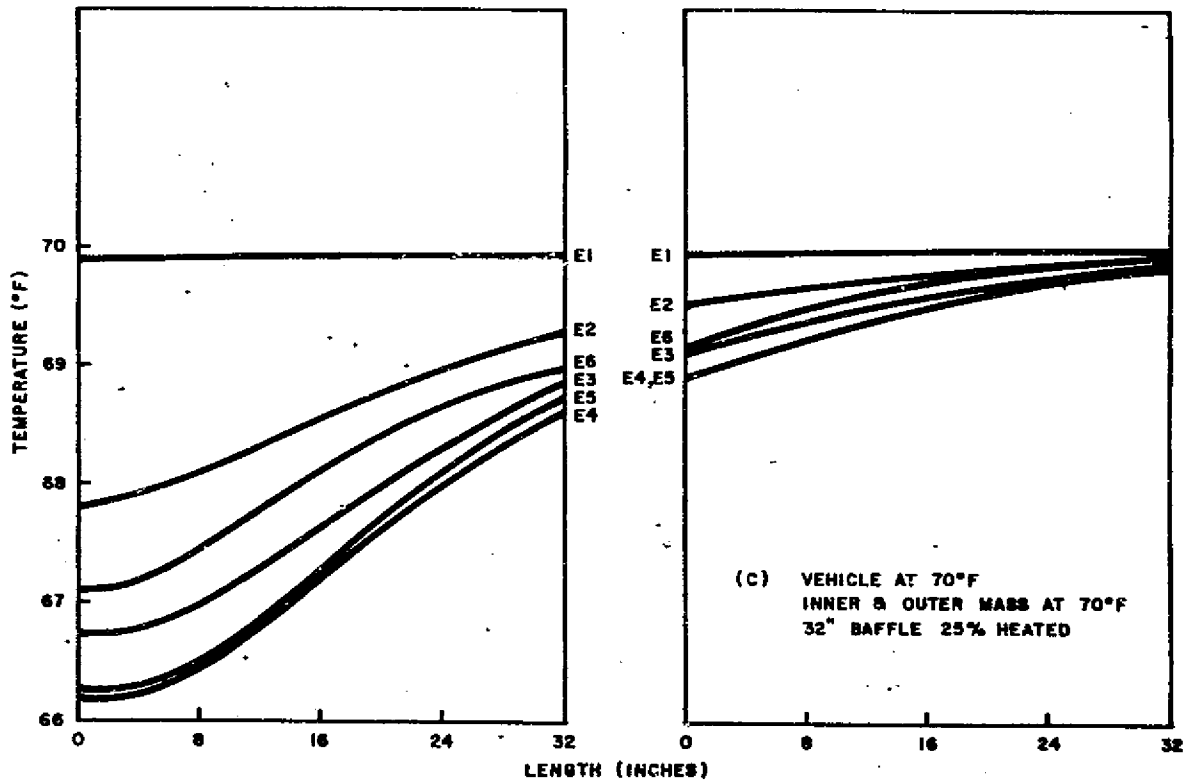

ELEMENT TEMPERATURE VS. ELEMENT LENGTH

FIGURE 9-9

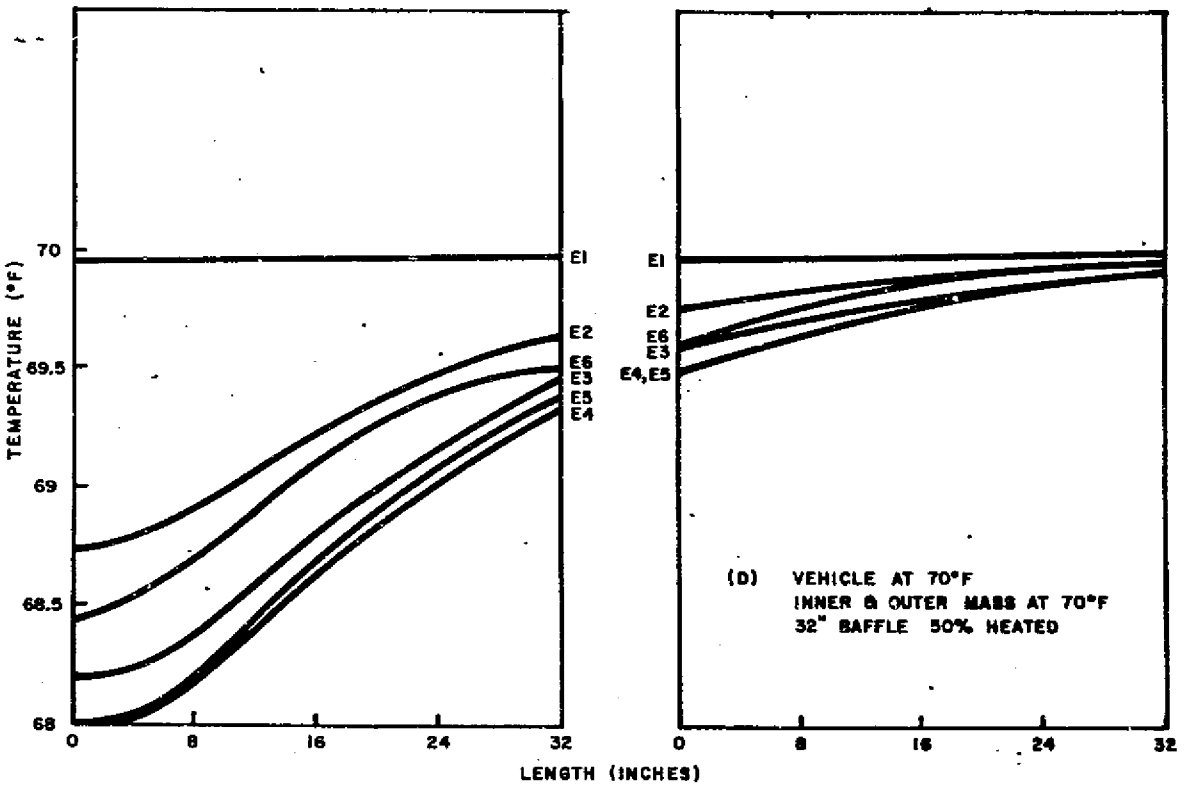

ELEMENT TEMPERATURE VS. ELEMENT LENGTH

FIGURE 9-10

ORIGINAL PAGE IS OF POOR QUALITY

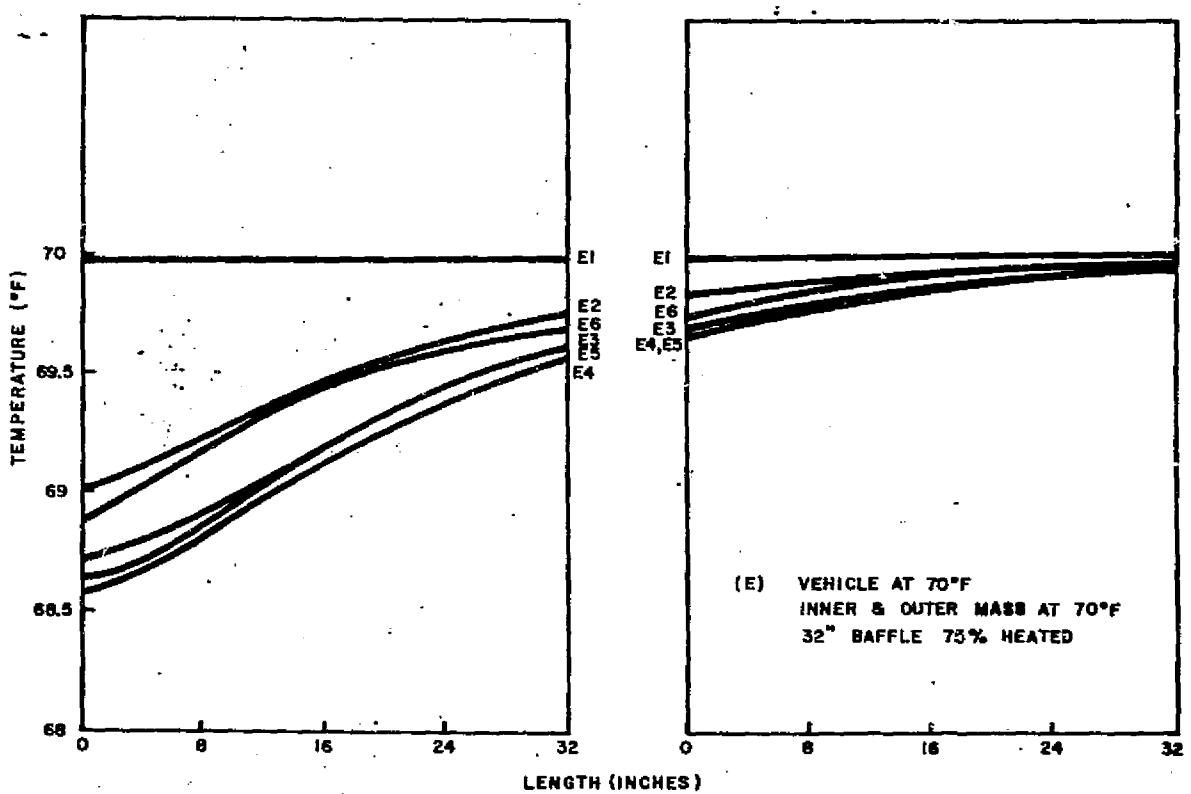

ELEMENT TEMPERATURE VS. ELEMENT LENGTH

FIGURE 9-11

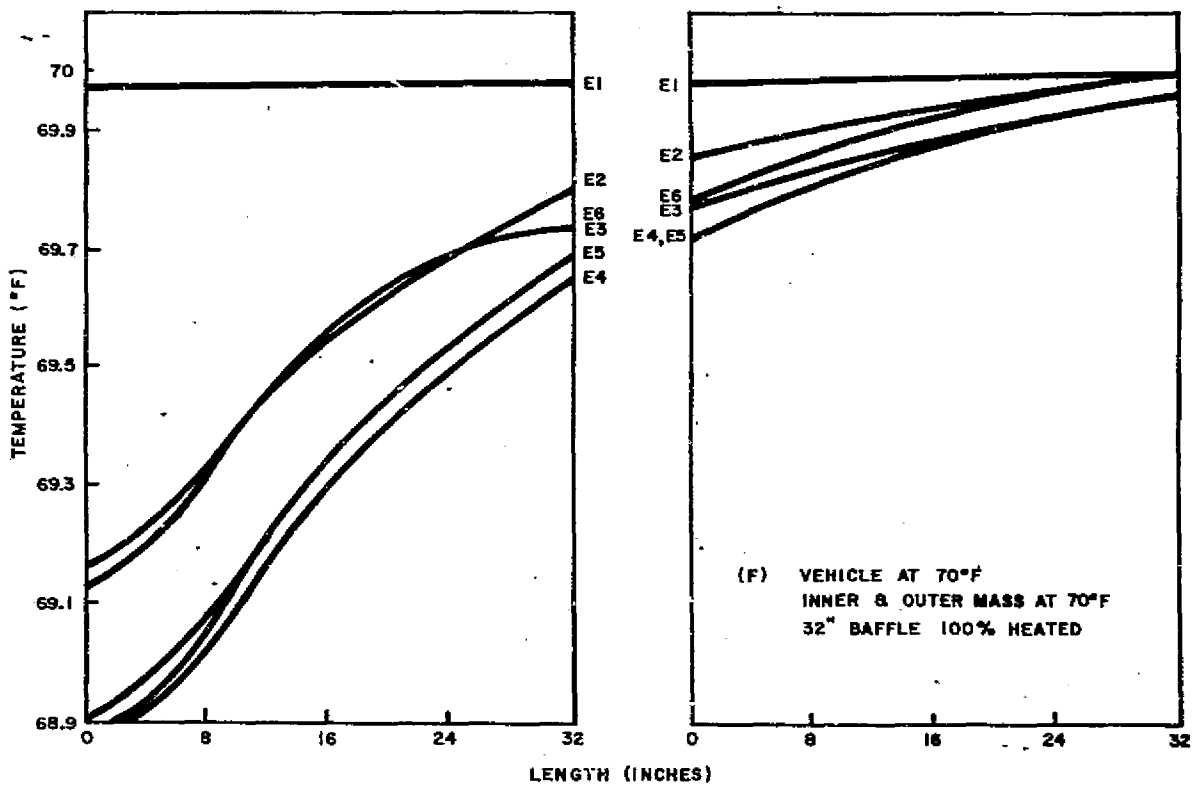

ELEMENT TEMPERATURE VS. ELEMENT LENGTH

FIGURE 9-12

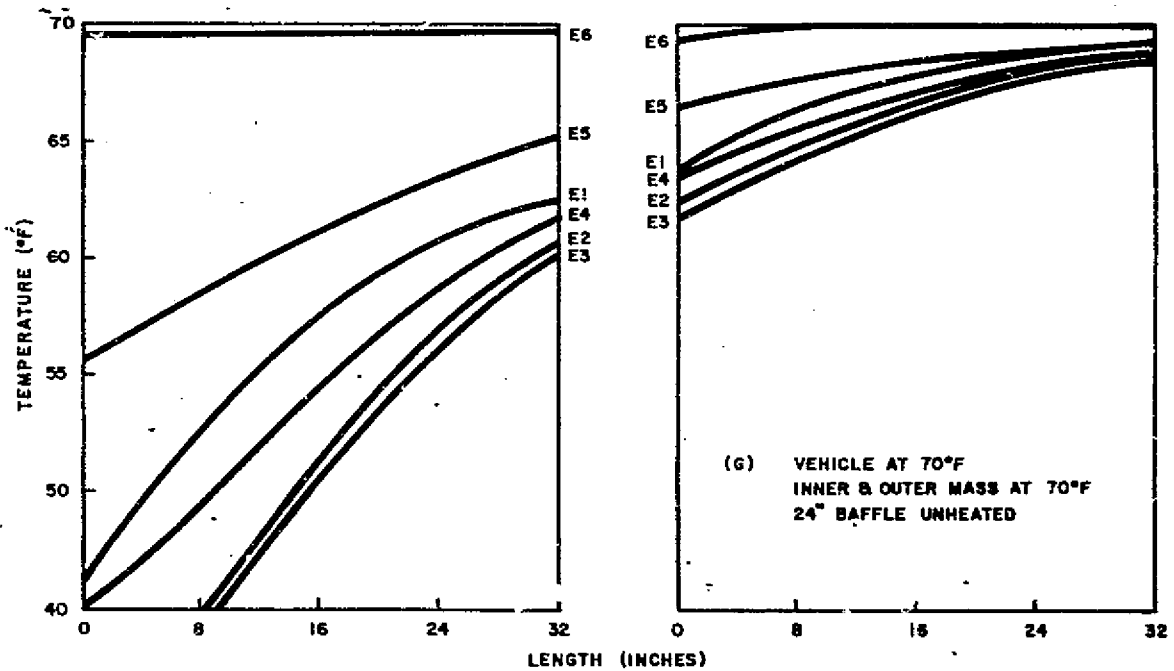

ELEMENT TEMPERATURE VS. ELEMENT LENGTH

FIGURE 9-13

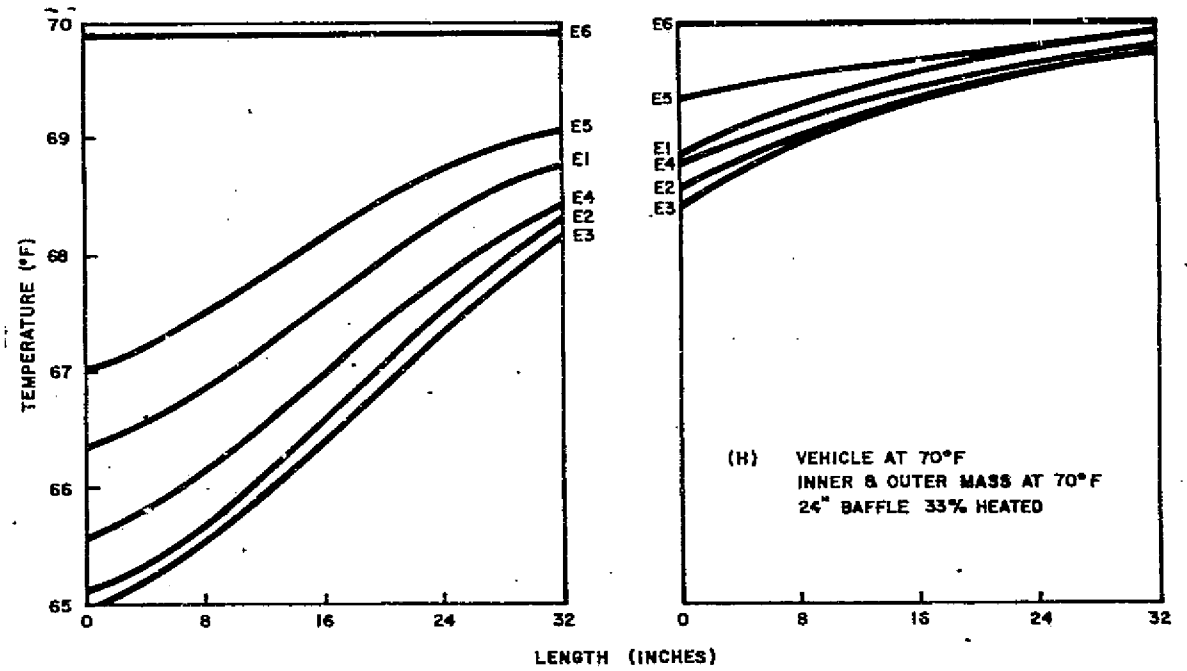

ELEMENT TEMPERATURE VS. ELEMENT LENGTH

FIGURE 9-14

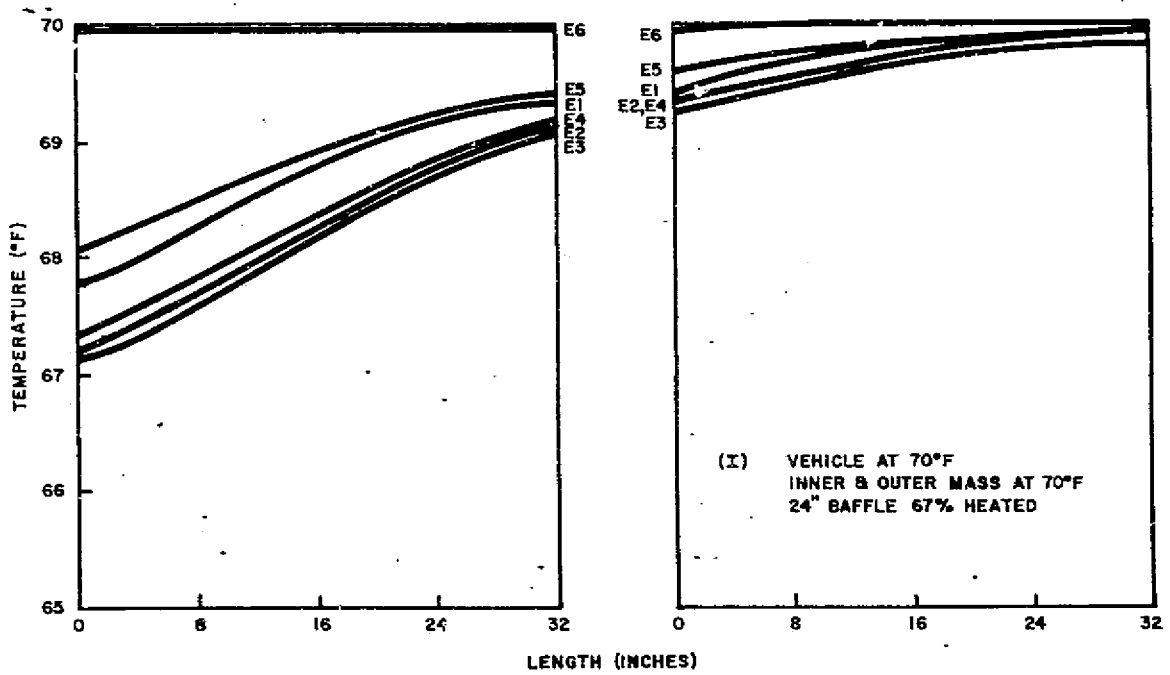

ELEMENT TEMPERATURE VS. ELEMENT LENGTH

FIGURE 9-15

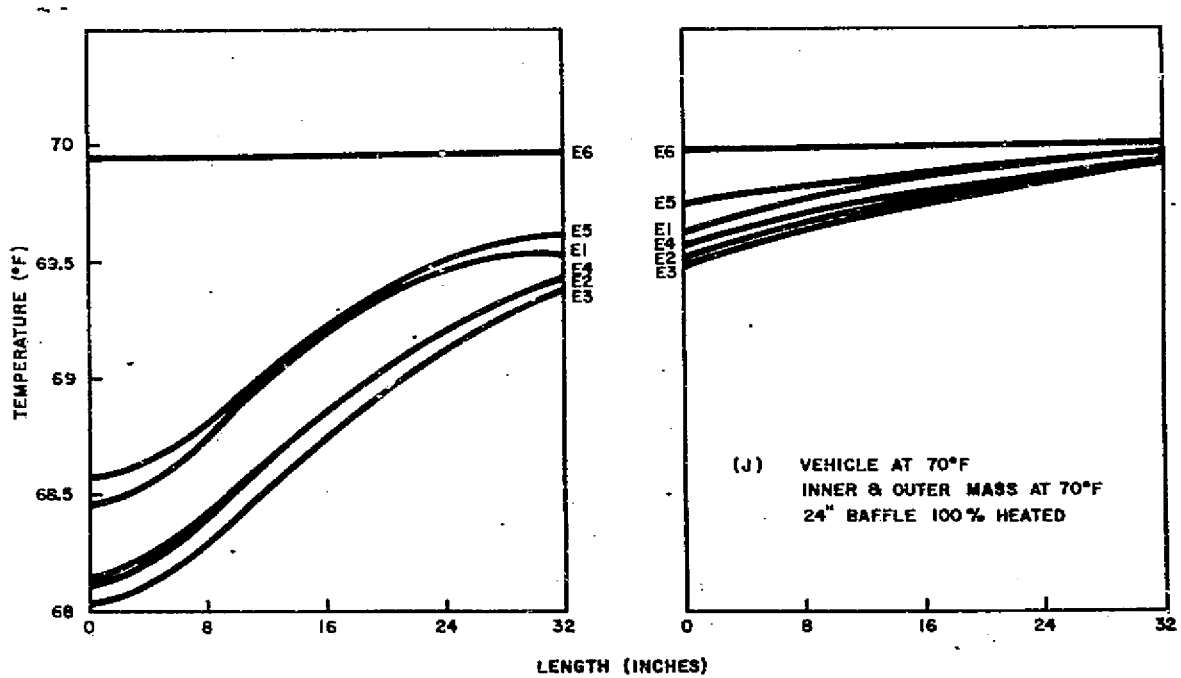

ELEMENT TEMPERATURE VS. ELEMENT LENGTH

FIGURE 9-16

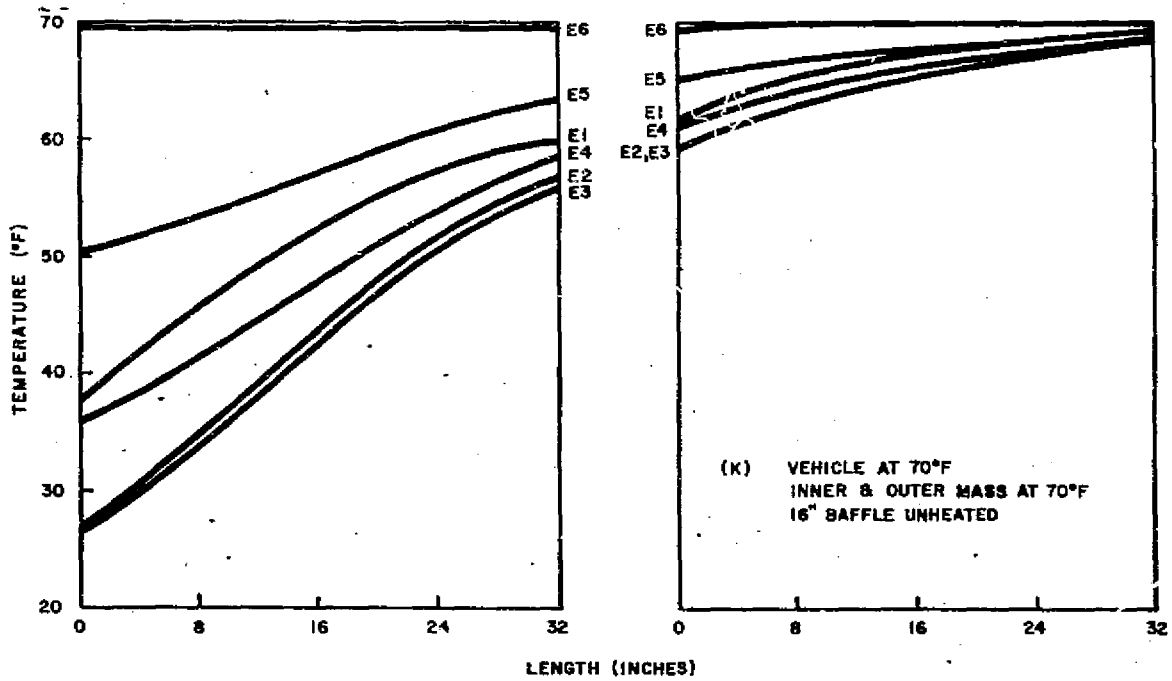

ELEMENT TEMPERATURE VS. ELEMENT LENGTH

FIGURE 9-17

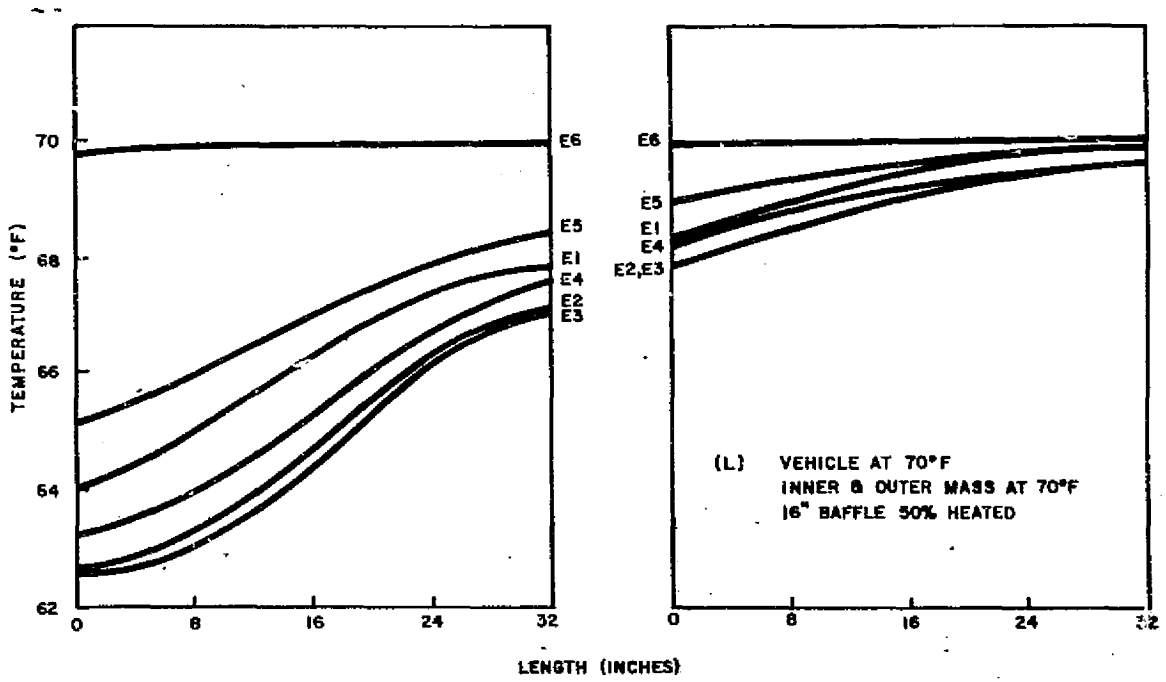

ELEMENT TEMPERATURE VS. ELEMENT LENGTH

FIGURE 9-18

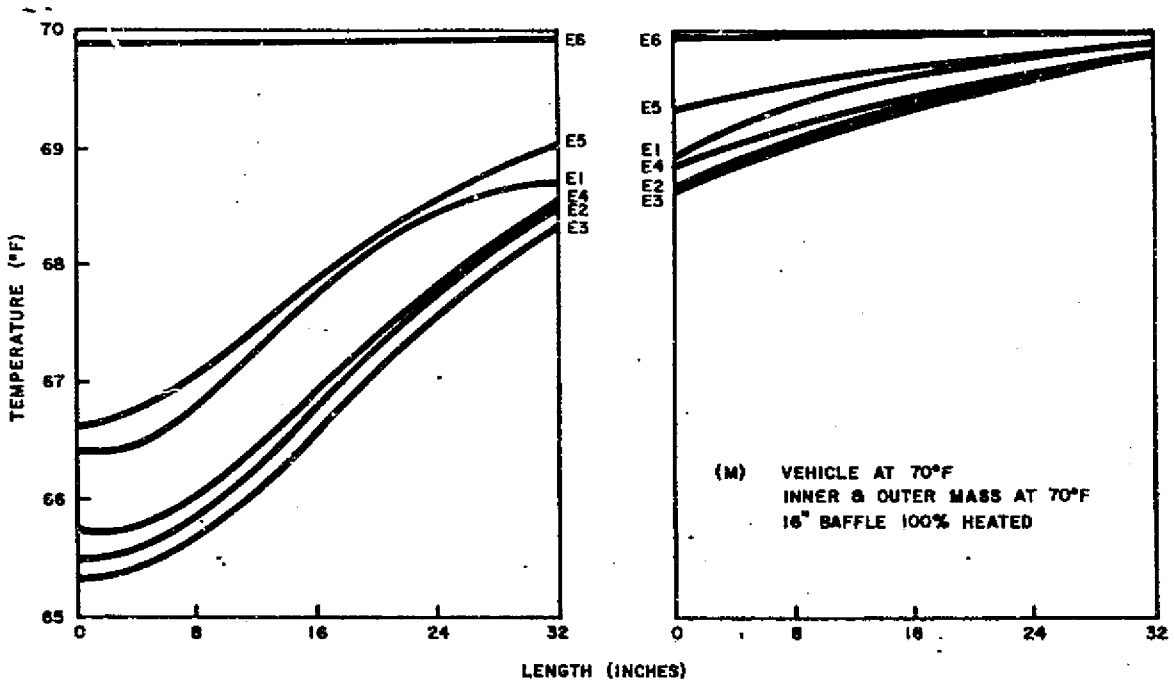

ELEMENT TEMPERATURE VS. ELEMENT LENGTH

FIGURE 9-19

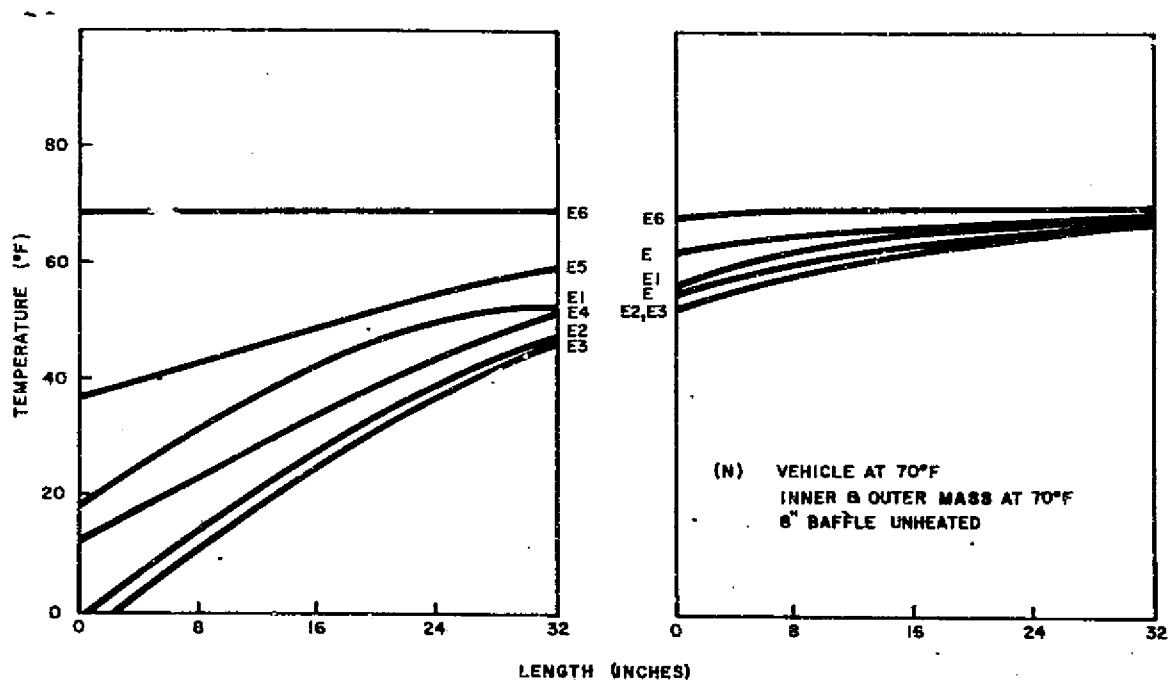

ELEMENT TEMPERATURE VS. ELEMENT LENGTH

FIGURE 9-20

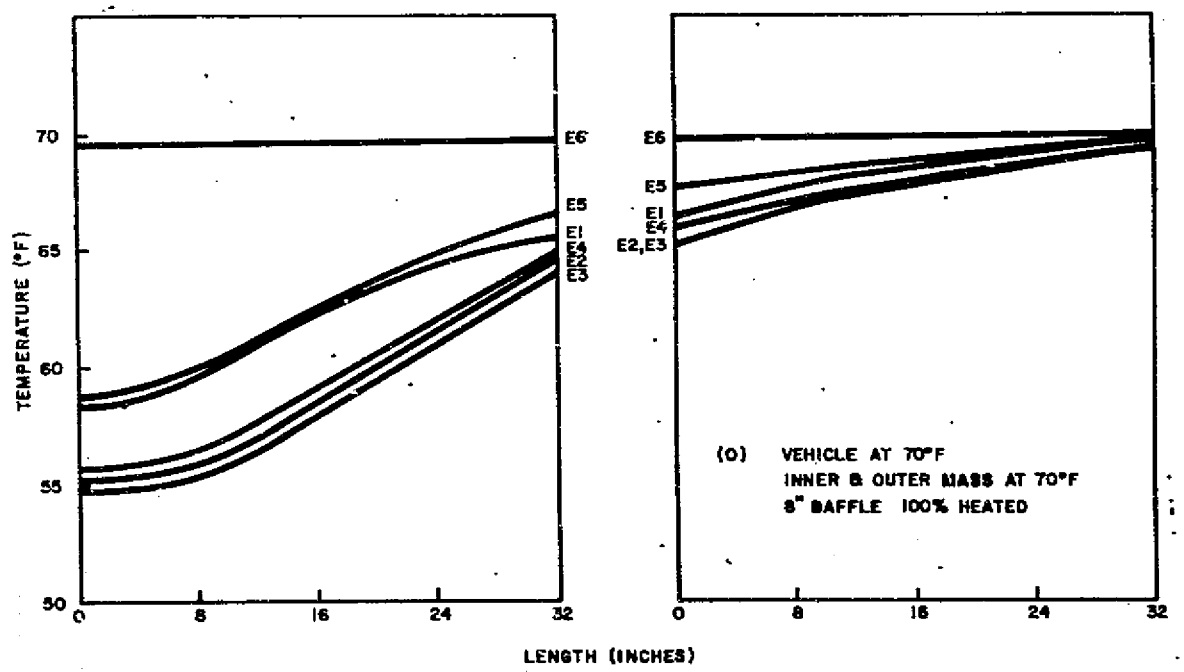

ELEMENT TEMPERATURE VS. ELEMENT LENGTH

FIGURE 9-21

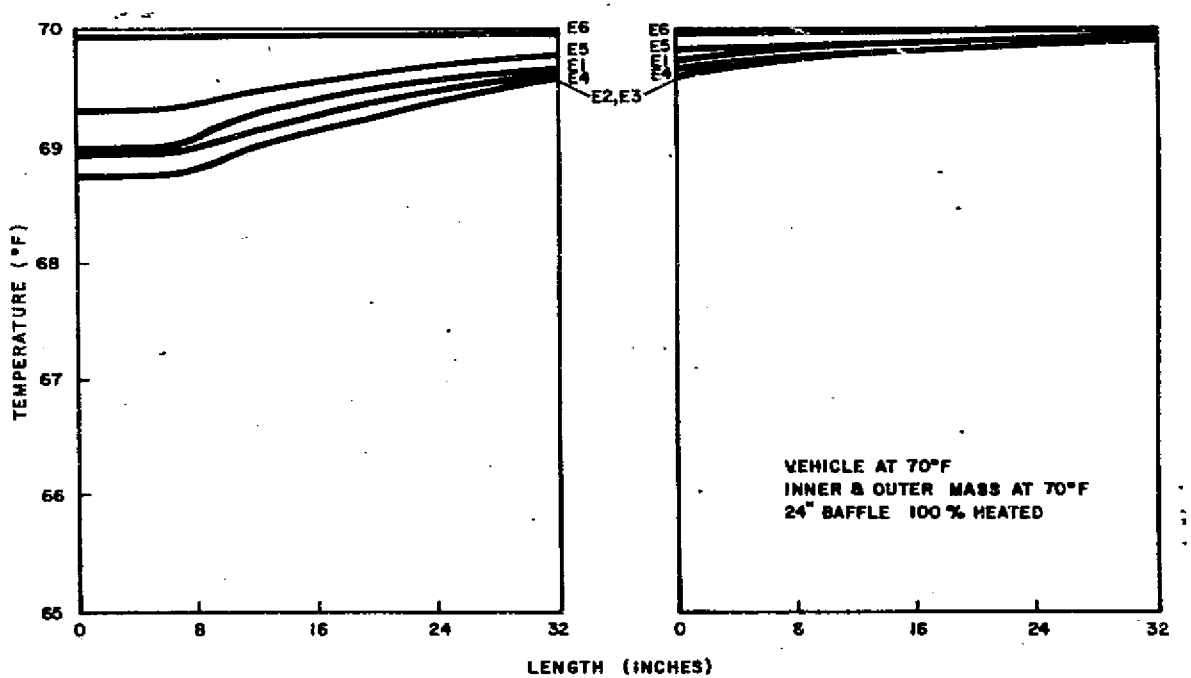

ELEMENT TEMPERATURE VS. ELEMENT LENGTH

FIGURE 9-22

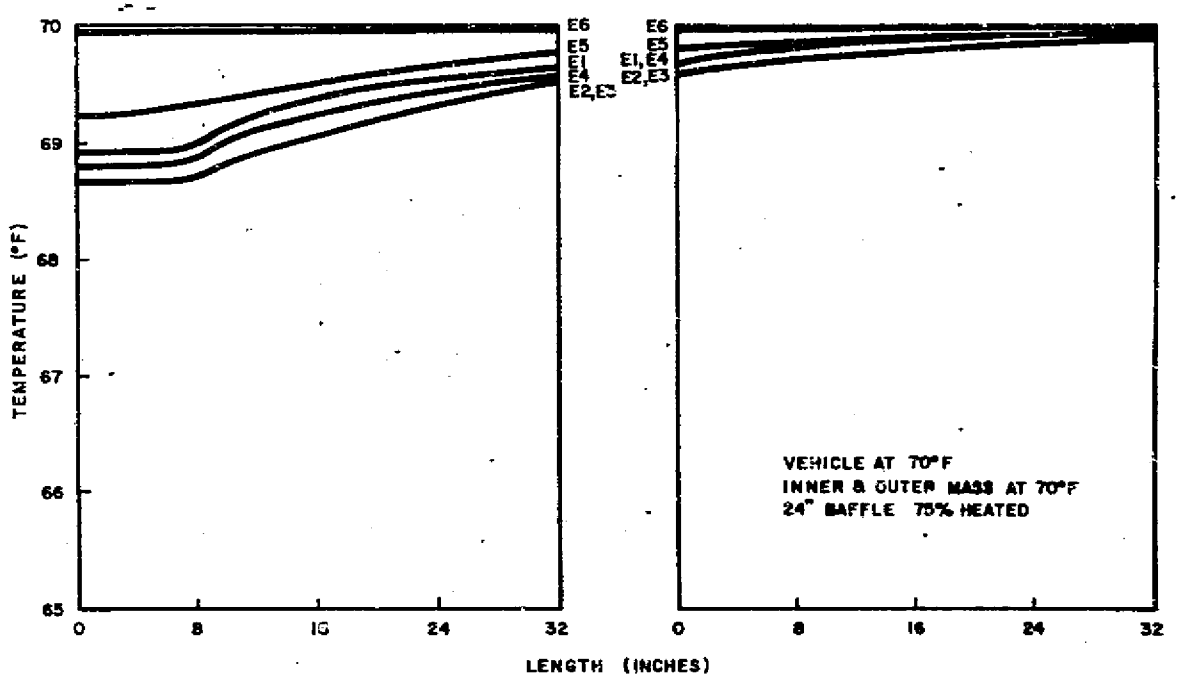

ELEMENT TEMPERATURE VS. ELEMENT LENGTH

FIGURE 9-23

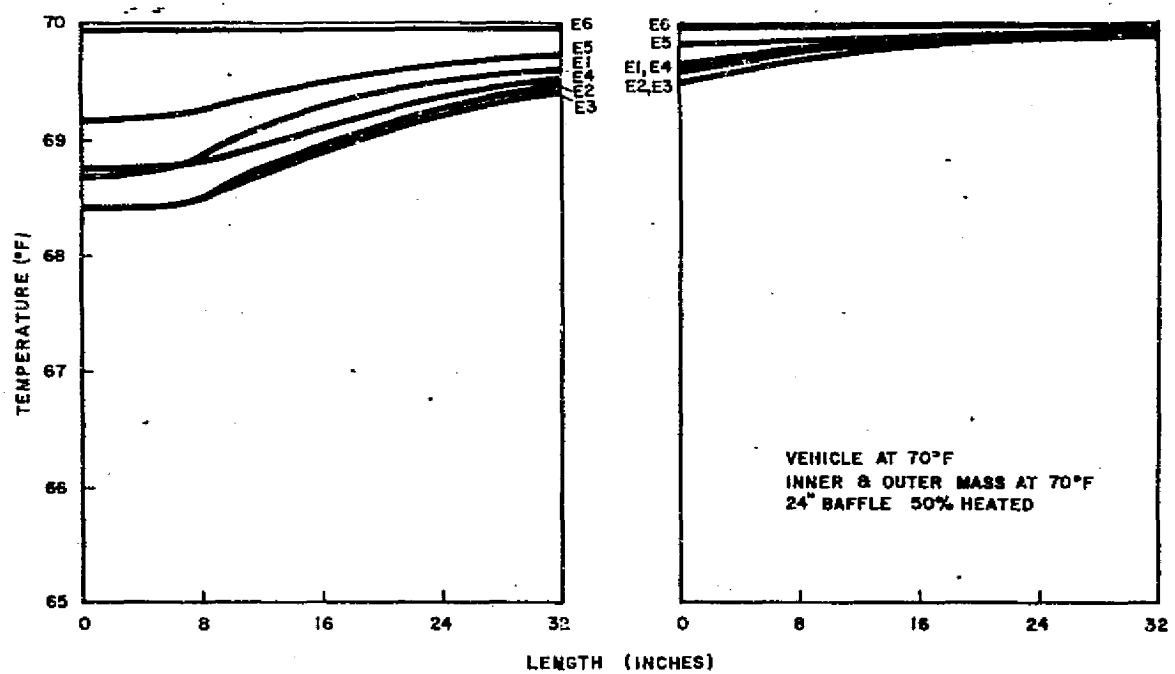

ELEMENT TEMPERATURE VS. ELEMENT LENGTH

FIGURE 9-24

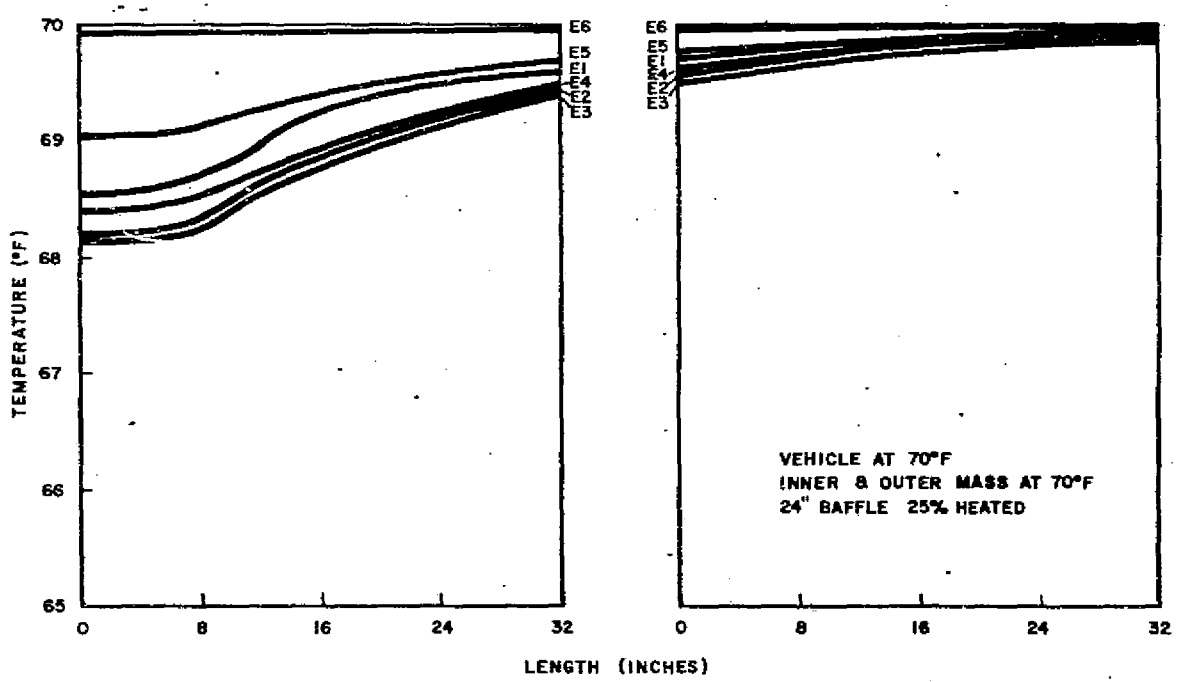

ELEMENT TEMPERATURE VS. ELEMENT LENGTH

FIGURE 9-25

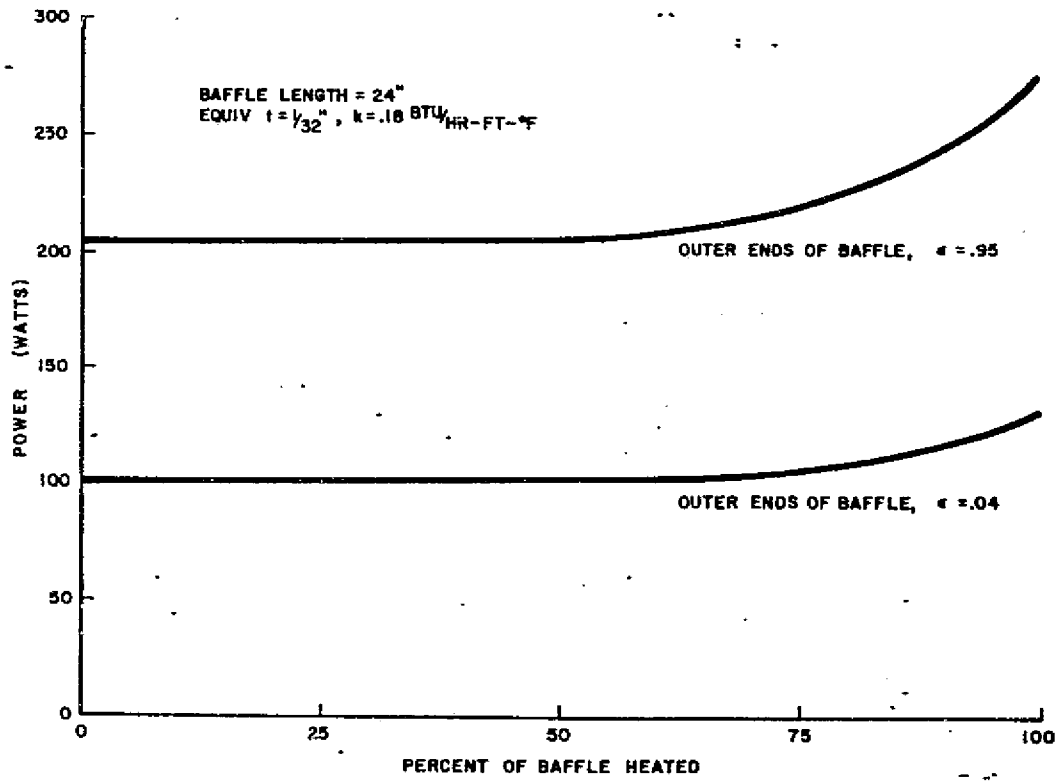

APERTURE POWER LOSS
VS.
PERCENT OF BAFFLE HEATED

FIGURE 9-26

10.0 ASPECT DETERMINATION SYSTEM

10.1 General

X-ray imaging of weak sources can require long observations encompassing many orbits during which changes of up to 30 arc-seconds in the AXAF optical axis pointing vector can occur (by the present strawman specification). Thus, even though the source is fixed in celestial coordinates, the detected events will be spread over the image plane by the vehicle motion during the observations. In order to reconstruct an X-ray image it is necessary to refer the point in the image plane at which the event was detected back to an apparent source position in celestial coordinates. This means that the instantaneous optical axis must also be reconstructed in roll, pitch, and yaw. Therefore, aspect data which reference the position of the X-ray image to the celestial sphere are truly part of the scientific data. A key point is that image reconstruction will, at least in general, be performed on the ground. Aspect solution can therefore also be post facto.

If the source viewed is a point source, the reconstructed image will have a spread determined principally by the resolution of the X-ray mirror (scattering), the uncorrectable effect of system motions, the resolution of the X-ray detector used, and the relative accuracy of the total aspect determination system. The present goal is to ensure an aspect solution whose relative accuracy is 0.5 arc-sec. Work to date indicates that such an accuracy approaches state of the art. Consequently, the aspect determination system is, along with the mirror assembly, the major system driver and an area requiring a great deal of study.

10.2 Aspect Determination System (Baseline)

The AXAF Aspect Determination System (ADS) is a system which includes but need not be limited to the items in Table 10-1.

The basic concept consists of thre elements:

1. Appropriate fine aspect sensors mounted in a stable and well defined way to the mirror assembly view the sky and projected fiducial lights (targets) from the focal plane.

2. Fiducial lights and associated optics refer radial motion of the focal plane to the axes of the fine sensors.

3. System absolute alignment is determined on-orbit by viewing known X-ray sources which have well defined and located optical (visible) counter parts.

Examination and estimation of ADS performance must take into account all portions of the system which can contribute to its inaccuracy. Fig. 10-1 shows the major elements to be considered. Realization of the 0.5 arc-sec relative accuracy goal depends upon the understanding and control of all the interrelated phenomena and effects.

Work to date at SAO has concentrated on the fine aspect sensors and fiducial calibration system with major emphasis being given to the sensors *per se*. This activity, however, is now being expanded to include other system considerations such as mechanical and thermal stability. Already the on-going HEAO-2 (Einstein) aspect determination activities are providing useful

TABLE 10-1

Aspect Determination System Elements

1. Fine Aspect Sensors
2. Fiducial System
3. Control/Data System
4. Auxiliary Sensors (if req'd)
5. Sensor Interconnecting Structure/Mount
6. Star Catalog/Plates
7. Simulation Software
8. Processing Software
9. Attitude Control System (if req'd)

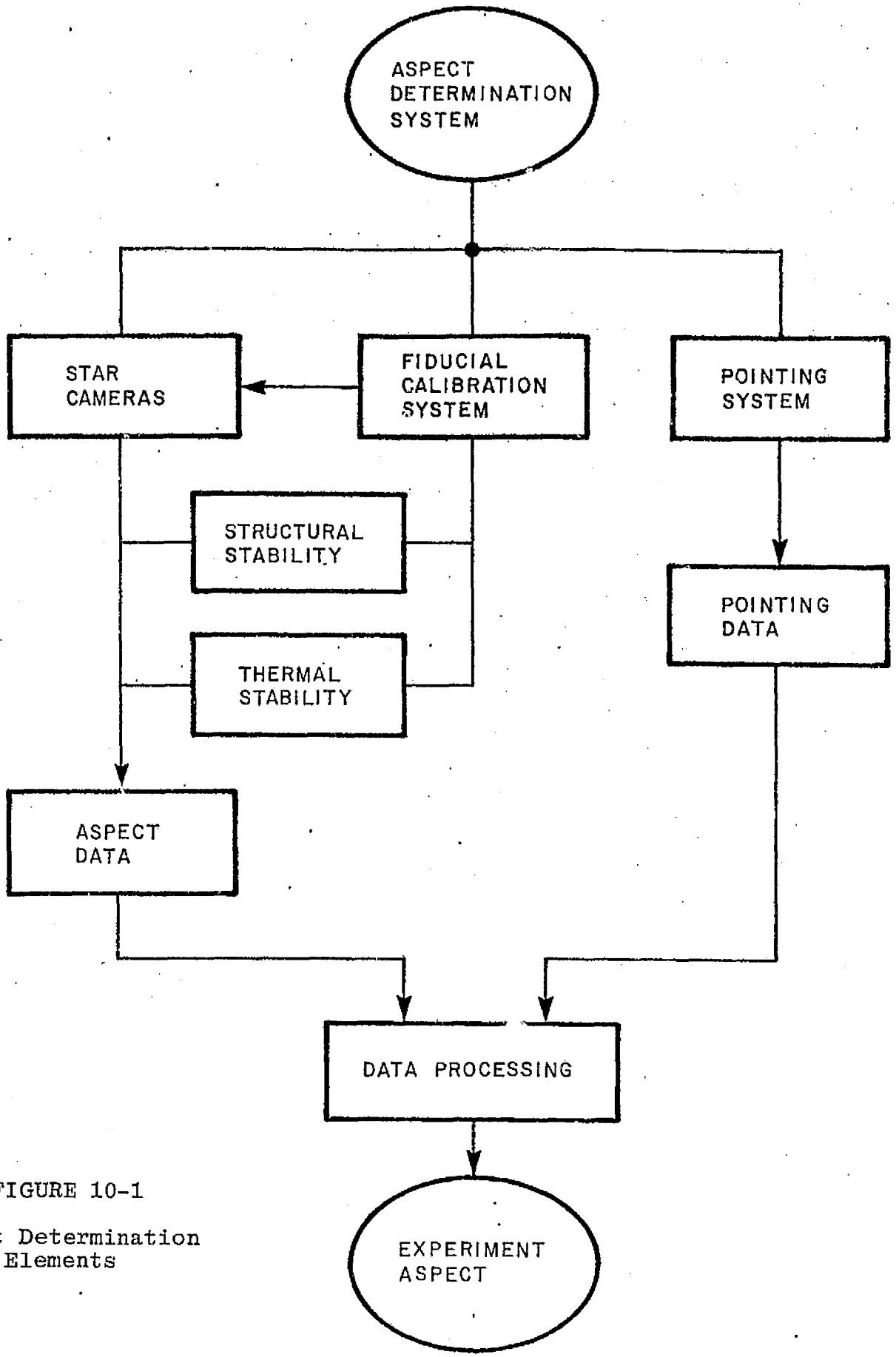

FIGURE 10-1

Aspect Determination Elements

insight and guidelines for improving total system performance to the levels required by the AXAF mission.

10.3 Control Of Focal Plane Motion

If uncalibrated, one of the major contributors of error in the aspect solution is radial motion of the focal plane with respect to the mirror optical axis. Such motions can be caused by a wide variety of effects such as optical bench bending from thermal or vibrational forces and mounting compliances.

Motions which are slow enough can be "tracked" by the fiducial system. Here "slow" simply means slow enough to be tracked by a feasible fiducial system/aspect sensor combination with reasonable data rates. For purposes of this study, such motions are considered to be limited by design to less than .010 inch which corresponds to about 5.0 arc-sec in the focal plane. As indicated in previous sections, such a constraint appears entirely feasible, at least in the context of concepts examined to date. However, in order to track such motions it is necessary to use the fiducial system regularly and possibly continuously. This situation directly drives the aspect sensor selected for use and results in a desired characteristic of (if not a firm requirement for) multiple target viewing capability.

High frequency motions are defined as those which are too fast to track with whatever fiducial system is implemented. These motions have been assumed to be constrained to values less than .0002 inch (~ 0.1 arc-sec). This situation sets a constraint on optical bench and other dynamics and establishes a requirement for detailed simulation studies of on-orbit dynamic behavior. It probably establishes a viable basis for the comparison of various X-ray Telescope Assembly configurations.

10.4 Preliminary Error Budget

A preliminary error budget has been established as follows:

Fine Aspect Sensor	0.3 arc-sec
Fiducial System & Structural Stability	0.2 arc-sec
Effect Of "Fast Motions"	0.1 arc-sec
Sampling Error Due To S/C Motion	0.1 arc-sec
Electronic To Spatial Transformation	0.1 arc-sec

The RSS error is less than 0.5 arc-seconds when the requirement for at least two aspect sensors is included. Although some of the error terms or components are systematic, because of their variability with time, the RSS combination is appropriate.

The error budget deals with relative accuracy. This means the degree of repeatability with which source locations can be reconstructed with respect to each other and with respect to fixed stars. Absolute accuracy requires knowing the relation between the X-ray telescope instantaneous axis and fixed stars whose position is well established. In practice, this will be done by viewing an X-ray source which is also an accurately located optical source. There are comparatively few such sources at present, but HEAO-2 (Einstein) can be expected to significantly increase the number of available "bore-sight" X-ray sources. The absolute position or aspect accuracy will be determined by the absolute accuracy of the optical position determination. This can be expected to be less than 0.5 arc-seconds. Thus, at present, SAO is pursuing its systems studies in the context of the stated goals of 0.5 arc-sec post facto relative accuracy and 1.0 arc-sec post facto absolute accuracy.

10.5 Fine Aspect Sensor Studies

10.5.1 General

Regardless of the final ADS configuration, a requirement will exist for precise, accurate and stable star sensors. Initial study activities were directed towards answering three questions:

1. could image dissector tube* (IDT) sensor performance meet or be extended to meet the AXAF objectives?

2. do alternative sensors exist or could they be developed?

3. would such alternate sensors offer improved performance re the IDT and would they meet the AXAF requirements?

The first result of these considerations was that the IDT sensor is not feasible for the AXAF application. Secondly, preliminary analysis showed that Charge Coupled Device (CCD) sensors can, with some development, meet the AXAF requirements. Recent developments at General Electric make the Charge Injection Device (CID) another potential candidate. SAO conducted a survey of a significant amount of CCD activity as summarized in Table 10.2.

---

*In the context of these studies, IDT is the ITT4012 unit used in the NASA Std Tracker, Shuttle Tracker, HEAO-2 tracker, HEAO-1 tracker, and SAS-3 tracker. It is the only available viable candidate.

TABLE 10-2

CCD Activities

Array Development/Production	Sensor System Development
Fairchild	Ball Aerospace Systems Division
Texas Instruments	Rockwell
RCA	Hughes
Rockwell	Honeywell EOC
Itek/Northern Bell	JPL
Hughes	Draper Lab
Westinghouse	TRW

10.5.2 IDT vs CTD Trade Study

A supporting trade study which assessed the IDT and CTD sensors on their own merits and then compared them was conducted by Ball Aerospace Systems Division under subcontract to SAO. The report described in Reference 2, which summarizes their work, has been accepted and is in final publication at BASD. It will be distributed under separate cover.

The rejection of the IDT is not at all subtle. For HEAO-2 one requires two FOV's about $2^{o} \times 2^{o}$ to ensure a reasonable probability of viewing a detectable star of sufficient intensity to produce an acceptable noise equivalent angle (NEA) over an integration period consistent with vehicle stability. This star is $+9m_v$ and the integration period is about 0.5 sec. With this FOV there is an irreducible systematic error that will certainly be no less than 0.5 arc-sec.. To meet the required 0.3 arc-sec accuracy of the AXAF ADS error budget requires a systematic error of no more than about 0.1 arc-sec. Thus the FOV is scaled by five in each dimension with the result that 25 IDT's are required for each single IDT used in HEAO-2. Since one needs two such FOV's for a roll solution the minimum number is 50 IDT's. THIS IS NOT REALISTIC.

If one gives up the notion of using pre-programmed and cataloged star positions or accepts the notion of limited region star catalogs for each X-ray target it is certainly possible to utilize dimmer stars thereby cutting the FOV required for acceptable probability of acquisition. However, this requires much better vehicle stability. The error allowable due to vehicle motion is taken as 0.1 arc-sec. The stability rate is specified by MSFC at 0.5 arc-sec per sec but it is generally agreed that 0.05 arc-sec/sec can be realized using the existing concept. One could therefore integrate something like 2-3 seconds and keep

the expected error within bounds (depending on error distribution assumptions) which would result in an improvement in NEA by a factor of only about two: It is still necessary to periodically view the fiducial lights. If the flexure of ±5 arc-sec allowed occurs once per orbit, the rate is roughly .004 arc-sec/sec. A fiducial measurement must therefore be taken about every 50 seconds or every 25 or so star measurements. At the expense of complexity a shorter integration time could be used to view the fiducial lights. If the same timing is used as for the dim star it will take about 8 seconds to view four fiducial targets. This is a 16% loss of aspect information. One must also provide a means of returning to the previously tracked star or if more than one star appears in the field of view a new aspect solution may be required.

Finally, one needs to recognize the sole source nature of the 4012IDT and the fact that it is a commercial item of which thousands are currently sold each year. The incentive on the manufacturer to produce space qualified versions is small. Moreover, the IDT commercial applications will most certainly be assaulted by solid state imaging devices over the next few years.

The conclusion which is documented in more detail in Ref. 2 is that the 4012IDT is not a viable candidate for the AXAF fine aspect sensor.

10.5.3 CCD Sensor Studies

Although the CCD sensor as a class of detector appears to offer a great deal of promise, a significant amount of detailed study is necessary to ensure an in-depth understanding of both the use of the devices and their performance within the context of the AXAF requirements.

SAO is engaged in a series of in-house studies that complement or extend on-going work to the extent that it has been published or determined from continuing contacts that have been established within both the open and classified areas of the CCD sensor activity.

The thrust of effort is to identify and evaluate the systematic effects that will ultimately limit the performance of any CCD sensor. We are also examining the CID sensor as a separate case and are considering various sensor control concepts and requirements. The activity is well underway. Work to be performed is defined in the study plan being submitted under separate cover. Basically the effort consists of:

1. array response simulations
2. sensor system studies
3. definition of candidate optics
4. experimental studies to be performed under subcontract

We comment on the first two.

10.5.3.1 Array Response Simulation Studies

A computer program has been written at SAO to simulate up to an N x N array where N is the number of pixels examined in a centroid calculation. The variables presently included in the simulation are:

1. point response function (Gaussian, tophat)
2. different centroid calculation algorithms
3. variable image diameter
4. variable pixel size
5. variable input signal level with respect to assumed fixed noise.
6. simulation of statistical variations

Some preliminary outputs are being evaluated for documentation as separate technical notes within the near future.

The simulation will be expanded and used to examine the sensitivity of determined position to:

1. point response function form and distortions therefrom
2. "fixed pattern" noise levels
3. "fixed patter" noise level variations
4. blur circle diameter
5. pixel to pixel response variation
6. star color

A total system will be configured on paper and simulated to examine dynamic response to deterministic and random motion and intensity variations. On-board processing will be identified and evaluated. <u>One objective is an equivalent linearized model of the aspect sensor for use in total AXAF system simulation studies</u>.

10.5.3.2 <u>Other System Studies</u>

Systems issues under examination include:

1. control/data handling concepts for multiple target tracking and acquisition
2. dynamic range extension and control
3. array packaging
4. mosaic mounting
5. array to optics alignment
6. array cooling
7. power management
8. shutter requirements

9. fiducial system interface
10. thermal interface with mirror assembly

10.6 Summary Comment

At this point in time preliminary studies at SAO, MSFC, and other organizations have shown the CCD and possibly the CID to be suitable sensors for the AXAF application. However, little detailed evaluation and identification of limiting systematic effects seems to have been carried out. The program established at SAO is directed not towards the detailed design of a specific sensor, but towards an in-depth understanding of the nature and the control of all effects that limit the AXAF as a total scientific facility out of which will come an incisive, feasible, and adequate specification for an AXAF fine aspect sensor. This activity is already benefitting from the on-going HEAO-2 (Einstein) experience at SAO where the transfer of the HEAO learning experience to the AXAF occurs continuously.